KU LEUVEN

ARENBERG DOCTORAL SCHOOL
Faculty of Bioscience Engineering

Structure-property relationships in vegetable cell wall suspensions

Ashwin K Sankaran

Dissertation presented in partial fulfillment of the requirements for the degree of Doctor in Bioscience Engineering

July 2015

Structure-property relationships in vegetable cell wall suspensions

Ashwin K SANKARAN

Examination committee:
Prof. H. Ramon, chairman
Prof. A. Van Loey (Promoter, KU Leuven)
Dr. ir. J. Nijsse (Co-promoter, Unilever R&D)

Prof. M. Hendrickx (KU Leuven)
Prof. P. Moldenaers (KU Leuven)
Dr. K. P. Velikov (Unilever R&D, Utrecht University)
Prof. L. Ahrne (Chalmers University)

Dissertation presented in partial fulfillment of the requirements for the degree of Doctor in Bioscience Engineering

July 2015

Uitgegeven in eigen beheer, Ashwin K Sankaran, Kasteelpark Arenberg 22 box 2457, B-3001 Heverlee (Belgium)

Abstract

Plant cell wall suspensions are widely present in daily food, such as soups, dressings and sauces. Cell walls of edible plants are made up of an intricate biopolymer network of mainly cellulose microfibrils, pectins, and hemicelluloses. Foods such as soups, ketchup, etc are made up of cell wall components. Modern processing methods alter the chemical and physical nature of the cell wall which in turn affect the properties of the end product. There is a need in the industry to build a fundamental toolbox for controlling the physical properties of products. To reach this goal, the relationship between the properties and microstructure of cell wall biopolymers has to be established. This work aims to build a qualitative scientific foundation of how various biopolymers present in cell wall suspensions affect the bulk properties. In this quest, novel processing methods are used which engineer the biopolymers to deliver needed functionalities.

Carrots and tomatoes were used as model systems in this study. Enzymes were used to hydrolyze specific classes of biopolymers. By correlating the changes observed in the properties to the specific biopolymer, the functional role of that particular biopolymer was hypothesized. The cell walls of carrot are known to be relatively resistant to disruption by heating and shear. In addition to standard treatments, enzymes were added to hydrolyze specific classes of biopolymers and disrupt the cell wall. Incubation with pure cellulases, pectinases or hemicellulases resulted in suspensions with a different physical structure. The effect of the enzymes was measured on the rheology over an 8 hour period and the microstructure was investigated by cryo-scanning electron microscopy. A homogenization step was applied after the enzyme incubation, resulting in distinctly different cell wall microstructures based on the type and extent of the pre-treatments. It was observed that there is an increase in storage modulus after homogenization due to the increase in particle size, hence the volume fraction of particles. Particle size and particle-serum interactions were pinpointed as the most important contributors to the bulk rheological properties of these cell wall suspensions.

Linking particle-serum interactions to the physical properties is crucial for tomato suspensions. Ion exchange resins were used to tune and investigate these interactions. Two types of resins were used, a hydrogen form cation exchange resin and an anion resin in the hydroxide form. The serum phase of tomato suspensions were treated with either a cationic or an anionic resin to exchange various ionic compounds with hydrogen and hydroxide ions respectively. The treated serum was then reconstituted to the tomato pulp and the suspension was re-suspended with shear. Effect of the resins was dependent on the concentration of resin used. The linear storage modulus varied with the different types of resin treatment. Samples treated with the anion exchange resin resulted in a higher modulus than the untreated tomato puree and the puree treated with the cation resin. The anion treated sample contained a network structure which was quite sensitive to pH. This was attributed to long range electrostatic interactions caused by protein-pectin interactions. Using Infrared spectroscopy conformational changes in the protein structure as a result of resin treatment were detected by analyzing the amide-I and amide-II regions.

In addition to particle size and particle interactions, the role of particle hardness on rheological properties are yet to be established. Hence, an experimental method was developed to study the effect of particle elasticity and electrostatic interactions on the rheological properties of cell suspensions. Enzymes were used to selectively depolymerize the pectin (backbone) and proteins in suspensions. The enzymatic treatments affected the physical properties, thus a hypothesis for the structure-function relationship of these biopolymers was formulated. The enzymatic treatments directly affected particle properties, resulting in loosened cell walls as visualized by cryo-SEM. The effect of the enzymatic treatment on the storage modulus was measured as a function of total solid content (below critical packing fraction). Furthermore, experiments were performed in the presence of varying concentrations of sodium chloride in order to change the Debye screening length. Such a method assisted in decoupling the electrostatic effects from particle elasticity. In addition, particle properties were measured directly by applying a compressive strain on the particles and measuring the normal force. By fitting the normal stress relaxation with a Maxwell model, particle properties such as time scale of relaxation and elasticity were obtained. It is suggested that for carrot suspensions, pectins on the cell walls could contribute to the particle hardness. The pectins on carrot cell walls were responsible for electrostatic interactions between particles. Thus, the structure-property relationships in cell wall suspensions were hypothesized.

Samenvatting

Plantgebaseerde suspensies (bestaande uit een partikel- en een serumfase) komen vaak voor in onze alledaagse voeding, bijvoorbeeld soepen, dressings en sauzen. Celwanden van eetbare planten bestaan uit een complex netwerk van biopolymeren, met name cellulose microfibrillen, pectine en hemicellulose. Moderne procestechnologieën kunnen de chemische en fysische eigenschappen van plantaardige celwanden wijzigen, wat bepalend is voor de structurele eigenschappen van het eindproduct. Vanuit de voedingsindustrie is er vraag naar een fundamentele toolbox om de fysische eigenschappen van een product te kunnen beheersen. Om dit doel te bereiken moeten de relaties tussen de eigenschappen en de microstructuur van de celwand biopolymeren onderzocht worden.

Dit doctoraatsonderzoek beoogt om een kwalitatieve wetenschappelijke bijdrage te leveren omtrent de impact van celwand gerelateerde biopolymeren op de reologische bulk eigenschappen van wortel- en tomaatgebaseerde suspensies. Hierbij worden in dit werk nieuwe procesmethoden toegepast die de biopolymeren doelgericht wijzigen om zo de structuur-functie relaties te onderzoeken. In een eerste deel werden enzymen doelgericht ingezet om specifieke klassen van biopolymeren in de celwand van wortels te hydrolyseren en zo inzicht te verwerven in de functionele rol van deze biopolymeren. Wortelcelwanden zijn relatief resistent tegen warmte en 'shear'. Naast thermische en mechanische behandelingen werden enzymen toegevoegd om specifieke klassen van biopolymeren in de celwand van wortelen te hydrolyseren. Incubatie met cellulase, pectinase of hemicellulase resulteerde in suspensies met verschillende structuren. Het effect van de enzymen op reologie werd opgevolgd gedurende een periode van 8 uur en de microstructuur werd onderzocht met cryo-scanning elektronenmicroscopie (cryo-SEM). Na enzymincubatie werd een homogenisatiestap toegepast, wat resulteerde in een duidelijk verschillende microstructuur afhankelijk van het type en de omvang van de voorbehandeling. De toename in opslagmodulus na homogenisatie kon worden toegeschreven aan

de toename in partikelgrootte, en bijgevolg de volumefractie van de partikels. Partikelgrootte en interacties tussen partikels bleken de belangrijkste factoren die bijdragen tot de bulk reologische eigenschappen van deze celwand suspensies.

In een tweede deel werden kation- en anion-uitwisselaars gebruikt om de partikel-partikel interacties in tomatensuspensies te onderzoeken. De serumfase van tomatensuspensies werd in contact gebracht met ofwel een kation- ofwel een anion-uitwisselingshars. Het behandelde serum werd vervolgens terug toegevoegd aan de tomatenpulp en de suspensie werd geresuspendeerd door middel van shear. Het effect van de harsen bleek afhankelijk van de concentratie van de gebruikte hars. De lineaire opslagmodulus varieerde met de verschillende harsbehandelingen. Stalen behandeld met de anion-uitwisselingshars hadden een hogere opslagmodulus dan de onbehandelde tomatenpuree en de puree behandeld met de kation-uitwisselingshars. Het staal behandeld met de anion-uitwisselingshars bevatte een netwerkstructuur die heel pH gevoelig bleek. Dit werd toegeschreven aan de lange afstand elektrostatische interacties veroorzaakt door proteïne-pectine interacties. Met behulp van infraroodspectroscopie (nl. door analyse van de amide-I en amide II-gebieden) werden conformatieveranderingen in de eiwitstructuur ten gevolge van de harsbehandeling gedetecteerd. In een derde deel werd naast partikelgrootte en partikelinteracties de rol van partikelhardheid op de reologische eigenschappen van wortelgebaseerde suspensies onderzocht. Hiervoor werd een experimentele methode ontwikkeld om het effect van partikelelasticiteit en elektrostatische interacties op de reologische eigenschappen van suspensies te bestuderen. Enzymen werden gebruikt om het pectine (backbone) en de eiwitten in de suspensies selectief te depolymeriseren en zo een hypothese voor de structuur-functie relatie van deze biopolymeren te formuleren. De enzymatische behandelingen hebben rechtstreeks effect op de partikeleigenschappen, wat resulteerde in verzwakte celwanden zoals gevisualiseerd door cryo-SEM. Het effect van de enzymatische behandeling op de opslagmodulus werd gemeten als functie van het totale gehalte aan solids (onder de kritische pakkingsfractie). Bovendien werden experimenten uitgevoerd in aanwezigheid van variërende concentraties natriumchloride om de Debye screening lengte te veranderen. Een dergelijke werkwijze heeft geholpen bij het ontkoppelen van de elektrostatische effecten van deze van de partikelelasticiteit. De partikeleigenschappen werden direct gemeten door een drukspanning aan te brengen en de normaalkracht te meten. De partikeleigenschappen relaxatietijd en partikelelasticiteit werden geschat door het modelleren van de data met het Maxwell model. Bij wortelsuspensies bleek dat pectines op de celwanden kunnen bijdragen aan de partikelhardheid. De pectines op de wortelcelwanden bleken verantwoordelijk voor elektrostatische interacties tussen partikels. Op basis hiervan werden hypotheses over structuur-functie relaties in plantgebaseerde suspensies geformuleerd.

Abbreviations

ATR	Attenuated Total Reflectance
CLSM	Confocal Laser Scanning Microscopy
cryo-SEM	cryo Scanning Electron Microscopy
DM	Degree of Methoxylation
FTIR	Fourier Transform Infrared Spectroscopy
GalA	Galacturonic Acid
HGA	Homogalacturonan
HPH	High Pressure Homogenization
HPLC	High-Performance Liquid Chromatography
ICP	Inductively Coupled Plasma
MALLS	Multiple Angle Laser Light Scattering
OES	Optical Emission Spectrometry
pKa	Acid Dissociation Constant
PSD	Particle Size Distribution
RG-I	Rhamnogalacturonan-I
RG-II	Rhamnogalacturonan-II

RI	Refractive Index
RMS	Root Mean Square
SAOS	Small Angle Oscillatory Shear
SEC	Size Exclusion Chromatography
UV	Ultra Violet

List of Symbols

ω	Angular frequency [rad/sec]
γ, γ_o	Angular strain
x, y	Cartesian coordinates
K	Consistency coefficient
a, B, B_1	Constants
$D[4,3]$	De broucker diameter [μm]
l	Distance [m]
ϵ	Extensional strain
n	Flow behavior index
F	Force [N]
$[\eta]$	Intrinsic viscosity [ml/mg]
G''	Loss modulus [Pa]
η/η_o	Matrix/solvent viscosity [Pa.s]
ϕ_m	Maximum packing fraction
M_w	Molecular Weight [Da]
F_N	Normal force [N]
δ	Phase angle [rad]
μ_{rel}	Relative viscosity [Pa.s]

$\dot{\gamma}$	Shear rate [1/s]
k	Spring constant
G'	Storage modulus [Pa]
σ	Stress [Pa]
t	Time (s)
τ, τ_o	Shear stress [Pa]
w	Total solids
u	Velocity [m/s]
η	Viscosity [Pa.s]
ϕ	Volume fraction
σ_y	Yield Stress [Pa]
E	Youngs modulus [Pa]

Contents

Chapter 1

Literature review

1.1 Introduction

This work investigates the structure-function relationship in plant cell wall suspensions. These systems are found widely in food products such as soups, sauces, smoothies and purees. The functionalities of food suspensions can be determined by measuring either the physical or chemical properties. Physical properties determine parameters such as mouth feel, texture, shelf life, etc. It is important to understand the effect of biopolymers on these functionalities in order to tune processing conditions or develop novel products.

This thesis aims to contribute in gaining insight into the complex biopolymeric interactions that occur in plant cell suspensions. The introduction provides the reader with needed theory in combination with a literature review in fields of rheology and plant cell wall biopolymers. Each field covered in the introduction is divided into subsections. Furthermore, the subsections are written using a bottom-up approach, starting from basic concepts and advancing to more

complex theory that is needed to understand the results presented in subsequent chapters. A brief conclusion and future outlook is provided at the end of the literature review to help the reader appreciate the scientific progress made in this study.

1.2 Rheology

Rheology can be described as the study of deformation and flow of matter. Matter being widely classified as liquid, solid, gas, plasma and substances which exhibit intermediate properties. The science of rheology as understood in modern times has been developed over the last century, but its origins have been traced back to the early Greeks, Chinese and Egyptians. It is mentioned in the ancient Jewish scriptures that the prophetess Deborah proclaimed "The mountains flowed before the lord" [129], which was intended to convey a philosophical message. However, rheologists look at it differently, i.e even the mountains flow when observed for a sufficiently long time. This concept provides the etymology for the Deborah number, which is defined as the ratio between the material's relaxation time and characteristic flow time scale.

Rheology has become a vital tool in modern research, due to its widespread applications and importance in many processes. How materials behave under a given deformation field or an applied stress has become an important measurement. The rheological behavior of any material is dictated by two factors, the deformation it experiences and the microstructure. This was observed as early as 50BC by Lucretius (a Roman poet), who noted in his work, "Of the nature of things", the difference in flow behavior between wine and oil through a colander. He concluded that the difference in "rheological" behavior between percolating wine and oil had to be linked to the internal "elements".

What Lucretius might not have realized is that the flow through a colander is a complex flow consisting of two components, shear flow and extensional flow. How you deform an object also plays an equally important role in determining its flow behavior. In our age of advanced measurement techniques it is easy to call such a phenomenal discovery as trivial. However, it was not until 1600's that a better understanding of flow was developed. Issac Newton wrote in his work Principia "the resistance which arises from the lack of slipperiness of the parts of the liquid, other things being equal, is proportional to the velocity with which the other parts of the liquid are separated from one another". Newton's law of viscosity states that shear stress is equal to the viscosity times the shear rate (equation 1.2.1). As this is not a fundamental equation of nature, it only holds good for certain fluids. Fluids which satisfy this condition are hence called Newtonian or ideally viscous fluids, common examples are liquids like water and oil.

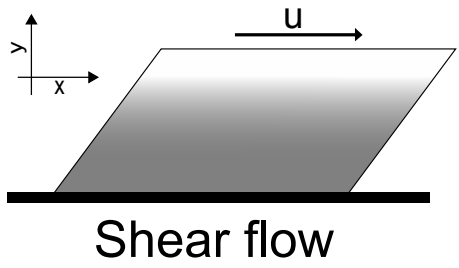

Figure 1.2.1: Schematic diagram of shear flow.

$$\sigma = \eta \cdot \dot{\gamma} = \eta \cdot \frac{\partial u}{\partial y} \tag{1.2.1}$$

where, σ is shear stress [Pa]; η is viscosity [Pa.s]; $\dot{\gamma}$ is shear rate [1/s];
u is velocity [m/s]; x, y are cartesian coordinates.

During the same time as Newton was researching on the laws of fluids and

$$F = k \cdot l \tag{1.2.2}$$

$$\sigma = E \cdot \epsilon \tag{1.2.3}$$

where, F is force [N]; k is spring constant; l is length [m]; σ is tensile stress [Pa]; E is youngs modulus; ϵ is strain [m].

gravity among other things, Robert Hooke was investigating the mechanics of solids. His very famous experiment involved measuring the stiffness of springs using hanging weights. He formulated what is known today as Hooke's law (equation 1.2.2) which states that for an ideal spring the force on the spring is equal to the spring stiffness multiplied by the stretch length. Materials obeying this relation are called Hookean solids. In reality, this equation is valid only for small strains, whereas at larger strains the force response becomes non-linear for all materials. In 1807, Thomas Young published an idea relating the stress (pressure) and strain (ratio of the change in length to the original length). The stress on a material is equal to the modulus multiplied by the strain (equation 1.2.3). Although this idea had existed prior to Young's paper in 1807, the concept of a modulus is named after his contribution, hence called Young's modulus denoted by E.

Most materials that are encountered in daily life have properties combining those of a viscous fluid and an elastic solid. Materials have unique rheological properties depending on the relative contributions from each material domain. For example, steel has a much higher elastic contribution compared to water which is purely viscous. Materials that have intermediate properties between that of a viscous liquid and an elastic solid are termed "viscoelastic", a popular example is ketchup. When dispensing ketchup from a bottle it flows like a liquid, but once it is deposited on a plate it ceases to flow and behaves like a "solid". Measuring these processes, however trivial it might seem, involves complex rheology which has to be precisely controlled. Materials can be classified

depending on their rheological behavior they exhibit, as shown in figure 1.2.2.

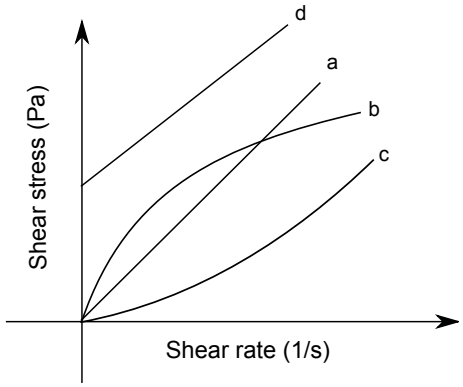

Figure 1.2.2: Graph showing the variation of stress with shear rate for different types of materials. Newtonian liquid (a), Shear thinning liquid (b), Shear thickening liquid (c) and Bingham plastic (d).

- Non-newtonian viscous behavior
  - Shear thinning: viscosity decreases with shear rate
  - Shear thickening: viscosity increases with shear rate
  - Bingham plastic: flows like a liquid if stress exceeds a critical value
- Viscoelasticity
  - Linear viscoelasticity: viscous and elastic moduli independent of applied stress/deformation
  - Non-linear viscoelasticity: high normal stresses and high extensional viscosity
- Time dependent viscous effects
  - Thixotropic: flow causes reversible viscosity decrease
  - Rheopeptic: flow causes reversible viscosity increase

1.2.1 Shear rheometry

Rheometry refers to the science of measuring the rheological properties of a certain system. There are two distinct classifications for rheometers based on the type of deformation applied: shear and extensional rheometers. Shear flow (figure 1.2.1) is the most frequently used flow type for characterizing material properties and will be the focus of this study. Within shear rheometers there exists two classes: capillary rheometers and rotational rheometers.

The underlying principle of capillary rheometers is the laminar flow of liquid through a pipe or capillary, as shown in figure 1.2.3. Either the flow-rate or pressure drop is controlled while the other is measured. As the capillary's dimensions are precisely known, the shear rate can be calculated from the flow rate and shear stress from the pressure drop. By controlling either parameter, a flow curve can be established. This method of determining flow properties is rudimentary and has limitations. As there is a variation in the shear rate across the cross section of the capillary, interpreting results for non-newtonian fluids is not phenomenological. However, for Newtonian fluids, as the viscosity does not vary with shear rate this method can yield precise measurements of viscosity.

Ubbelohde viscometer is a capillary based method of measuring the viscosity for Newtonian fluids (figure 1.2.3). It is a U-shaped device with a reservoir on one side and a measuring bulb with a capillary on the other. The end of the capillary is connected to a third arm which is open to the atmosphere. Sample liquid is loaded into the reservoir which is then sucked into the measuring bulb through the capillary. Once the liquid passes the calibrated mark A, it is allowed to drain under gravitational force. The time taken for the liquid to travel from the calibrated mark A to B is a measure of viscosity. The measurement is independent of the total volume of liquid as the pressure drop of the flow is not dependent on the column of liquid present within the arms.

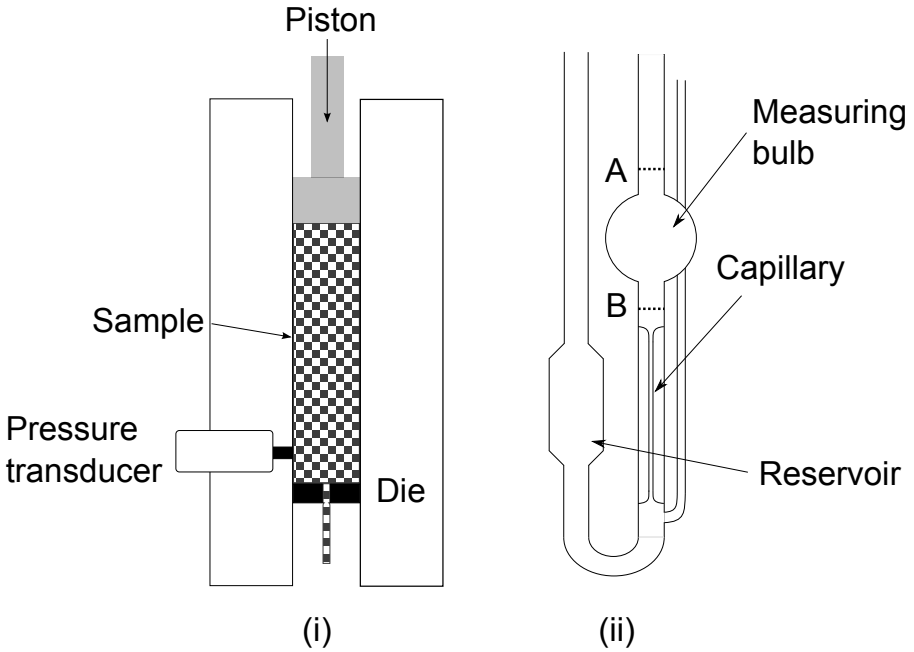

Figure 1.2.3: Schematic diagram of capillary rheometers: (i) Capillary rheometer, (ii) Ubbelohde viscometer.

This method allows for a precise measurement of the viscosity for Newtonian fluids. This viscometer is typically used for measuring the intrinsic viscosity of dilute polymeric solutions.

Typical rotational shear rheometers are shown in figure 1.2.4 with the use of plate geometries. In principle, this device can independently control and measure the torque and/or angular velocity applied. As a result, there are two control types for rotational rheometers. A stress controlled machine, wherein the device applies the stress and measures deformation on the sample. The other is the strain controlled type wherein a motor controls the rate of deformation while the torque applied on the bearing is measured. Although the control system may have the flexibility to run experiments in both modes, the parameter that the instrument is controlling should always be noted, as the other can only be

applied indirectly via a feedback control loop. Stress controlled rheometers are the most commonly used rheometers to characterize various material functions because of their cost benefit and ease of use.

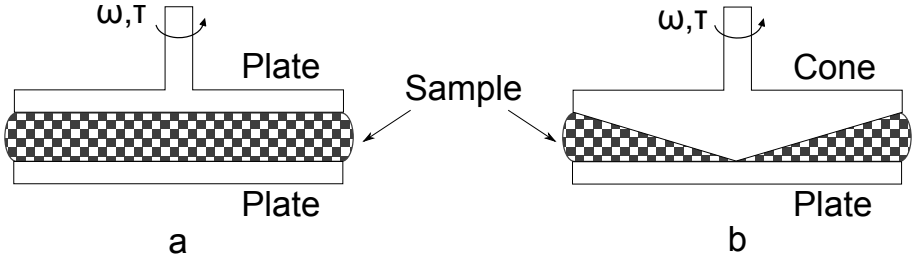

Figure 1.2.4: Schematic diagram of rotational rheometers, (a) parallel plate and (b) cone-plate geometry.

Viscoelastic properties of materials such as the storage (G') and loss (G") modulus indicate the contributions of elastic and viscous characteristics of the material respectively. They are determined either by performing a small amplitude oscillatory shear, creeping test or stress relaxation within the linear viscoelastic region. The most frequently used test is the small amplitude oscillatory shear performed in the strain controlled mode, colloquially known as oscillatory experiments. Here the rheometer inputs a strain deformation in the form of a sine wave while simultaneously measures the resulting stress signal from the sample (figure 1.2.5). This resulting stress signal is the superposition of the elastic (equation 1.2.4) and viscous (equation 1.2.5) response of the material. The elastic part of the signal is in phase with the strain applied, whereas, the viscous part lags by 90°. Hence, G' the storage modulus, G" the loss modulus and δ the phase difference, can be calculated.

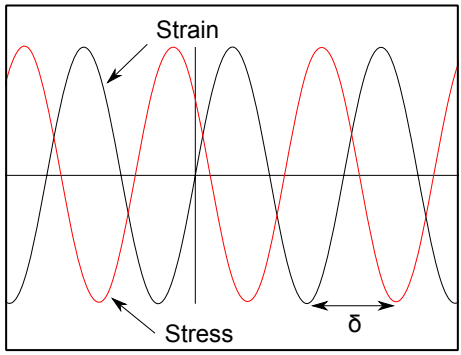

Figure 1.2.5: Oscillatory stress-strain diagram for viscoelastic materials.

$$\gamma = \gamma_o sin(\omega t)$$

$$\tau = \tau_o sin(\omega t + \delta)$$

$$\tau = \tau_o[sin(\omega t)cos(\delta) + cos(\omega t)sin(\delta)]$$

$$\tau = \frac{\tau_o}{\gamma_o}\gamma cos(\delta) + \frac{\tau_o}{\gamma_o}\frac{\dot{\gamma}}{\omega}sin(\delta)$$

$$G'(\omega) = \frac{\tau_o}{\gamma_o}cos(\delta) \tag{1.2.4}$$

$$G"(\omega) = \frac{\tau_o}{\gamma_o}cos(\frac{\pi}{2} + \delta) \tag{1.2.5}$$

where, G' is storage modulus [Pa]; G" is loss modulus [Pa]; ω is angular frequency [rad/sec]; t is time [s]; τ_o and τ are shear stress [Pa]; δ is phase difference; γ and γ_o are strain.

The moduli are dependent on two independent parameters, the strain amplitude and frequency of oscillation. Within the region of linear viscoelasticity, the modulus is independent of the strain amplitude, which is valid for small values of strain. As the strain increases beyond a critical strain (γ_c) , G' and G" become non-linear and dependent on the applied strain. The storage modulus

in the linear viscoelastic region is called the linear storage modulus. This linear storage modulus is an important measure for food products as it is an indicator of properties such as product stability, physical shelf life, mouth feel and consistency.

The limit of linear viscoelasticity of a material can be determined by keeping the frequency constant and varying the strain. Subsequently, a frequency sweep is performed at a fixed strain ($\gamma < \gamma_c$) to give a deeper insight into the materials microstructure. The dependence of the storage and loss moduli on frequency provides an understanding of the material's microstructure from the relaxation spectrum. For gelled systems, the elastic moduli indicate the stiffness of the gel, whereas, the slope $G' \backsim \omega^n$ indicates the gel type being either a strong or weak gel. In addition to these properties, the elastic nature of the gel can be determined by $\tan(\delta)$ which is the ratio of the G' to G".

Shear rheometers also perform flow measurements, in which the device measures the viscosity under well defined flow conditions. In a rheological steady shear rate test, a constant deformation rate is applied and the equilibrium torque on the bearing is measured. Depending on the geometry used, the viscosity as a function of the shear rate can be evaluated from the torque. As the control system is flexible, a shear stress can be imposed while measuring the shear rate. This method can also be used to determine the dynamic yield stress present in the sample. After a critical stress, the material starts to flow, indicative of the yield stress within the sample. In addition, advanced tests such as creep, step strain experiments, can reveal more detailed information about the relaxation processes and non-linear viscoelasticity of the samples. However, interpretation of these results is not straight forward for heterogeneous systems as investigated in the present work.

1.2.2 Suspension rheology

Most food products are either suspensions, emulsions, or a combination of both. Suspensions are systems that consist of particles in a viscous medium. Common examples of suspensions are paints, milk, ketchup, sand in water, etc. The rheology of these systems can become very complicated as it depends on a wide range of factors such as particle volume fraction, particle shape, particle-particle interactions, ions/electrolytes, particle orientation and so on, depending on the system. The approximation for viscosity of a dilute suspension of hard spheres (no interactions) as a function of concentration was given by Einstein [40] (equation 1.2.6). According to this approximation, the viscosity of the suspensions depends only on the viscosity of the suspending medium (η_o), the volume fraction of particles (ϕ) and the intrinsic viscosity [η].

$$\eta = \eta_o(1 + [\eta]\phi) \tag{1.2.6}$$

The intrinsic viscosity [η] is defined as,

$$[\eta] = \lim_{\phi \to 0} \frac{\eta - \eta_o}{\phi \cdot \eta_o}$$

where, η is suspension viscosity [Pa.s]; η_o is solvent viscosity [Pa.s]; ϕ volume fraction.

The intrinsic viscosity depends on the particle shape, being 2.5 for rigid spheres and larger for anisotropic particles. With this as the starting point of modern suspension rheology, many advances have been made in the last century to better understand more complex systems. Taylor [130] extended the Einstein equation to deformable spheres also known as soft spheres or droplets. Jeffery [56] formulated a theory for non-spherical objects that were rigid. It was found

that the viscosity of ellipsoids was higher compared to hard spheres at the same volume fraction.

As the concentration of the particles starts to increase, the interactions between particles become more dominant. In such a case, the linear relationship between the viscosity and volume fraction of the particles fails. Hence, higher order terms are needed to describe the physics more accurately. Early work towards formulating a viscosity relationship for semi-dilute suspensions was done by Batchelor with a second order polynomial [8] (equation 1.2.7). The coefficients B and B_1 were correlated from particle-particle interactions [69, 138]. With B=2.5 and B_1 varied between 7.35 and 14.1, depending on the system [9, 88].

$$\eta = \eta_o(1 + B\phi + B_1\phi^2) \tag{1.2.7}$$

where, η is suspension viscosity [Pa.s]; η_o is solvent viscosity [Pa.s]; ϕ volume fraction; B and B_1 are constants.

One of the short-comings of polynomial relationships is that they fit experimental data poorly when the particle-particle interactions become significant ($\phi \gtrsim 0.25$). The viscosity does not tend to infinity as the volume fraction tends towards unity, i.e $\phi \to 1$. However, it can be easily realized that volume fraction of hard particle suspensions cannot approach unity in reality. By percolation theory, at a certain critical concentration of particles the systems loses its fluidity. As the concentration of particles increases, the system goes through a phase transition. Once there is sufficient crowding of particles, they are more restricted in motion by their adjacent neighbors and these systems start to exhibit glassy behavior. As the concentration approaches the random close packing limit, the particles pack into a lattice structure and behave like a crystalline solid. This critical volume fraction is referred to as the maximum volume fraction (ϕ_c).

Theoretically, the maximum packing fraction for hard spheres is 0.74, although random packing of spheres are at a lower volume fraction [88]. For a system of uniform hard spherical particles, a $\phi_c = 0.64$ is sufficiently accurate for most purposes [93].

A different approach to model concentrated suspensions was formulated by Roscoe [1952] and Brinkman [1952] using a so-called differential scheme. Considering that a suspension had a volume fraction ϕ and an infinitesimal amount of particles $\delta\phi$ were added, the corresponding increase in viscosity was evaluated (equation 1.2.8). The parameter B_1 depends on the size distribution of the spheres, for a uniform size distribution it was found to be 1.35 [108]. This equation seems to satisfy the limiting condition, i.e when the volume fraction tends to the maximum packing fraction of hard spheres $\phi \to 0.74$, the relative viscosity tends to infinity, $\eta_r \to \infty$.

$$\eta = \eta_o(1 - B_1\phi)^{-2.5} \tag{1.2.8}$$

where, η is suspension viscosity [Pa.s]; η_o is solvent viscosity [Pa.s]; ϕ volume fraction; B_1 is a constant.

Krieger and Dougherty [1959] evaluated the viscosity considering the contribution from successive packets of particles to the total volume fraction and formulated what is known as the functional equation (equation 1.2.9). The main advantage of this model is that it incorporates the main characteristics for a hard sphere suspension. This model is compared with experimental data, as the parameters B and ϕ_m can be determined from experimental results.

$$\eta = \eta_o(1 - \frac{\phi}{\phi_m})^{-B\phi_m} \tag{1.2.9}$$

where, η is suspension viscosity [Pa.s]; η_o is solvent viscosity [Pa.s]; ϕ volume fraction; ϕ_m packing fraction; B is a constant.

1.2.3 Soft particulate suspensions

Most real systems like concentrated emulsions [11, 72], foams [53], gelled star polymers [26] and pastes [27], contain particles that are not ideally "rigid". These kind of soft particulate systems do not behave like hard spheres because of the inherent deformability of the particles or forces that stabilize them. As concentrated soft particulate suspensions exhibit glassy dynamics, these systems are often called as soft glassy materials [14, 118]. A notable difference between hard and soft particle suspensions is that soft particles can be packed more densely. As the volume fraction of these systems tends towards unity $\phi \to 1$, the zero shear-viscosity tends to a finite value. These systems undergo a jamming transition as a result of increased volume fraction. Concentrated systems of particles are restricted in their ability to diffuse over large length scales due to the presence of adjacent neighbors [102]. This point corresponds to the onset of significant particle-particle interactions. Although the particles are capable of local movements, they are constrained in a cage formed by their neighbors, which leads to a frozen glassy state of the material [28, 57, 101, 102, 137]. The nature of the "cages" could either be due to direct particle-particle contact or mediated by particle-particle interactions (repulsive or attractive) [27, 62, 98], as shown in figure 1.2.6. Hard sphere systems start to interact mainly by steric interaction of finite sized particles, governed by nature's law that two particles cannot occupy the same space at the same time. However, particle systems that are stabilized by inter-

forces are capable of interacting at a much lower volume fraction compared to

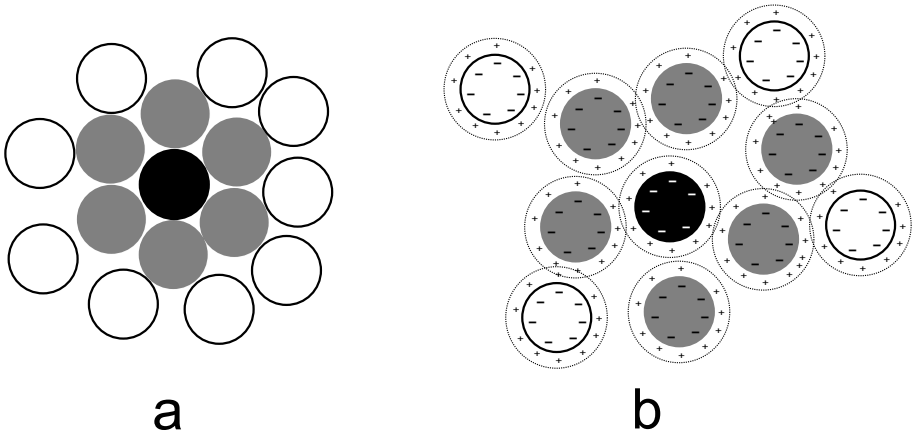

Figure 1.2.6: Two dimensional illustration of caged particle in a concentrated suspension. The particle in the middle (black circle) is 'caged in' by the presence of the nearest neighbors (grey circles). Figure a, depicts a hard sphere scenario. Figure b, depicts a scenario for soft spheres stabilized by electrostatic interactions.

their hard sphere counterparts. These systems start to experience the presence of a neighboring particle due to "soft force fields" that surround their hard core shell. Hence, systems with repulsive interactions such as emulsions or granular materials, exhibit jamming at a volume fraction lower than the random close packing.

The rheology of soft systems originates from two factors, a disordered microstructure and metastability of the particles [118]. Concentrated soft particle systems have complex stress relaxation phenomena, usually having two relaxation time scales, a short (β regime) and a longer time scale (α regime) [27]. Using mode-coupling theory, the shear stress versus shear rate behavior can be described for soft systems starting from microstructural information. At a higher volume fraction of particles (jammed state), they cease to flow at low stress levels and behave like a soft solid at rest exhibiting a yield stress [52]. This yield stress occurs as the applied force is balanced by the force

network between particles and the cages. However, as the stress increases, the particles start to overcome the energy barrier imposed by their cage. Beyond the yield stress, the particles undergo macroscopic flow, which induces a state of continuous rearrangements causing a shear thinning viscosity. Mode-coupling theory fits the experimental data; at small time scales the particles undergo subdiffusive motion (β regime) and at longer time scales they are trapped (α regime) [27, 137]. The slow diffusion time scale in the β regime is dependent on the hydrodynamic interactions between the particles at equilibrium [24, 63]. This time scale is similar to the Stoke-Einstein equation, an important consideration when brownian motion is predominant. When subjected to a shear flow with a characteristic time scale larger than the time for subdiffusive motion, there are structural rearrangements taking place which cause relaxation. A simple flow essentially causes long range structural re-arrangements and relative motion between neighbors. Under these conditions, stress relaxation occurs in the α regime. This is governed by elastic recoil of the particles themselves as they are "locked" in a metastable state under flow conditions [95, 114]. Due to crowding of particles, it is reasonable that this effect will be more predominant in concentrated systems than dilute systems. The rate of relaxation decreases by a factor of approximately 50 for concentrated systems compared to dilute systems [114, 136]. At certain conditions of particle type, concentration and shear rates, some systems are capable of showing shear thickening effects. This occurs due to a localized jamming transition in the system with the increase in shear rate, a typical example being corn starch in water [79]. Shear thickening systems are out of scope of the current study.

Often softness in particulate suspensions arise from two distinct effects, the particles being soft themselves or particles can be stabilized by repulsive forces (electrostatic or steric). Stabilization of particles is broadly classified into electrostatic or polymeric stabilization. Furthermore, electrostatic stabilization

can be further classified by the nature of the force into attractive and repulsive interactions [115]. Polymeric stabilization can be subdivided into either steric or depletion stabilization [151]. These types of stabilization makes the particles seem softer compared to hard core models due to the inherent forces that act on the particles.

Electrostatically stabilized suspensions are commonly found in many day to day products, such as foods, paints, oils, etc and hence is more relevant to this work. When particles are dispersed in a liquid, ionic groups can adsorb onto the surface of the suspension to form a charged layer (figure 1.2.7). To maintain local electro-neutrality around the particle, counter ions surround the particle to form a charge neutral shell around it, called the stern layer. The stern layer extends itself until the stern plane, as shown in figure 1.2.7. After which, there is a diffuse layer caused by the migration of ions present in the suspending medium. This layer contains a higher concentration of counter ions with a gradient starting from the stern plane. The electrical double layer is held together by the electrostatic force caused by the charged particle. This electrical double layer surrounding the particle helps in stabilizing the system by charge repulsions from neighboring particles. The thickness of the double layer primarily depends on factors such as ionic strength, concentration of ions and size of the particle. Therefore, electrostatically stabilized systems are very sensitive to the amount of ions present in the system.

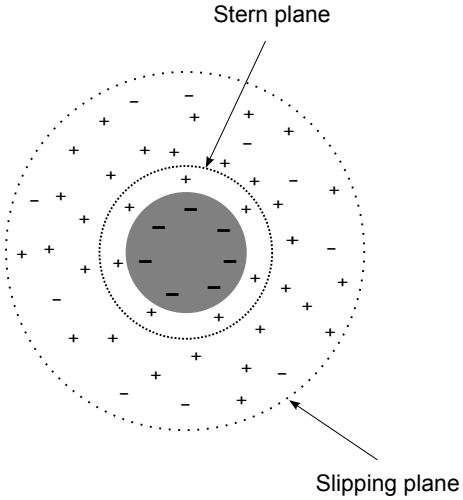

Figure 1.2.7: Schematic diagram showing double layer around a single particle. The particle is negatively charged in the schematic.

Steric stabilization is achieved by attaching a macro-molecule of sufficient molecular weight onto the surface of the particles. This process is usually done by either grafting the macro-molecule onto the surface or by chemisorption. The grafted macromolecules provide stabilization when two particles are close enough to each other by steric hindrance (figure1.2.8a). Depletion stabilization (figure 1.2.8b) occurs when there is 'free', non-absorbing polymer present in the dispersing medium. A depletion region is created around the particles as the polymer molecules do not approach the surface of the particle. This is because the entropy of the system decreases as the polymer chains interact with the particle surface, creating an energetically unfavourable state. When two particles start to overlap in the depletion region, the polymer present gets squeezed out and creates an osmotic pressure that keeps particles separated. A relatively high concentration of polymers is required for this type of stabilization to occur, and sometimes the polymers can also be weakly flocculating. Depletion flocculation occurs when the polymer in the solution is able to form a bridge

between particles. This mechanism is possible when each end of the polymer attaches to different particles. Usualy flocculation causes de-stabilization in the system and promotes coagulation between particles. Each type of stabilization has its own advantages and disadvantages: electrostatic stabilization is less robust but cheaper and easier to formulate compared to polymeric stabilization. In addition, electrostatic repulsion can act over significantly longer distances.

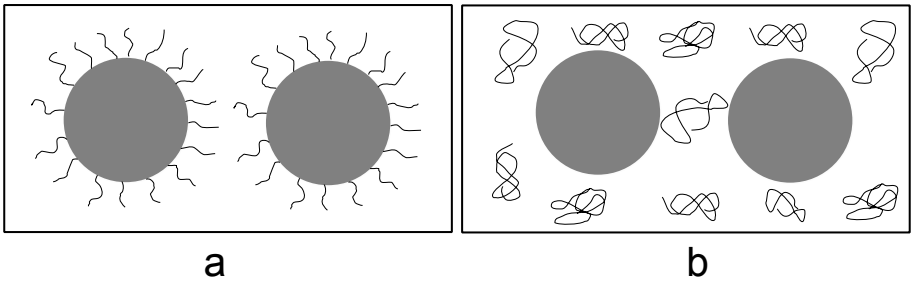

Figure 1.2.8: Schematic diagram showing polymeric stabilization of particles. (a) Steric stabilization, (b) depletion stabilization.

The rheology of systems can vary considerably depending on the method of stabilization. Electrostatically stabilized suspensions can be found abundantly in nature and many manufactured products. The effect of an electric double layer around a particle on the rheology is referred to as electroviscous effect. In dilute concentrations of these suspensions, the particles are not packed close enough to "feel" the neighboring particle's double layer, and thus, electrostatic effects are small. As the concentration increases to a point where the diffuse layers of neighboring particles begin to overlap, the interactions become more complex. Due to the electrostatic potential, the particles experience inter-particle repulsion. The distance to which the electrostatic effect persists is called the debye length. Causing a substantial increase in the viscosity, this effect is termed as the secondary electroviscous effect [79]. Under flow conditions, these systems typically shear thin similar to hard sphere suspensions

of comparable volume fraction. Shear thinning behavior can be greatly enhanced by inter particle repulsion due to the higher zero shear viscosity. The secondary electrovisous effect can be mitigated by the addition of salts like NaCl. As salts reduce the debye length surrounding each particle, there is a decrease in inter-particle repulsion, which can greatly reduce the zero-shear viscosity or the storage modulus [54].

1.3 Biopolymers in the primary cell wall of plants

Primary cell walls of plants are complex nanostructured systems. There are many models that describe the plant cell wall, the most influential model was proposed by McCann and Roberts (figure 1.3.1)[76]. In this model, the primary cell wall is believed to be made up of interconnected matrices composed of cellulose, pectins, hemicelluloses and proteins. These cell wall biopolymers form a complex structure through non-covalent bonding giving the plant its needed mechanical properties among other functionalities. In recent decades, understanding the structure-property relationships in plant cell walls has become of research interest to both academics and industry. It is important to understand the microstructure of these systems to engineer their properties for suitable applications. From the food industry perspective, Aguilera [1] highlights the importance of studying food microstructure to understand its impact on nutrient availability, texture and physical properties.

1.3.1 Cellulose

Cellulose is the most abundant carbohydrate polymer in the primary cell wall of plants, notably also the most abundant polymer in the world. It is a polysaccharide made up of repeating D-glucose monomers linked together

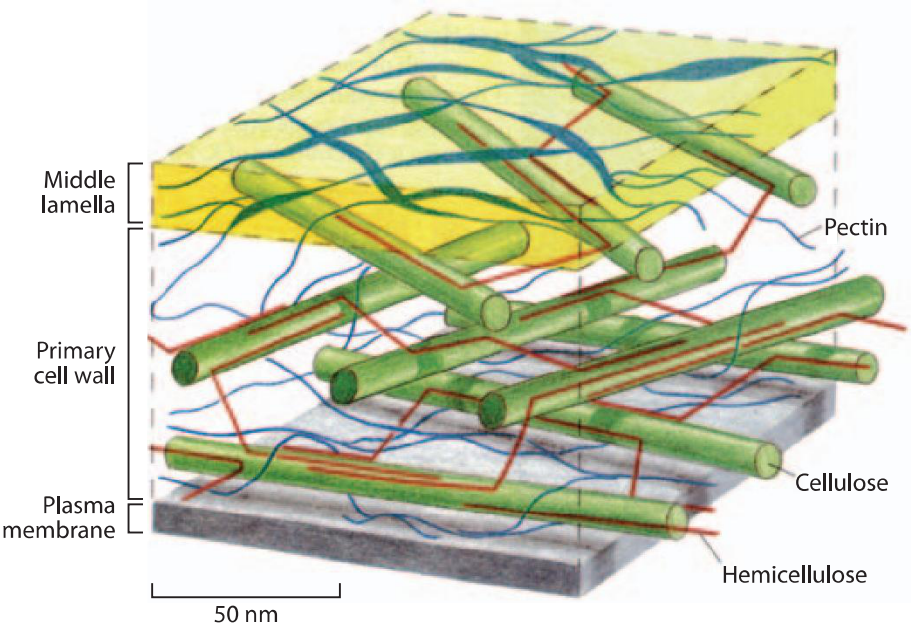

Figure 1.3.1: Schematic diagram representation of the cell wall model proposed by McCann and Roberts [76].

by β-1,4 glycoside bonds. Cellulose is a crystalline structure made up of 1-α and β crystals, this is by far the most ordered polysaccharide in the cell wall [123, 134, 146]. This crystalline nature of cellulose is responsible for the cell wall's rigidity and mechanical strength. Dimensions of cellulose fibrils are about 2-3 nm in diameter and can be upto 22-24 monomers in crosssection, which are created during cell growth [134]. Golgi vesicles carrying cell wall matrix material and cellulose synthase deposit them on the plasma membrane. Cellulose synthase consists of rosetta particles which spin out cellulose polymers. Subsequently these polymers crystallize to form microfibrils [36]. Microfibrilar deposition and orientation is determined by the spinning pathways along the plasma membrane [25]. The orientation of the fibrils arise due to many factors like turgor pressure, the template for growth, environmental factors and composition of cell wall

substances [89]. Cellulose is deposited in successive layers which forms a lamellar structure where the fibers are arranged in parallel to each other [121]. As a result of this orientation, the resulting fibers are stronger in the direction of fiber orientation compared to the transverse direction [89]. The presence of proteins within the cell wall during growth could result in cross linking with other polysacharides as well, improving the tensile strength of plants [60, 61]. During the creation of the cell wall, various polysacharides like hemicelluloses and pectins are deposited on the cellulosic matrix. This results in a complex polysaccharide network inside the cell wall of plants.

1.3.2 Pectins

Pectins are a diverse class of polysaccharides, which play a crucial role in plant growth, cell-cell adhesion, wall structure and cell expansion [85, 148]. Pectins are grafted naturally onto the cellulose backbone and are also found in inter-cellular spaces. Being a multifunctional component within the cell wall, pectin also has a diversified chemical structure. Pectins are made up of smaller hetero-polysaccharides that consist of unique domains (figure 1.3.2). They were suggested to have three possible domains along its backbone: homogalacturonan (HGA), rhamnogalacturonan-I (RG-I) and rhamnogalacturonan-II (RG-II) (figure 1.3.2) [85]. HGA is the acidic polymeric backbone made up of (1→4)-α-linked-D-galacturonic acid, which consists of about 100-200 galacturonic acid (GalA) monomers [133]. The GalA of HGA can be methyl esterified or acetylated which significantly affects the functionality. The RG-I domain is made up of repeating (1→2)-α-L-rhamnose-(1→4)-α-D-galacturonic acid disaccharides [90]. These are abundant in pectic polysaccharides and contain other chemical groups that branch off from its backbone. The most common branching observed are galactose and arabinose neutral sugar residues [85]. These side chain sugars may

also vary in their structural linkages [23, 133]. RG-II does not share structural resemblances with RG-I, despite the naming convention. They are made up of nine (1→4)-α-linked-galacturonic acid monomers with 4 hetero-polymeric side chain branchings [91]. RG-II does not seem to have significant structural diversity within the pectic domain.

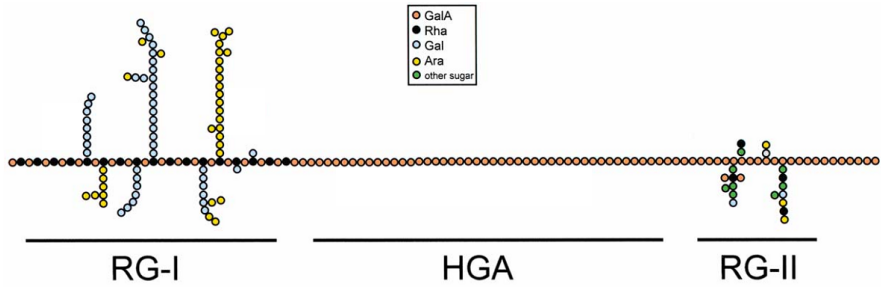

Figure 1.3.2: Schematic diagram representation of pectin structure, picture adapted from Willats et al. [148].

The heterogeneous nature of pectins arises from branchings and substitutions on the backbone. The chemical structure of pectins allows for an interesting interplay with other bio-polymers through hydrogen bonding, hydrophobic interactions, ionic and maybe even covalent coupling [117]. Pectin-pectin interactions have been studied quite well and the most exploited use in the industry is in gel formation. Pectin gels and their physical properties are known to be significantly affected by the processing conditions and environmental factors [12, 126]. Two main mechanisms of gelling have been identified depending on the degree of methoxylation (DM) of the HGA backbone of the pectins. A high degree of methoxylation (DM $>$ 50%) present in the pectin chains makes them gel only at pH values lower than 3.5 and in the presence of high sugar content (higher than 55%) [132, 147]. The high sugar content promotes hydrophobic interactions between the methoxyl groups and the low pH helps to maintain the carboxyl groups from dissociating, hence reducing electrostatic

repulsion. This effect, combined with hydrogen bonding between the carboxyl and secondary alcohol groups promotes gellation [132]. On the other hand, low methoxylated pectins (DM $< 50\%$) interact with other pectin chains to form a gel at a higher pH and in the presence of ions. In the presence of Ca^{2+} ions, homogalacturonan chains present in pectins interact with each other according to the "egg box model" [49]. The carboxyl groups present between two galacturonic acid molecules creates a negative charge that is capable of holding in place a calcium ion [20]. The environmental factors such as pH, sugar content, presence of ions and temperature play an unequivocal role in pectin-pectin interactions [45].

1.3.3 Hemicellulose

Hemicelluloses are the third class of polysaccharides present in the cell wall, they are different in chemical structure and physio-chemical properties from other polysaccharides. The key structural feature that differentiates hemicellulose from the other polysaccharides is their β-(1→4)-linked backbones with an equatorial configuration. Hemicelluloses can include xyloglucans, xylans, mannans, glucomannans and glucans, depending on the type of plant. Xyloglucans are able to form non-covalent links with cellulose which facilitate the cross-linking of cellulose microfibrils. This provides structural strength to the cell wall [76]. In addition, there is evidence to suggest hemicelluloses are non covalently bound to the pectic matrix via hydrogen bonding [41]. During the process of cell wall expansion, xyloglucans are capable of functioning as signal molecules. This helps in regulating the auxin mediated cell wall expansion [112]. In conclusion, the role of hemicellulose in the cell wall is to interact with other polymers to ensure proper physical properties of the cell wall.

1.4 Food rheology: Rheology of cell wall suspensions

Food products that are consumed in daily lives of people are heterogeneous systems. The complex microstructure and the underlying physics of such systems are quite fascinating. Soft food systems are often classified under a branch of soft condensed matter, materials such as emulsions (mayonnaise), foams (ice cream), particle suspensions (ketchup) or colloidal suspensions (milk) [80]. Even though food systems are everyday products, there is a need for better understanding to control their properties. This helps to exploit endogenous structuring potential without artificial thickeners and for solving problems encountered in daily life [80]. For example, Len Fisher discussed a common problem, the physics of dipping a biscuit in tea so that it does not become "soggy" and fall apart. He was awarded the physics Ignoble in 1999 for the same work. According to his analysis, the optimal way to dip a biscuit is at a shallow angle into the tea instead of dipping it vertically. This ensures that only the bottom is wet and the upper regions of the biscuit remains dry and maintains the mechanical strength needed to hold it [43].

Controlling the rheological properties of food is important for the physical shelf life (eg. sedimentation), mouth feel (eg. creaminess) and processing conditions of a product. Rheology, microstructure and processing are inherently interconnected. A common example of soft matter in food is ketchup, a typical problem is dispensing the required quantity of ketchup from a glass bottle. As per the instructions on the bottle, the ideal method is to shake the bottle before trying to get it on your plate. This ensures the ketchup flows easily out of the bottle. If one does not shake the bottle before, it is more difficult to dispense the needed amount of ketchup. The underlying physics behind this problem is linked to the microstructure and rheology. Ketchup can be considered as

a jammed particulate system; it behaves like a thixotropic yield stress fluid. When the bottle is shaken hard enough, the applied stresses can overcome the yield stress and cause structural re-arragements allowing for the ketchup to flow. This creates a time window before the microstructure relaxes to its orignal state. Dispensing within this time window would be ideal as the ketchup still has the ability to flow without a yield stress. After dispensing the ketchup on your plate or burger, it ceases to flow unlike it did from the bottle. As the microstructure relaxes, the yield stress is restored and the thixotropy is reversed, hence, the ketchup retains its shape after dispensing it onto the plate. Ironically, the yield stress that once caused the problem of dispensing, solves the problem of the ketchup being too thin or runny on your plate.

Rheology of plant based suspensions obviously depend on the microstructural characteristics. The three corner stones of plant food rheology are the particle phase, the serum phase and respective interactions between them. Particles can vary by their shape, size, surface charge and hardness. The serum phase contains solubilized pectins, proteins and sugars. In addition to these, the chemical heterogeneity of these systems can also cause considerable interactions either between the particles or particle/serum phase of the suspension. The interactions between either of the components can be electrostatic, frictional or elastic, depending on other factors such as particle concentration, plant type and ionic content.

It is common knowledge that cooking softens vegetables and blending results in products with disintegrated plant tissue similar to a juice, puree or a sauce. However, the structure-property relationship of these everyday processes that result in cell wall suspensions is less clear. Rheological behavior of these suspensions depend upon the particle and serum properties. The properties of both these phases largely depend on the thermal, mechanical and enzymatic processes used to formulate the suspension.

1.4.1 Particle phase

Particle concentration is a key factor in determining the rheological behavior in plant cell suspensions. In dilute concentrations of these suspensions, they flow like a liquid and do not exhibit a yield stress. This is primarily due to the lack of a percolated network between particles. As the concentration increases, the particles start to "crowd" which can help to form a network held by either electrostatic, elastic or frictional interactions, resulting in a yield stress [83]. Once the suspension is subjected to a stress higher than the yield stress, it flows like a shear thinning fluid. There have been attempts to model the rheological flow properties, yet there is no phenomenological model to describe the physics. This is primarily due to the heterogeneity and complex interactions present, hence approximating these systems to hard sphere models can be erroneous [19]. However, empirical models such as the Herschell–Bulkley model was used to fit experimental data [15, 50]. The Herschell–Bulkley model has three independent parameters, the flow behavior index (n), yield stress (σ_y) and consistency coefficient (K). It was found in plant based suspensions that the flow behavior index (n) decreased, whereas the consistency coeffecient (K) increased with increase in particle concentration. This meant that a suspension behaved more as a non-Newtonian fluid with an increase in the concentration of particles. The effect of particle concentration on the influence of K seemed to vary with a power law dependence [5, 149]. As a general trend in plant cell based suspensions, the yield stress and storage modulus also seem to vary with a power law dependence on the concentration of particles [33, 64, 128, 140, 149].

Particle sizes in plant cell suspensions are polydisperse, which plays a critical factor in determining the rheological properties. The size range of insoluble particulate matter can be very broad, ranging from 0.5 μm upto 500 μm. In this work, the term particle refers to the larger insoluble material such as

cells, agglomerated cells or cell wall fragments, which can be about 50-500 μm. Smaller colloidal particles from intra-cellular material can also exist in the form of nutrients, phospholipids, carotenoid crystals, etc. These smaller colloidal particles are referred to as the serum phase or serum. Estimating an accurate volume fraction is a daunting task, because of the polydispersity in particle size and varied particle shapes. Hence, researchers tend to use particle concentration on a dry weight basis as a qualitative indicator for the volume fraction of particles [64, 83]. Without an accurate volume fraction it is quite difficult to formulate a conclusive hypothesis of how particle size can affect the rheological properties. Previous studies trying to understand the effect of particle size on rheological properties has not yielded unambiguous and universal results [83]. The general trends observed in tomato suspensions is that smaller particles result in higher rheological parameters compared to larger particles of the same volume fraction. It is reasoned that since smaller tomato particles have larger surface area, there is higher particle-particle interactions which result in the enhanced rheological properties [103, 149]. A contrasting trend is observed in an apple system, smaller particles resulted in lower rheological parameters, due to a better packing of the particles [113]. It is clear that the trends of particle size and their rheological properties are not universal. This is primarily due to the unique nature of particle-particle interactions within each system.

Particle morphology and shape were also found to affect the texture and rheological properties of plant cell suspensions. These properties can be tuned by a combination of thermal and mechanical processing. The resulting particle morphology is dependent on the order and intensity of the treatments [65], as shown in figure 1.4.1. Cell clusters were formed when either carrot or broccoli purees were cooked for 10 minutes at 70 °C followed by blending. On the other hand, when the vegetables were cooked for 40 minutes at 90 °C the blending of the cooked material resulted in individual cells [65]. Prolonged heating

at higher temperatures resulted in weaker cell-cell adhesion caused by pectin solubilization. When mechanical shear is applied, the particles have a single cell morphology as it breaks along the cell boundaries [92]. In recent times, a high pressure homogenizer is used to apply a more severe mechanical treatment. The homogenizer works by pumping the samples through a narrow orifice at high pressures. The resulting turbulence causes a larger stress on the particles than conventional blending, hence disrupting the particles more effectively. In a subsequent work, Lopez-Sanchez et al. [66] investigated the effect of the homogenization pressure and the number of cycles on the microstructure of tomato and carrot emulsions. It was concluded that tomato fibers resulted in an intricate network of cellulose microfibrils, known as microfibrilated cellulose, whereas, carrot cell wall fibers were more resistant and resulted in cell wall fragments. In addition to the variation in the type of tissue, morpholopgy seemed to vary as a function of homogenization pressure [97]. There is a progressive change from cell clusters to single cells and subsequently cell wall fragments with increase in the homogenization pressure. This change in the morphology of the particles directly influences the physical properties such as texture and rheology [33].

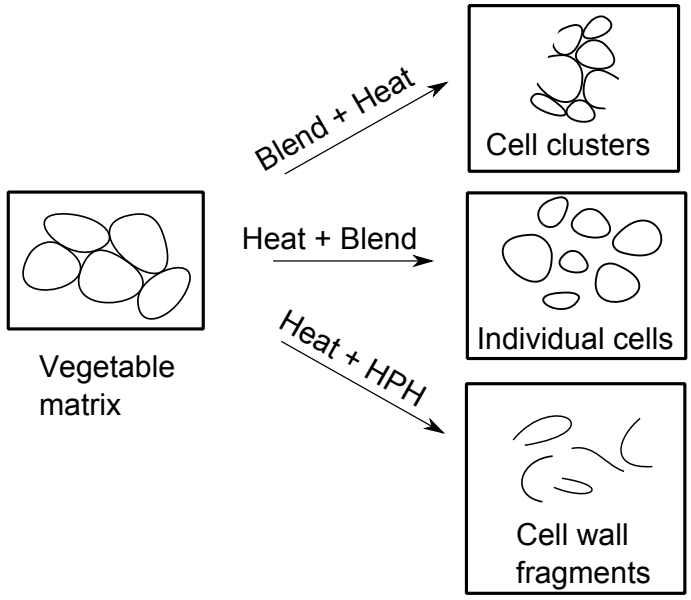

Figure 1.4.1: Schematic diagram on the types of microstructure in cell wall suspensions.

The effect of particle hardness on the rheology of cell wall based suspensions is quite sparse in literature. Lopez-Sanchez *et* al. [2011] proposed a model for the storage modulus of concentrated cell suspensions based on the elastic properties of particles. The model was based on a non-affine network of folded elastic sheets as observed from microscopic images, shown in figure 1.4.2. Under an applied shear stress, the stretching of sheets results in a storage modulus directly proportional to the Young's modulus of the sheets at constant volume fraction. The theory seemed to correlate well with the experiments for tomato and carrot suspensions of different particle shapes [64]. These results show the importance of particle elasticity on the rheology of these systems. Den Ouden and Van Vliet [1997] also concluded that tomato cells were highly compressible as the average size after sieving is much larger then the sieve size itself. Maximum viscosity and yield stress were obtained for particle sizes of 90-180 μm. Similar results

were also obtained by Yoo and Rao [1994]. It is quite clear that the role of particles on the rheology of vegetable based cell wall suspensions arise from two distinct factors, namely the volume fraction and particle-particle interactions. So far, a hypothesis connecting the particle hardness and rheology is yet to be established.

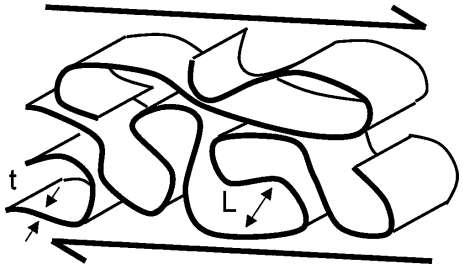

Figure 1.4.2: Schematic representation of folding sheet behavior of cell walls. t is the sheet thickness and L the separation between contact points. Picture is taken from [64].

1.4.2 Serum phase

The serum phase can directly alter the physical properties of the suspension or it can control particle-serum interactions. In vegetable cell suspensions the serum properties are dependent on the amount of dissolved compounds i.e sugars, proteins and pectins as a result of thermal and mechanical processing [127]. Intense heat treatment and high pressure homogenization of tomato suspensions resulted in a higher pectin solubilization into the serum phase. However, this higher concentration of solubilized cell wall components does not affect the consistency and rheology of carrot and tomato cell suspensions [82]. The serum viscosity is affected by the amount of pectin dissolved, a higher concentration can increase the viscosity of the serum phase [127]. On the other hand, pectin depolymerization by either heat or enzymes can cause a decrease in the serum viscosity [86]. After hot break processing of tomato paste, the pectin molecules

were found to be more compact, resulting in a lower serum phase viscosity [38]. This had an impact on the consistency and yield stress of tomato ketchup, which was dependent on the amount of pectin solubilization and pulp content [104].

Interactions can also occur between the serum and particle phase. Insoluble pectins present on the particle surface can cause an electric charge around the particle, causing an electroviscous effect [145]. For example, tomato suspensions are comprised of a network of pectin polysaccharides, which suspend the particles and other components [105]. This network contributes significantly to the physical properties of tomato suspensions as pectins are the main agents of physical interactions [120]. The addition of electrolytes, such as NaCl or $CaCl_2$, can alter these electrostatic interactions by changing the debye length around the particles, thus reducing the effective volume fraction of the particles and thereby reducing the viscosity [82, 106]. The extent to which the electroviscous effect affects rheological properties is dependent on the type of system. Tomato suspensions are more sensitive to addition of salts compared to apple systems [106].

Pectin is a versatile polysaccharide, which is capable of interacting with other biopolymers such as cellulose and proteins. Particle-serum interactions can also originate from pectin-protein interactions in addition to pectin-pectin. Takada and Nelson observed the occurence of pectin-protein interactions by measuring the viscosity of tomato juice at different pH [126]. It was seen that both the viscosity of the serum phase as well as the suspension showed a local maximum at a pH of 4.4, very close to the natural pH of tomatoes. This was mainly attributed to pectin-protein interactions present in tomato suspensions as empirically shown with model systems. Tinzani and Vodovotz [135] investigated the addition of soy protein isolate to tomato juice. Interaction of proteins with pectins resulted in an increased viscosity of the tomato juice.

The system with soy protein also exhibited typical behavior of a physical gel stabilized by long range electrostatic forces. It is quite clear that the rheology of cell wall suspensions depend on a large number of disparate variables.

1.5 Conclusions and outlook

So far, the essential concepts needed to understand the structure-function relationship between cell wall polymers has been covered. It is clear that microstructural characteristics of plant food suspensions are based on processing parameters and the type of matrix. The resulting microstructure (figure 1.5.1) influences the functional physical properties such as rheology and texture. These suspensions are essentially comprised of two components, serum and particle phase. Particle phase is made up of insoluble cell wall material and directly contributes to the volume fraction of the suspensions. Factors like particle concentration, particle size distribution, particle morphology, surface charge and particle elasticity directly affect the physical properties. In addition, serum phase components such as solubilized pectins, salts, sugars and proteins, have an impact on the rheological properties by affecting the interactions between particles. There has been considerable research in the past to understand the effect of processing on the microstructure and physical functionality of cell suspensions. However, there is a lack of knowledge in understanding the role of polysaccharides on the physical properties. Therefore, this thesis aimed to investigate the role of polysaccharides on particle size, particle-particle interactions and particle hardness, which in turn affect the bulk rheological properties. This is facilitated by using innovative processing methods such as enzymes, homogenization and ion exchange resins. These processing methods result in new microstructures with novel physical functionalities. Moreover, a fundamental material science approach is followed to characterize these

microstructures, which helps in establishing a hypothesis for the micro-structure to physical functions for specific polysaccharides.

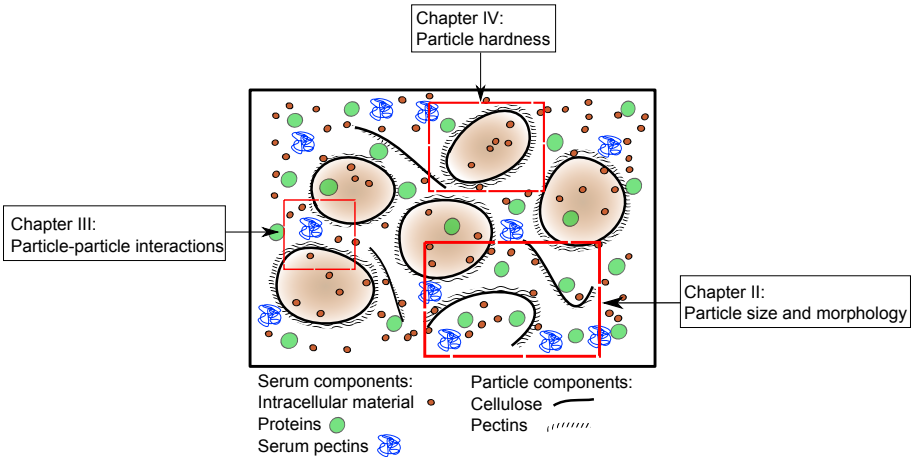

Figure 1.5.1: Schematic diagram of a cell wall suspension with the individual components.

It is known that the physical properties of these suspensions depend on the microstructural characteristics. The three main characteristics are particle size, particle-particle or particle-serum interactions or particle hardness. The effect of these three properties on the rheological properties are investigated in the subsequent chapters (figure 1.5.1). The second chapter presents the importance of particle size and morphology effects on the physical properties of carrot suspensions. The third chapter discusses the importance of particle-serum interactions in tomato suspensions. The fourth chapter discusses the effect of particle hardness on the rheology of carrot suspensions. These three chapters cover different aspects on how physical properties of cell suspensions can be controlled. Furthermore, in each chapter a polysaccharide's function towards each physical property is presented. Finally the conclusions chapter highlights the contribution of this thesis in the field.

Chapter 2

Effect of enzymes on particle size and morphology of carrot cell wall fragments[1]

2.1 Introduction

Primary cell walls of plants are mainly made up of various carbohydrate polymers. These cell wall polysaccharides form a complex structure through various interactions giving the plant its needed mechanical properties. In recent years, the understanding of structure-property relationships in plant cell walls has become of research interest to both academics and industry. Applications are found in food, bio-fuels and bio-plastics. It is important to understand the

[1] A.K. Sankaran, J. Nijsse, L. Bialek, M.E. Hendrickx, and A.M. Van Loey, Effect of Enzyme Homogenization on the Physical Properties of Carrot Cell Wall Suspensions, Food and bioprocess technology 8, 1377 (2015)

microstructure of these systems to engineer their properties for a wide range of uses.

In addition to conventional thermal and mechanical treatments, enzyme treatments can be applied to modify biopolymers. In a review paper, Bhat [16] elucidated the use of enzymes for applications in industrial processes. In the food industry, enzymes are used to clarify juices, produce nectars and purees, extract olive oil, to name a few. One of the earliest works on carrots was by Sreenath et al. [119], where carrots were mechanical sheared, subsequently cooked and incubated with enzymes. Enzymes used were Cellulase from *Trichoderma reesei* and Rohament P from *Aspergillus alleacecs*. Both enzymes had a high activity of cellulases but pectinase activity was found only in Rohament P. The resulting micro structure was different for each of the individual enzymes compared to the combined enzymatic hydrolysis. Rohament P caused damaged tissues, disintegrated cells and cell debris, whereas Cellulase showed disintegrated cell walls. Sreenath et al. [119] concluded that a mixture of both enzymes was crucial in obtaining a higher liquefaction of cell wall polysaccharides. To better understand the biochemical composition, Massiot and coworkers [73, 74] extracted carrot fibers from alcohol insoluble residues and characterized the residual sugars. Carrot pectins were found to be mainly branched with neutral sugars of galactose and arabinose polysaccharides. Hemicelluloses were mainly comprised of xylans, xyloglucans and glucomannans being strongly bound with cellulose and proteins [73]. Using fibers from the alcohol insoluble residues, the effect of exogenous enzymes was investigated in a later study [75]. A combination of SP249 from *Aspergillus aculeatus* which had a strong pectinase activity, and Cellucast from *Trichoderma reesei* with a strong cellulase activity, was used. Complete liquefaction was not possible due to the formation of a network of lignin, proteins and phenolic acids, although 95% of the cell wall polysaccharides were solubilized [75]. Anastasakis et al. [3] studied the effect

of cellulase, pectinase and hemicellulase on the yield of carrot juice. Upon the addition of pectinase to raw carrots, there was a decrease in birefringence as a function of time within the cell walls, indicating the role of pectins as the "glue" that holds ordered cellulosic fibrilar structures together. In a later work, Kotcharian et al. [58] looked at the functional properties of carrots with macerating and liquefying enzymes. Enzymatic treatments on re-hydrated samples resulted in decreased juice yields, reduced galacturonan content and greater solid densities. The functional properties were also dependent on the type of carrots and the extent of cell wall degradation due to the microstructural changes caused by enzymatic degradation. Pickardt et al. [97] followed up the work of Kotcharian, investigating the effect of a homogenization step in addition to the action of enzymes. The rheology seemed to vary as a function of chemical composition (content of pectins) and structure/physical state (microstructure). For novel functional foods the understanding of these bio-polymer interactions is critical. Stoll et al. [122] formulated a process using enzymatic hydrolysis to enhance the α- and β- carotene bio-accessibility in carrot juice. Upon enzymatic hydrolysis and subsequent homogenization (180 bar) the viscosity of juice increased. However, the reason for this increase was not addressed. Anyhow the process was performed on a pilot scale and would be a viable means of naturally increasing nutritional content of juice, instead of adding supplementary carotenoids. As reviewed above, the effect of enzymes on the physical functionalities of cell wall suspensions has been investigated previously with heterogenous enzymes, yet there is a need for a more fundamental approach with pure enzymes [75].

In the current work, the effect of different enzymes on bulk rheology and microstructure of carrot suspensions was investigated. Mixes of pure enzymes and enzyme cocktails were used to selectively hydrolyze biopolymers of carrot cell suspensions. An additional homogenization step was performed after

enzyme incubation to physicaly break down the microstructure further. Enzyme hydrolysis resulted in a weaker cell wall by hydrolyzing the polysaccharide links that hold it together. Homogenizing of an enzyme treated cell wall caused it to fracture along the weak points created by the enzyme hydrolysis, thus resulting in new microstructures and physical properties of the suspensions depending on the type of enzyme used. These properties were measured by rheology, particle size distribution and by high resolution microscopic imaging. Carrots were used in this particular study because it is known that carrot cell wall is quite resistant to thermal and mechanical treatments. The results presented in the work is applicable to a broader range of systems. Different systems should show similar trends with enzyme treatment as most vegetables and fruits are made up of similar cell wall architecture.

2.2 Materials and Methods

2.2.1 Sample preparation

Frozen carrots used in this study were procured from Ploegmakers Food Ingredients BV (Breda Netherlands). The carrot cubes of edge 1 cm were blanched at 80 °C for 2 minutes by the supplier to inactivate endogenous enzyme activity. The cubes were stored and transported at -20 °C. Before experiments, the cubes were thawed overnight at room temperature. Thawed carrot cubes and an equal weight of water were cooked at 90 °C for 45 minutes. Evaporated water was replenished after cooling the carrots to room temperature in an ice bath. The mixture was then blended using a lab scale Waring Variable Speed Lab Blender LB20EG 0.40 HP (Waring commercial, Stamford USA) at maximum speed for 5 minutes to obtain a puree. A Panda plus homogenizer (Niro Savi, Parma Italy) was used to homogenize the sample at 800 bars and

the pH was adjusted to 4.5 with 1 M acetic acid. Optimal enzyme activity was obtained at a pH of 4.5, as stated by the suppliers. Henceforth this sample is referred as the reference sample and is the starting material for further experiments with enzymes.

2.2.2 Enzymes

In this study mixes of pure enzymes were used to degrade the major polysaccharides present. The mixes are divided by enzyme class and are named based on the type of substrate they hydrolyse, e.g. cellulase, pectinase and hemicellulase. All these enzymes were bought from Megazyme International. Mixtures of pure enzymes were also applied, to understand how they compare with the pure enzymes applied separately. In addition, a heterogenous cellulase enzyme cocktail (Cellulase from *Aspergillus Niger*, Sigma Aldrich) was used. Table 2.2.1 gives an overview of the enzymes and their concentrations used in this study. Enzyme concentrations were optimized between activity and cost of the enzymes.

Table 2.2.1: Summary of enzymes used in this work. Activity of enzymes as provided by Megazyme International.

Enzyme Class	Constituent Enzymes	EC Number	Concentration (v/w %)	Activity (U/ml)
Cellulase	endo-1,4-β-Cellulase	3.2.1.15	0.1	820
	β-Glucosidase	3.1.1.11	0.05	40
	Cellobiohydrolase	3.2.1.8	0.05	0.5
Pectinase	endo-Polygalactaronase	3.2.1.151	0.1	1800
	Pectinmethyl esterase	3.2.1.4	0.01	10
Hemicellulase	endo-1,4-β-Xylanase	3.2.1.21	0.1	2300
	Xylogloglucanase	3.2.1.91	0.1	1000
Other glycosidases	endo-Arabinanase	3.2.1.99	0.1	200
	β-Galactosidase	3.2.1.23	0.1	3200
Cellulase (A.Niger)	Heterogeneous cocktail	N/A	1	1

The carrot puree with addition of enzymes was incubated in a water bath at 45 °C. This was the condition for maximum activity of the enzymes as specified by the supplier. At different time intervals, aliquots were taken and placed in a water bath at 90 °C for 10 minutes to irreversibly inactivate the enzyme. The deactivation procedure was as per the suppliers instructions. Additionaly, certain enzyme treated aliquots were subjected to a second homogenizing step at 1000 bars.

2.2.3 Confocal laser scanning microscopy

Confocal laser scanning microscopy (CLSM) was used to visualize the microstructural changes of cell wall fragments. The images were taken using a Leica TCS SP5 with a DMI6000 inverted microscope (Leica GmbH, Wetzlar

Germany). Congo Red was used to visualize fiber dispersions because of its strong affinity with cellulose. The dye was added by gently stirring 1 droplet of Congo Red (0.5% v/w) to 1 ml of sample. A 561 nm laser was used for excitation of the congo red dye. The emitted fluorescence signal was detected by a CCD sensor between 565 nm to 680 nm into grey scale. A 40x objective (NA=1.25; zoom 1) was used to capture images of 1024 x 1024 pixels each. Multiple pictures were stitched together to give a bigger picture of approximately 1 mm^2. For best visualization the images were inverted and color balanced.

2.2.4 Cryo-Scanning electron microscopy

Samples were analyzed using Cryo-Scanning Electron Microscopy (cryo-SEM) to visualize the cellulose structures at a higher resolution, giving information about fibrilar architecture which is not seen with the confocal microscope. For cryo-SEM a tiny volume of each sample (one droplet) was placed on top of a rivet and plunge-frozen in melting ethane. The sample was cryo-planed using a cryo-ultramicrotome (Leica Ultracut UCT EM FCS, Leica GmbH, Wetzlar Germany), to obtain a freshly prepared cross-section. Cryo-planing was done first with section thickness of 100 nm and a speed of 60 mm/sec using a glass knife. The last sections were made at decreasing thickness, down to 20 nm, with a speed of 2 mm/sec using a diamond knife (Diatome histo cryo 8 mm from DiATOME, Pennsylvania USA) at -110 °C. The rivet was mounted onto a holder and transferred into a Gatan Alto2500 (Gatan Inc, Pennsylvania USA) cryo-preparation chamber. To reveal the microstructures under the planed surface, the temperature of the sample was increased for a short while to -90 °C in vacuum, to remove a thin layer of water by sublimation. This yielded a semi-3D view on the planed sample. The sample was sputter coated with platinum (120 sec) for better SEM contrast and to prevent charging by the

electron beam. The sample was imaged using a Zeiss Auriga field-emission SEM (Zeiss, Oberkochen Germany) at -125 °C and an accelerating voltage of 3 kV.

The images shown are representative of the microstructure observed from a set of 20-30 images. Also, schematic interpretations were drawn to depict the observed microstructures.

2.2.5 Particle size distribution

Particle size distribution was measured by conventional laser light diffraction with a Malvern Mastersizer 2000 (Malvern Instruments Ltd, UK). After calibrating the sensors and lasers, a small volume of the sample was loaded into a Hydro 2000S (Malvern Instruments Ltd, UK). To disperse the suspension, an ultrasonication step was applied first for 10 seconds followed by a stirring step at a speed of 3000 RPM for 30 seconds. This suspension was pumped into the diffraction chamber for measuring the particle size distribution of the bulk solution. Samples were measured at least 3 times, average values of De Broucker mean diameter (D[4,3]) were reported.

2.2.6 Rheology

A stress controlled rheometer (TA-instruments AR-2000ex, Delaware USA) with parallel plate geometry of 40 mm diameter was used for all measurements. Wall slip occurs commonly in two-phase systems due to steric, hydrodynamic, viscoelastic and chemical constraints acting near the boundaries [6]. This wall slip is apparent for concentrated suspensions using a smooth geometry. To avoid this, the plates were stuck with a 3M 800 grit sand paper. The effects of slip were found to be negligble, after checking the occurence of slip as outlined by Yoshimura and Prud'homme [150]. The gap between the plates was 1500

μm, being an order of magnitude larger than the mean particle size but small enough to avoid flow effects arising from large gaps. The sample was subjected to a pre-shearing step at a shear rate of 5 1/s for 30 seconds, and allowed to equilibrate for 7 minutes prior to measuring. The storage modulus within the linear viscoelastic region was measured by performing strain sweeps from 0.01-100% strain at a frequency of 10 rad/sec. Each point in the strain sweep was averaged over 6 cycles of oscillations to ensure good quality of data. The reported linear storage modulus was obtained from the plateau of the linear viscoelastic domain. The measurements were repeated three times within each experimental batch and averaged over 2 batches.

2.3 Results and Discussion

Figure 2.3.1 is a representative of a strain sweep rheological experiment on the control carrot puree. The linear modulus reported hence forth is the plateau value at a strains below 0.1

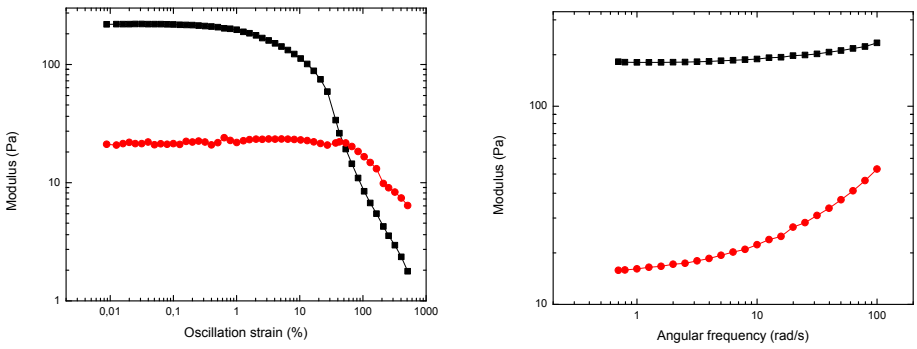

Figure 2.3.1: Representative rheological graphs of the strain (left) and frequency (right) profiles of carrot suspensions. Squares indicate storage modulus (Pa) and circles indicate loss modulus (Pa).

Rheology of the enzyme incubated samples was measured for different enzymes

over an 8 hour period. Figure (2.3.2) summarizes the results for the pure enzyme classes.

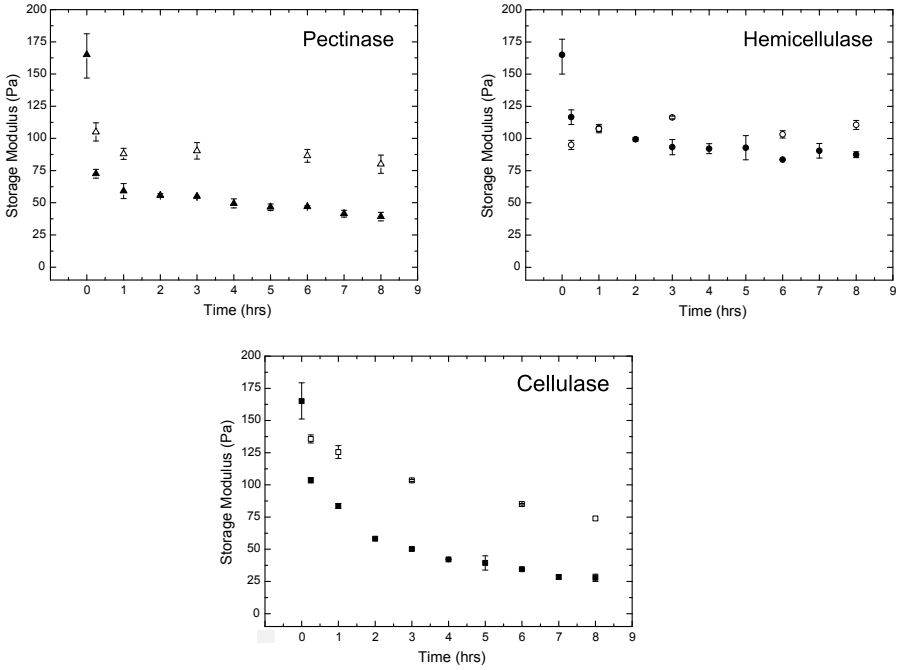

Figure 2.3.2: Graphs of linear storage modulus for carrot suspensions as a function of enzyme incubation time and post-homogenization. Filled symbols are used for enzyme incubated samples and open symbols are used for post homogenized samples. Pectinase is denoted by triangles, Hemicellulase by circles and Cellulase by squares.

2.3.1 Pectinase

This enzyme class consisted of an endo-polygalacturonase and pectin methylesterase (PME) which hydrolyses the galacturonic acid and de-esterifies the pectin backbone respectively. The pectinase incubated material has the largest drop in storage modulus in the first 2 hours compared to other mixes of pure enzymes. It is also interesting to note that there is approximately a 40% decrease in the

storage modulus within the first 15 minutes of enzyme incubation. It is probable that the quick drop in the storage modulus is due to a reduced particle-serum interaction and smaller mean particle size. Particle-serum interactions might be affected readily due to the hydrolysis of pectins on the exterior of the cell walls and in the serum phase. Confocal images in figure (2.3.4) highlight the changes in the microstructure. Individual cell wall fragments are well dispersed and less aggregated in the pectinase treated sample compared to the untreated sample. Cell wall fragments which are less aggregated result in a smaller mean particle size, which is observed from light scattering measurements, as seen in figure (2.3.3). The pectinase enzyme leads to disintegration of the aggregates into smaller fragments because pectins have an unequivocal role in cell-cell adhesion [3, 23, 99]. Samples imaged with an cryo-SEM show a more loosely packed fibrilar network within the cell wall fragments (figure 2.3.5a). This indicates that the pectins function like a ”zip tie”: when the galacturonic acid chains are hydrolyzed, then the cellulose fibers are no longer constrained by the pectin network. The current study shows that both the exterior (particle-serum interactions) and interior (loosely packed fiber networks) of cell walls were affected by the pectinase treatment. Further research is needed to investigate the extent of pectin hydrolysis quantitatively.

After homogenizing the pectinase incubated samples, there was an increase in the storage modulus throughout the period of enzyme incubation. This increase in storage modulus can be attributed to the increase in particle size and the volume fraction of particles (figure 2.3.3). Increase in the particle size can be directly visualized in the confocal images, which show the changes in particle morphology. The dispersed cell wall fragments have transformed into “wooly” like structures without sharp edges (figure 2.3.4). Cryo-SEM of the sample after homogenizing shows a multitude of smaller fibrilar bundles, which are different to the characteristic fibrilar network of the cell wall before homogenization.

It is also interesting to see that these fiber bundles are shorter as compared to the bundles resulting from other enzyme classes as seen in figure (2.3.5). Following the rationale that homogenization after enzyme treatment would break the structure at its weakest points, gives a qualitative indication of the spatial interactions between pectins and cellulose. The formation of smaller fiber bundles suggests that pectins play a crucial role in holding the cell wall together in both the radial and axial directions of cellulose fibers.

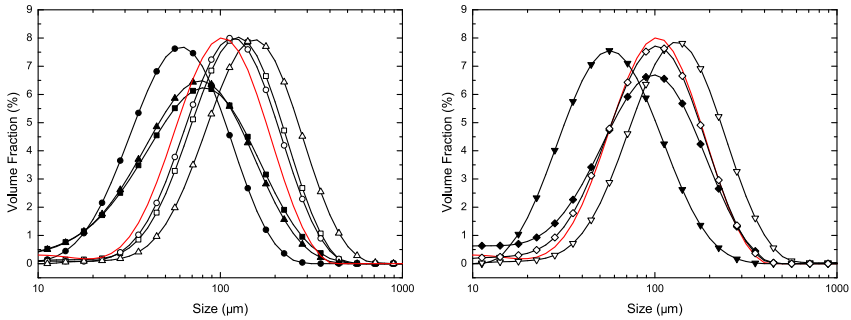

Figure 2.3.3: Particle size distributions of enzyme treated carrot puree samples for 8 hours before (closed symbols) and after homogenization (open symbols). Left graph is for the samples treated with mixture of pure enzymes, Hemicellulase(■), Cellulase(●) and Pectinase(▲). The right graph shows heterogeneous enzyme mixtures, Pure enzyme cocktail (▼) and Cellulase from A.Niger(◆). The solid line in both graphs is for the reference samples.

2.3.2 Hemicellulase

The used hemicellulase consisted of pure endo-xylanase and xyloglucanase that target the hydrolysis of xylans and xyloglucans, the two main hemicelluloses present in carrots [73]. Hemicellulase treated material caused the least decrease in bulk rheology as compared with the other mixed pure enzymes (figure 2.3.2). Microstructure observed from confocal microscopy after 8 hours of enzyme incubation resulted in cell wall fragments that were similar to the pectinase

treated sample (figure 2.3.4). The resulting particle size distribution was comparable to the pectinase treated material after 8 hours of enzyme incubation (figure 2.3.3). Even though the hemicellulase and pectinase treated samples have similar particle size distributions, the storage moduli show different trends. This indicates the importance of particle-serum interactions on bulk rheological properties. Cryo-SEM of the 8 hour incubated material shows a mildly loosened cellulose fibrilar network within the cell wall fragments. The cellulose fibrils appear to be more tightly packed compared to the pectinase treated sample, but looser compared to the control sample (figure 2.3.5). The marginal contribution of hemicelluloses to the bulk rheology could be explained by the fact that they are mainly present in the interior parts of the cell wall [31, 112, 144]. It is suggested that their breakdown would not largely affect particle-serum interactions or particle properties, hence having no significant impact on the rheological properties. Further research has to concentrate on measuring residual sugars to quantify the extent of enzyme catalyzed hemicellulose hydrolysis.

Upon homogenization of the hemicellulase incubated sample, the storage modulus decreased after 15 minutes of enzyme incubation. With prolonged enzyme incubation the storage modulus increased after homogenizing. Confocal images show that upon homogenizing the cell wall fragments transformed into a “wooly” like particle morphology (figure 2.3.4), very similar to the other classes of pure enzymes. Fiber bundles (or sheets) visualized in cryo-SEM are longer compared to the pectinase treated homogenized sample (figure 2.3.5b). Apparently, the cell wall fragments break in the axial direction of cellulose fibers which results in the formation of long fiber bundles. This is in agreement with earlier reports that xyloglucans are oriented in the parallel direction to the cellulose microfibrils within the cell wall [30, 76].

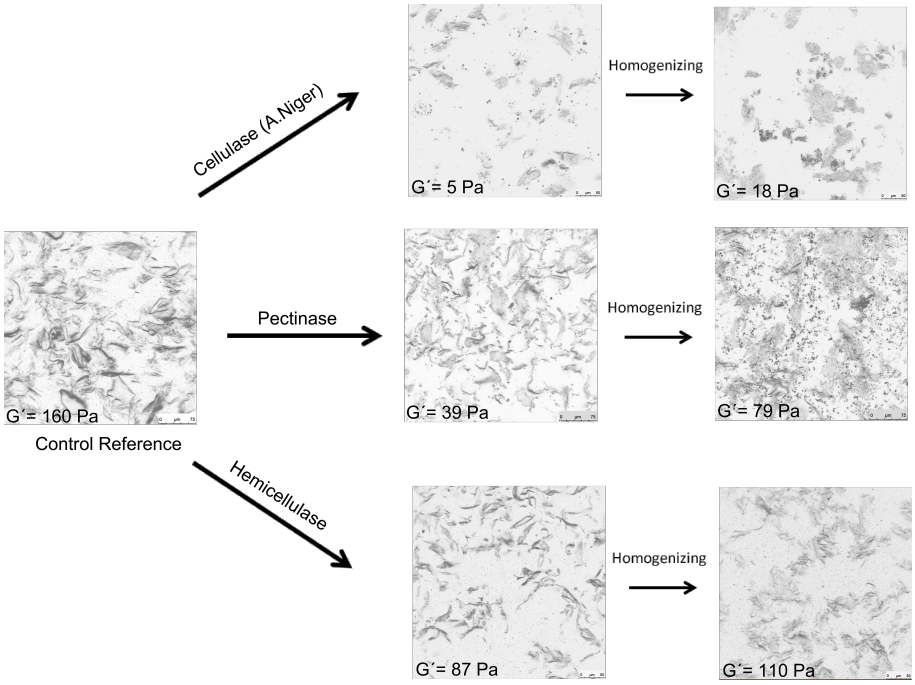

Figure 2.3.4: Confocal laser scanning microscopy images of microstructure progression of carrot puree treated with selected enzymes. The 8 hours enzyme treated samples are shown with their corresponding average linear storage modulus in the bottom left of every image. Homogenization was performed at 1000 bars.

2.3.3 Cellulase

The used cellulase consisted of three enzymes that are needed to completely hydrolyze cellulose to glucose: endo-cellulase which randomly cleaves the backbone, beta-glucosidase to cleave from the non-reducing end and cellobiohydrolase to convert cellobiose to glucose. The storage modulus of cellulase incubated material showed a gradual decrease (figure 2.3.2). After 8 hours of enzyme incubation there was no change in the volume fraction, but the particle size reduced (figure 2.3.3). A similar decrease in particle size was observed in Avicel cellulose with the addition of cellulase by Walker et al. [142]. The cellulase

treated cell fragments were smaller and less aggregated as compared to the other reference material (CSLM data not shown), like the other pectinase and hemicellulase treatments. When investigated with cryo-SEM the cell wall fragments appeared very similar to the untreated sample, with tightly packed cellulose microfibrils within the cell wall, as seen in figure 2.3.5. The observation that the cellulase treatment for 8 hours caused a decrease in rheology and smaller particles, but without a discernible change in the microfibril architecture of the cell wall, suggests that cellulase has been active on the exterior part of the cellulose matrix. Earlier, it has been proposed that cellulase activity is restricted by the pore size of the matrix, which is in the order of 5-10 nm. Hence, only exposing the external surface of the fibers for effective hydrolysis [42].

Homogenizing the cellulase treated samples resulted in an increase in the storage modulus throughout the period of incubation. The increase in storage modulus upon homogenization, is likely due to the increase in particle size (figure 2.3.3). The micro-structure of the particles after homogenization as visualized with a CLSM is comparable to the pectinase or hemicellulase treated samples. Visualizing the fibers using cryo-SEM shows cell wall fragments similar to the reference sample and fiber bundles occur sporadically. Within the cell wall fragments there is a network of closely packed cellulose fibrils similar to the reference sample (figure 2.3.5c).

2.3.4 Other glycosidases

Endo-arabinase and beta-galactosidase were used to hydrolyze arabinose and galactose, respectively. The storage modulus decrease for the material incubated with these glycosidases was small over an 8 hour period. The decrease after 8 hours of enzyme incubation was about 20 Pa, a 10% decrease only. Upon

homogenizing, the storage modulus did not change during the entire period of enzyme incubation. This suggests that galactose and arabinose side chains play a negligible role in contributing to the bulk rheology of these cell wall suspensions. Still, they might be important once the micro-structure is first “opened up” by using other enzymes like pectinase, which is not further addressed in this study.

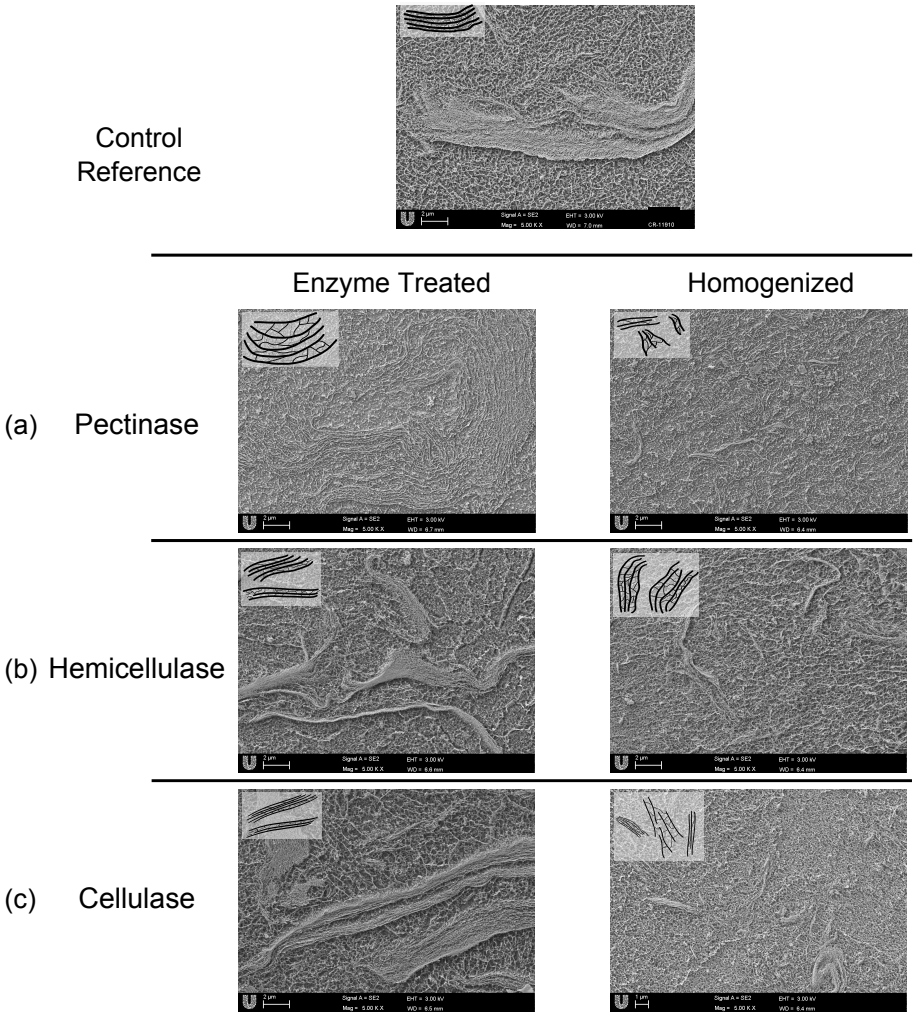

Figure 2.3.5: Cryo-SEM images of mixes of pure enzyme treated carrot samples for 8 hours (left) and homogenized samples (right). The picture insets are a schematic representation of the microstructures observed. Homogenization was done at 1000 bars.

2.3.5 Heterogeneous enzymes

Similar rheological experiments were performed with two enzyme cocktails (figure 2.3.6): Cellulase from *Aspergillus niger* and an enzyme cocktail consisting of all the pure enzymes classes used earlier (table 2.2.1) in this study.

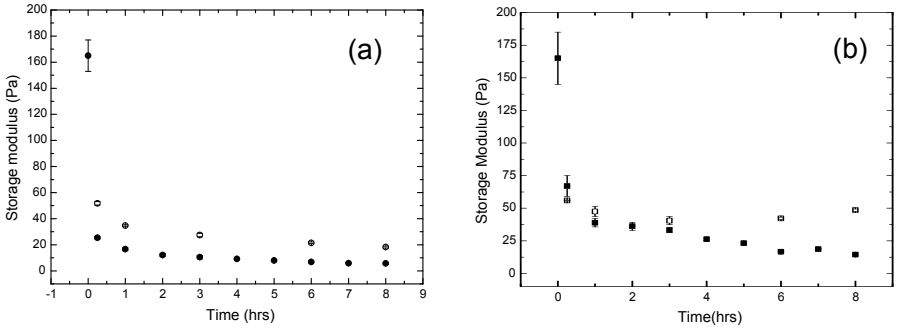

Figure 2.3.6: Graphs comparing the effect of enzyme cocktail on storage modulus as a function of incubation time and homogenizing. Filled symbols are used for enzyme incubated samples and open symbols are used for post homogenized (1000 bars) samples. (a) Cellulase from *Aspergillus niger* by circles (●). (b) Cocktail of pure enzyme mixes is denoted by squares (■).

The enzyme Cellulase from *Aspergillus Niger* was the most effective enzyme tested: it had the largest decrease in storage modulus compared to any other enzyme investigated here (figure 2.3.6a). From the CLSM images, the cell wall fragments appear to have disintegrated cell wall material and severely damaged fragments (figure 2.3.4). At a higher resolution, cell wall structure of the enzyme incubated sample shows loosening of the cell wall (figure 2.3.7a), considerably more than with the pectinase enzyme treatment. Upon homogenizing, there was an increase in the storage modulus over the entire period of enzyme incubation (figure 2.3.6a). Particle sizes increased upon homogenizing throughout the enzyme incubation period which probably caused the higher storage modulus (figure 2.3.3). The microstructure shows complete defibrilation of the cellulose fibers, forming into a loose network of cellulose

microfibrils known as microfibrilated cellulose. This type of microstructure was observed only in this homogenized sample treated with the enzyme Cellulase from *Aspergillus Niger*.

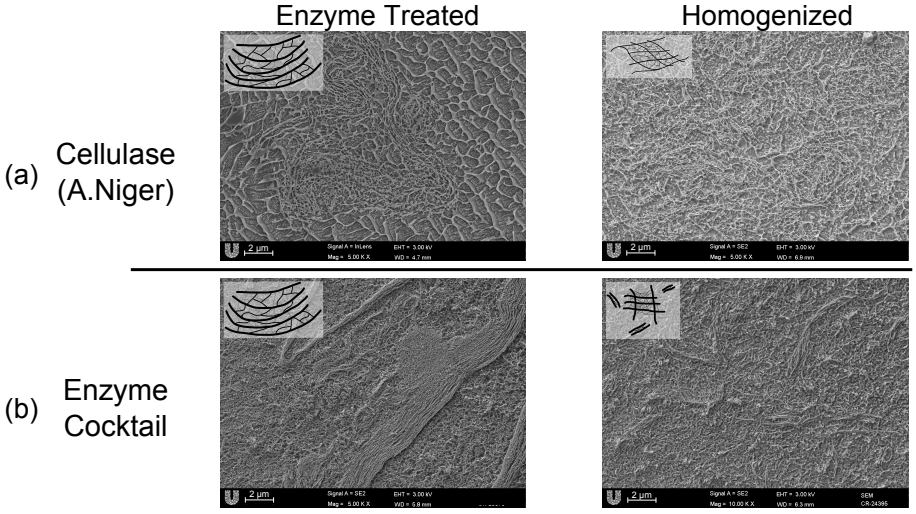

Figure 2.3.7: Cryo-SEM images of the carrot purees treated with heterogeneous enzymes for 8 hours (left) and homogenized samples (right). The picture insets are a schematic representation of the microstructures observed. Homogenization was done at 1000 bars.

The enzyme cocktail made by mixing the earlier applied pure enzymes classes was used to evaluate the synergistic effect of all the pure enzyme classes on the substrate. The decrease in rheology was much faster compared to any of the individual classes of enzymes. Cryo-SEM images show that after 8 hours of incubation with the pure enzyme cocktail, the cellulose network had loosened (figure 2.3.7b). Upon homogenizing, the samples showed an increase in the storage modulus after 3 hours of incubation (figure 2.3.6). Particle size distribution is comparable to the Cellulase from *Aspergillus Niger* and again the increase in mean particle size is likely to cause the increase in storage modulus. After homogenizing the 8 hour incubated material, there are short fiber bundles and defibrilated cellulose networks. Complete disruption of the cellulose network

like the sample treated with the Cellulase from *Aspergillus Niger* did not occur here. Enzyme cocktails are more effective in hydrolysis then any of the pure enzymes used, suggesting that the studied enzymes are synergistic in hydrolysis.

2.3.6 Nature of microstructural changes

In the current study, the carrot cell walls ruptured differently during homogenization, depending on the enzyme pre-treatments. This is schematically depicted in figure 2.3.8. Within an untreated cell wall, the cellulose matrix is held strongly together by the polysaccharide crosslinks and because of that, homogenization will fragment the cell wall into smaller pieces. Alternatively, by enzymatic pre-treatment the polysaccharide crosslinks are partially removed, thereby creating localized defects across the cell wall. When this enzyme treated cell wall is subjected to large stresses in a homogenizer, it causes the cell wall to rupture along these defects and swell. This results in larger particles and new microstructures with novel physical properties.

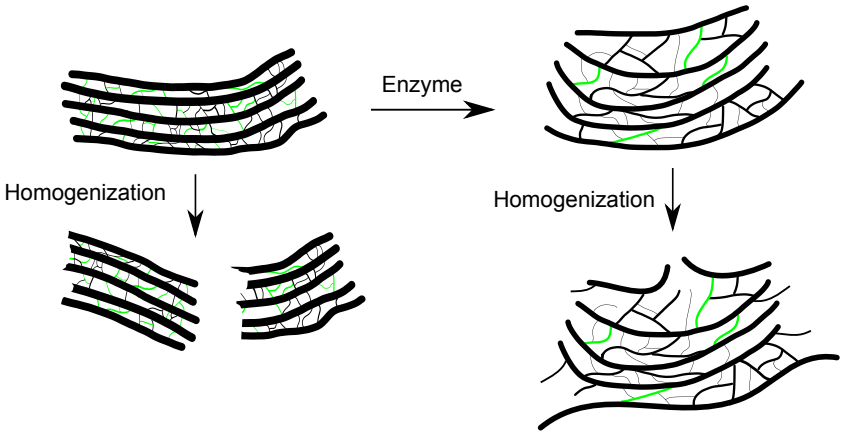

Figure 2.3.8: Two dimensional schematic highlighting the mechanism of cell wall fracture within a homogenizer. Left side schematic is an untreated cell wall and right side is for an enzyme treated cell wall. Green lines within the schematic indicate the polysaccharide crosslinks within the cell wall.

2.4 Conclusions

In this study, the structure-property relationship of bio-polymers in carrot cell wall suspensions was investigated. Rheology, microscopy and light scattering was used to characterize enzyme treated and subsequently homogenized samples. Linear storage moduli was measured over an 8 hour period of enzyme incubation, which showed a decrease for all enzymes that were investigated. Pectinase had the largest drop in storage modulus in the first two hours followed by hemicellulase and cellulase. After enzyme treatment there was considerable loosening within the cell wall fragments as visualized with cryo-SEM. Regarding the pure enzyme classes, pectinase treatment caused the largest loosening of the cell wall fibers followed by hemicellulase. It is concluded that the cellulose network swells if the bio-polymers that hold them together are hydrolyzed. Enzyme cocktails resulted in a lower storage modulus than the pure enzyme classes showing a synergistic effect in hydrolyzing the bio-polymers. Furthermore, homogenization of the samples after enzyme treatment largely resulted in an increased storage modulus. This increase in storage modulus was correlated to larger particle sizes. Particle size and particle-serum interactions were found to be important factors contributing to the bulk rheology of these suspensions. Various microstructures were formed with different enzymes and subsequent homogenization, respectively. Homogenization after enzyme treatment resulted in fiber bundles for the pure enzyme classes treated samples and microfibrilated networks treated with enzyme cocktails. It was observed that pectinases caused the formation of very small fiber bundles, suggesting that pectins hold the cell wall together in both the radial and axial directions. Hemicellulase formed more extended bundles, indicating that they tether to cellulose predominantly in the axial direction. Only the enzyme Cellulase from *Aspergillus Niger* showed complete microfibrilated cellulose upon homogenizing, which to our knowledge

is the first report of microfibrilated cellulose from carrot cell walls. Future research should also be focused towards investigating the effect of proteins on the cell wall architecture and measuring the residual sugars to quantify the extent of enzyme hydrolysis.

Chapter 3

Enhanced electrostatic interactions in tomato suspensions[1]

3.1 Introduction

Processed tomato products in the form of purees and sauces are a primary source of tomatoes in the modern diet. Tomato as a fruit primarily consists of cellulose, pectins, hemicelluloses, proteins and sugars. Functional role of these polysaccharides in cell wall suspensions arise inherently from their roles in the plant itself. Considerable research has been conducted in the past to elucidate the reason for natural consistency and structure of tomato products. Complex interactions among these building blocks are responsible for the structuring of

[1] A.K. Sankaran, J. Nijsse, L. Bialek, A. Shpigelman, M.E. Hendrickx, and A.M. Van Loey, Enhanced electrostatic interactions in tomato suspensions, Food Hydrocolloids 43, 442 (2015).

tomato products [7, 12, 127, 128]. During the various stages of processing many changes occur in these building blocks which in turn affect the characteristics of the end product [4, 65, 66, 110]. A better understanding of these natural interactions enables the food industry to create products with desired rheological properties.

Cellulose is the primary component in vegetable cell wall suspensions and also the primary contributor to the rheology by forming the backbone of the particles. Pectins are a diverse class of polysaccharides that are chemically heterogeneous and they are grafted naturally onto the cellulose backbone and are also found in the serum phase. They are known to contribute significantly to the structure depending on the processing conditions and extrinsic factors such as pH, ionic conditions etc.. [12, 126]. Pectins play a vital role in the quality of processed foods. Many processes may alter the structure of pectins which in turn change the tangible properties of foods. The unique characteristics of pectins allow for an interesting interplay with other components through hydrogen bonding, hydrophobic interactions, ionic and maybe even covalent coupling [117]. Pectin-pectin interactions have been studied quite well, the most exploited use of these interactions are in making gels. The main mechanism of gelling has been been discussed in section 1.4.2.

Polysaccharides are also known to interact with proteins to form complexes. These interactions play a role in the texture, rheology and micro-structure of many food systems [35, 39, 139]. Depending on various factors, there could be three possible scenarios for protein-polysaccharide interactions in mixtures. The interactions could result in the formation of two distinct phases, behaving like two immiscible liquids due to the incompatibility of the polymers. Alternatively the interaction may result in an homogeneous stable solution of macromolecules (no interaction). In this case, they are not stabilized by electrostatic interactions nor form complexes. Co-soluble complexes are the third type of interaction

that could occur, when two types of macromolecules exist in the same phase and result in the formation of protein-polysaccharides complexes. Bernal et al. [13] used a model system to investigate the gelling properties of pectin-protein gels. It was found that the addition of proteins to calcium-pectin gels improved the gel strength due to protein-pectin interactions. Protein-pectin interactions have also been observed in tomato suspensions by Takada and Nelson [126]. The highest viscosity of a tomato puree and the serum phase was at a pH of 4.40. The pH is an important factor as it determines the nature of interactions depending on the pKa of pectins and the isoelectric point of the proteins. In another work, an addition of 1% denatured soy protein to tomato juice increased the consistency and changed the rheological properties considerably [131, 135]. This system exhibited a weak physical gel behavior, stabilized by non-covalent interactions with a complex rheological response, indicating a network formation or aggregation among the proteins and pectins [135].

In this work, the electrostatic interactions present in tomato cell wall suspensions are investigated. A novel method for investigating these electrostatic interactions in tomato suspensions was explored with the use of ion exchange resins. A cation and an anion resin were employed to substitute ionic compounds with H^+ and OH^- respectively. It will be shown that processing with different resins can change the physical functionality of tomato suspensions by altering protein-pectin interactions. The main highlight of this chapter is to highlight the importance of particle-serum interactions and tomatos were chose for the high protein content [126]. These results may not be applicable to other plant-based systems and is currently relevant only with tomatoes. Using ion exchange resins seems to be promising and this needs to be explored further in other systems.

3.2 Materials and methods

3.2.1 Resin treatment

Ion exchanger I (Catalogue number 104765), a strong cation exchange resin in the H^+ form and Ion exchanger III (Catalogue number 104767), a strong anion exchange resin in the OH^- form were obtained from Merck Millipore International (Amsterdam, Netherlands). The cation and anion resins were loaded by incubating 100g of resin material in 100ml of 4M HCl or NaOH respectively for 3 hrs. Excess acid/base was washed away with de-ionised water until the filtrate was at neutral pH. A tomato suspension was prepared from an industrial supply of 28° brix tomato paste obtained from Unilever (Unilever R&D, Vlaardingen, Netherlands). The paste was hot breaked by the suppliers and contained no enzyme activity. This paste was diluted to 8.5% total solid content as measured by dry weight basis, which is referred henceforth as the control or reference sample. This tomato suspension was centrifuged at 12,000g for 20 minutes at room temperature of 20-25 ^{0}C. Serum phase was separated from pulp by decanting. Different concentrations (w/v) of each resin were added to this serum phase and incubated for a period of 1 hour at room temperature. After filtering off the resin material, the treated serum phase was reconstituted back into the tomato pulp. Using a high speed mixer Ultra-turrax T25 (IKA laboratory equipment, Staufen Germany), the mixture was re-suspended by shearing at a speed of 13,000 rpm for 1 minute at room temperature (20-25 ^{0}C). All samples were left in a refrigerator at 5°C overnight before performing any measurements. Experiments were repeated in duplo.

3.2.2 Enzyme treatment

Two classes of enzymes were used to treat tomato suspensions, a protease (Promod 144GL, Biocatalysts Ltd, Cardiff UK) and a pectinase, the pectinase being a mixture consisting of a pure polygalacturonase (Endo-polygalacturonase M2, EC 3.2.1.15, Megazyme International Ireland) and pectin methylesterase (pectin methylesterase, EC 3.1.1.11, Novozyme International Denmark). The mix was made up of ten parts Endo-polygalacturonase to one part of pectin methylesterase by volume. The tomato suspensions were incubated with the enzymes either before or after treating with the anion resin treatment, to qualitatively identify the nature of the interactions. Both enzymes were used at a concentration of 0.1% w/w in tomato suspensions. All enzyme treatments were performed at pH 4.5 and a temperature of 45 °C over a period of three hours. After enzyme treatment the samples were heated to 90 °C for 5 minutes to irreversibly inactivate the enzymes.

3.2.3 Rheology

The sample was subjected to a pre-shearing step at a shear rate of 5 1/s for 30 sec and subsequently was allowed to equilibrate for 10 minutes prior to measuring. Rheology of various samples was thixotropic, hence very sensitive to the pre-conditioning of the material. To ensure confidence in the rheological measurements, all samples were strictly subjected to the same pre-conditioning procedure, including the loading procedure in the rheometer. All measurements were done in triplicate. The samples were found to be very sensitive to the storage duration. As it was observed that the storage modulus for the anion treated sample increased over a period of a day, all rheological measurements were done after 24-28 hours from preparation to allow sufficient time for equilibration. While measuring the linear storage modulus as a function of pH,

the samples were measured immediately after adjusting the pH. The storage modulus within the linear viscoelastic region was measured by performing strain sweeps from 0.01-100% strain at a frequency of 10 rad/sec. Each point in the strain sweep was averaged over 8 cycles of oscillation to ensure good quality of data. The reported linear storage modulus is obtained from plateau of the linear viscoelastic domain.

3.2.4 Data analysis

Experiments were repeated twice, each set of data had at least 2 measurements. To determine significant differences in the means between samples, a pairwise Tukey test followed by a Bonferonni correction was used. The p value was compared with a critical limit of 95% to determine significant differences.

3.2.5 Fourier transform infrared spectroscopy

After the anion resin treatment of the tomato serum and reconstituting it back into the pulp phase the resulting pH was 9.9. Hence, the untreated tomato suspension was also adjusted to a pH of 9.9 and left overnight in the refrigerator. Small amounts of both these samples (less than 10g) were frozen in liquid nitrogen and lyophilized. The freeze fried samples were stored over P_2O_5 until measurement. From the dry material a small sample was firmly compacted to expel entrapped air and ensure smooth surfaces. After loading this material on the ATR-FTIR (Attenuated total reflectance-fourier transform infrared spectroscopy) sample holder (Shimadzu FTIR-8400S, Shimadzu Japan) the signal was measured with the IRAffinity spectrophotometer (Shimadzu Japan). The transmittance was recorded at wave-numbers from 2000 cm^{-1} to 800 cm^{-1} at a resolution 2 cm^{-1} and averaged over 100 scans per run per

sample. Each sample was recorded at least three times, the average of these three runs was base line corrected before further data processing using the software provided by the instrument manufacturer (IRsolution). The averaged spectra were converted into absorbance mode and smoothed using a third-order Savitzky-Golay smoothing filter over 9 data points. Due to the inherent heterogeneity of the samples, there was significant band overlap unresolvable by the instrument itself. To obtain narrower peak, resolution enhancement techniques were used. A fourier self deconvolution with Happ-genzel apodization and a band width of 14 was used to detect overlaid peaks. Their existence was also verified by the second derivative of the smoothed spectra. Upon this verification, a curve fitting algorithm was used to fit the smoothed spectrum with a number of Gaussian peaks. The algorithm was programmed to find the best fit to the smoothed spectra iteratively until the root mean squared error was less than 1% for all cases. Peak locations from the Fourier self deconvolution was used as a first estimate for the curve fitting algorithm. Best results were obtained only when the peak locations were optimized by the algorithm, hence the peak locations were not fixed during curve fitting. In certain cases, there was a disagreement between the peaks obtained from the Fourier deconvolution and second derivative spectra. The ambiguity in the existence of such peaks was resolved empirically in a systematic iterative approach following some of the principles outlined elsewhere [22].

3.2.6 Plasma emission spectrometry

The concentrations of calcium, magnesium, potassium, sodium and phosphorus were determined by plasma emission spectrometry with the following procedure. 0.5 grams of sample material was taken on a dry weight basis in a test tube. 20 ml of ultra pure water (Milli-Q water from Millipore corporation, Netherlands)

was added and the solution was heated to 90 °C in a regulated water bath for 5 minutes. To this solution, 5ml of 37% aqueous HCl was added while maintaining the solution temperature at 90 °C for 5 minutes with constant shaking. After cooling the solution to room temperature, it was diluted with 50 ml of ultra pure water. To remove any particulate matter before measuring the solution was passed through a 0.22 μm filter. This allowed the solution to be sprayed into a plasma emission spectrometer (Optima 7300DV ICP-OES type, Perkin Elmer, Seer Green UK), after which the emission wavelength was measured for calcium at 317 nm, potassium at 766 nm, sodium at 589 nm, phosphor at 213 nm and for magnesium at 280 nm [55]. All elements were determined by comparison with an acidified standard solution, thus enables absolute values for ion concentrations.

3.2.7 Determination of molecular weight distribution by SEC MALLS-UV-RI

The molecular weight distribution of the polysaccharides in the serum phase was determined using size exclusion chromatography (SEC) coupled to multiangle laser light scattering (MALLS) (PN3621, Postnova analytics, Germany). The refractive index (RI) was measured by a detector (Shodex RI-101, Showa Denko K.K., Kawazaki, Japan) and UV absorption was measured using a diode array detector (G1316A, Agilent technologies, Diegem, Belgium). The serum phase of the tomato suspensions was filtered (0.45 μm) prior to injection, using an auto-sampler (G1329A, Agilent technologies, Diegem, Belgium), to a series of three Waters columns (Waters Inc, Massachusetts USA), namely, Ultrahydrogel 250, 1000, and 2000 with exclusion limits of 8104, 4106, and 1107 g/mol, respectively. An eluent was used based on the starting pH of the sample: 0.1 M acetic acid buffer (pH 4.4) with 0.1 M $NaNO_3$. The eluent was prepared using

demineralized water (organic free, 18 MΩ-cm resistivity), filtered (0.1 mm) and degassed by an on-line degasser of the HPLC system (Agilent technologies 1200 Series, Diegem, Belgium). The flow rate was 0.5 ml/min and the columns were kept at 35 ^{0}C. Before injection all samples were allowed to equilibrate overnight after filtration. A dn/dc value of 0.146 mL/g was used for all samples, as this value was found to be accurate for both pectins [44] and for starch [107] in different buffers. The molecular weight was calculated using the Debye fitting method (up to 2nd order) of the software provided by the MALLS detector manufacturer (Nova Mals, version 1.0.0.18, Postnova analytics, Germany). The presented elution profiles are averaged chromatograms of two repetitions.

3.3 Results and discussion

3.3.1 Concentration of resins used

The effect of resin concentration used to treat the tomato serum was investigated. Effect of resin concentration on the rheology, pH and total solid content is depicted in figure 3.3.1. It can be observed that the anion resin treated sample resulted in a higher storage modulus compared to the cation resin and the untreated sample. For the cation treated sample, the linear storage modulus was lower than for the control sample throughout the concentration range investigated. The anion resin treated sample showed a contrasting result, as the rheology was increasing until 15% resin concentration. This could suggest that exchange of certain anionic compounds in the tomato serum with OH^- triggers an increased interaction between particles, resulting in an increased storage modulus. As a result of the resin treatments the pH of the tomato suspensions also varied with the concentration of resin used as shown in figure 3.3.1a. The effect on pH seems reasonable as the resins increases the concentration of

hydrogen and hydroxide ions. When tomato suspensions were not treated with resin, but subjected to similar pH changes, the storage modulus did not increase. This shows that the effect of resin treatment is more than a change in pH.

Total solid content measured on a dry weight basis was measured, the results are shown in figure 3.3.1b. It is interesting to note that the total solids reduced significantly with an increase in resin concentration above 10%. The differences in solid content between the cation and anion resin treated were found to be statistically significant for the 15% resin concentration pair (p value of 0.012 between the cation and anion resin treated samples). These measurements indicate that certain "solids" were removed from the system as a result of treatment with the resins. It is counter-intuitive that despite the decrease in total solids content the storage modulus increases with increasing anion resin concentration.

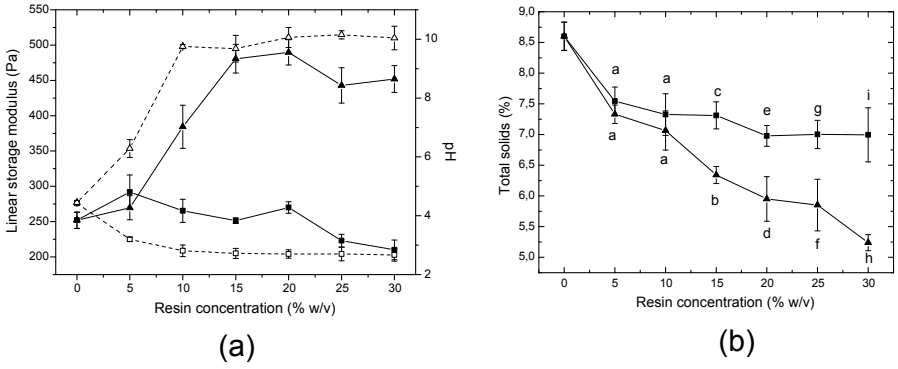

Figure 3.3.1: The effect of resin concentration on the rheology, pH (a) and total solid content (b) of tomato suspensions. In graph (a), Black solid symbols indicate the storage modulus and black hollow symbols the pH of the samples as a function of the concentration of resin used. Upright triangles indicate the anion resin treated samples and squares are for the cation resin treated samples. In graph (b), the triangles indicate the anion resin treatment and square represent the cation resin treatment. The control reference sample is marked as 0% resin concentration.

3.3.2 Inorganic salt analysis

The changes in the inorganic ions such as Ca, Mg, K, Na and P were measured by plasma emission spectrophotometry, the results are shown in table 3.3.1. There are differences in the type and quantity of ions removed by the resin treatments. The cation resin is capable of removing a substantial quantity (approx 70%) of the potassium, magnesium and sodium ions from the system, whereas, the anion resin removes the phosphorous and magnesium by about 55% from the initial value. A 20% reduction is observed in calcium ion concentration, which are notable for their potential interaction with pectins in forming egg-box structures, after the anion resin treatment, whereas a 40% reduction in calcium is observed for a similar cation resin treatment. The trends observed in the inorganic salt content with increasing resin concentration are inconsistent with the effect of resin treatment on the rheological properties. Therefore it is suggested that the increase in storage modulus caused by the anion resin treatment is not due to the removal of cations. It is probable that the anion resin also has an affinity towards organic compounds and not limited to only inorganic ions, as the decrease in total solids can not be explained by the decrease in cations only.

Table 3.3.1: Table indicating the concentration of various ions present in the resin treated samples. Percentage change is calculated with respect to the control sample, which is the untreated tomato sample.

	Sample	Ca		K		Na		P		Mg	
		mg/kg	%change	mg/kg	%change	mg/kg	%change	mg/kg	%change	mg/kg	%change
	0% (w/v)	137		3170		173		271		158	
Anion resin	5% (w/v)	121	11,6	2990	5,6	163	5,7	207	23,6	87	44,9
	10% (w/v)	106	22,6	2960	6,6	163	5,7	142	47,6	73	53,8
	15% (w/v)	112	18,2	2950	6,9	166	4,0	108	60,1	68	56,9
	20% (w/v)	109	20,4	2440	23,0	133	23,1	101	62,7	76	51,9
Cation resin	5% (w/v)	76	44,5	1340	57,7	87	49,7	234	13,6	48	69,6
	10% (w/v)	78	43,1	880	72,2	55	68,2	226	16,6	45	71,5
	15% (w/v)	75	45,3	820	74,1	49	71,6	209	22,8	45	71,5
	20% (w/v)	76	44,5	800	74,7	45	73,9	202	25,4	47	70,2

3.3.3 Effect of pH

For further experiments to investigate the nature of the phenomena, the resin concentration was kept constant at 15% w/v. Variation in rheology as a function of pH for the various samples indicates the importance of electrostatics as seen in figure 3.3.2. The pH of the samples was adjusted by adding 4N HCl/NaOH drop-wise to the samples while stirring to avoid pH overshoots. The measurements were done immediately after adjusting the pH. Storage modulus of the control sample has a local maximum close to the natural pH of 4.4 for tomato suspensions, which has been previously reported by Takada and Nelson [126]. However, this maximum value of the storage modulus at a pH of 4.4 was not found to be statistically significant. Cation resin treated samples did not show much variation in rheology with pH. Throughout the pH range investigated, it had the lowest storage modulus, even lower than the untreated sample. Electrostatic interactions dominate the anion resin treated samples which causes the larger storage modulus (figure 3.3.2). Furthermore, the maximum storage modulus for the anion resin treated samples has a peak at a different pH compared to the control sample. At a pH around 5-6, the anion resin treated sample shows the highest storage modulus of around 520 Pa. This is considerably higher than the storage modulus of the untreated tomato suspensions which is around 270 Pa at the natural pH of 4.4. It is clear that the anion resin treatment caused significant demethoxylation of pectin that increases the charges allowing more interactions with proteins and other divalent ions. The fact that the control sample in figure 3.3.2 treated at pH 10 did not reach the same high storage modulus like the anion treated sample suggests that the effect cannot be explained only by the pectin demethoxylation.

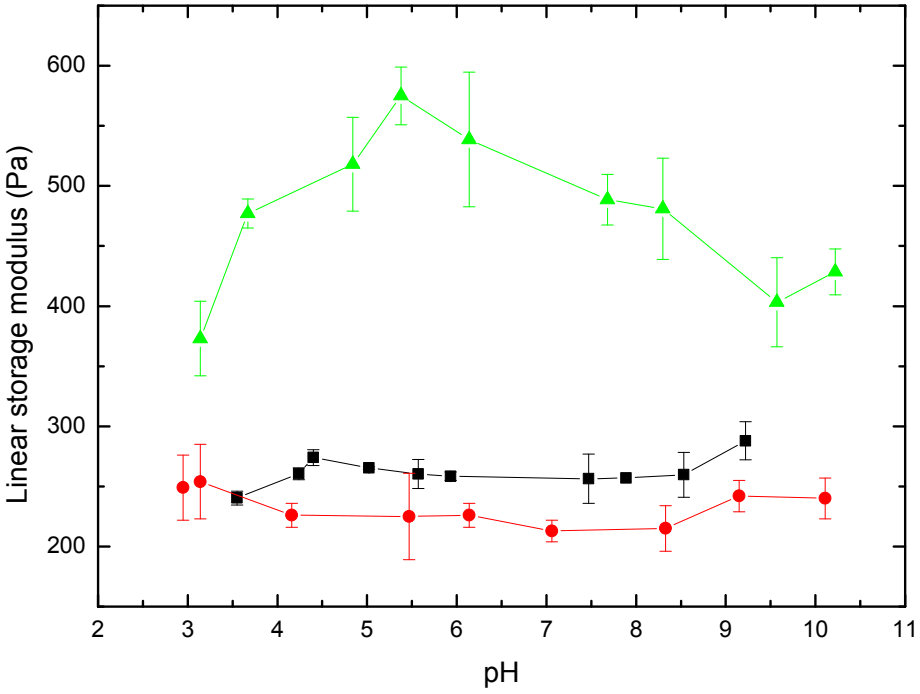

Figure 3.3.2: The effect of pH on the linear storage modulus of untreated and resin treated tomato slurries. Green upright triangles denote the anion resin treated sample, black squares denote the control sample and the red circles denote the cation resin treated sample.

Observing that the anion resin treated samples are more sensitive to pH than the control and cation treated samples indicates the presence of strong non-covalent interactions, likely being dominated by long range electrostatic interactions [39]. The rheology of tomato suspensions has been reported to depend on the pH as it controls the interactions between pectins and proteins. Favorable interaction occurs between them only when the pH is higher than the pKa of pectins but lower then the isoelectric point of the proteins [48, 126]. Similar observations have been reported by Messiaen et al. [78], they observed a maximum absorbance of cations and polyamines towards cell wall material close to a pH of 6. A

similar type of pH response has been reported for casein-pectin systems as well. There is a maximum absorption of casein micelles towards the pectins close to a pH of 5.3. As a result of this, casein micelles were found to have an increased intra-particle repulsion, resulting in a higher viscosity [71]. It is likely that a similar interaction mechanism between pectins and proteins is present in the anion resin treatment of the current study. Proteins present in the bulk absorb onto the pectins on the cell wall material which could result in an enhanced intra-particle repulsion causing the higher storage modulus observed. The sensitivity of pH observed for the anion resin treated sample depends on the pKa of pectins and the isoelectric point of the proteins. Highest storage modulus occurs around a pH of 5.5-6, just higher than the pKa of pectins which has been reported to be in the range of 3-5 [48, 51, 126]. The rheological behavior of the anion treated sample and tomato juice with added soy protein isolate described in Tiziani and Vodovotz [135] are alike in several aspects. They both behave like a stronger physical gel compared to their respective untreated tomato suspensions. Both systems surprisingly show similar rheopectic behavior as well. Given the close resemblance between the anion resin treated sample and systems that show pectin-protein interactions, it is hypothesized that the anion resin changed the native conformation of proteins present in tomato cell suspensions by removing some compounds (as observed by reduction in total solid content).

3.3.4 Microscopy

No changes were observed in the physical micro-structure of the cell wall fragments after processing the suspension with either of the resins as seen in the upper images of figure 3.3.3. This result is to be expected, as the processing only involves the serum phase of the tomato suspension. Although the resins change

the natural electrostatic balance in tomato suspensions, swelling of cellulose, like previously reported due to alkaline pH and organic liquids [46, 70], was not observed here. In the resin treated samples, only the particle-serum interactions seem to play a role in the structure-property relationships. Samples were stained with a fluorescent Rhodamine red dye to highlight proteins and intracellular substances, making it possible to directly visualize these interactions as seen in the bottom series of image, in figure 3.3.3. It can be observed that agglomerates of intracellular material and proteins with the cell walls were formed in the anion treated sample. These agglomerates were not found in the control reference, nor in the cationic treated sample. This visualization, although qualitative, presents further evidence for pectin-protein interactions with the observation of agglomeration of protein and intracellular substances towards the cellular matrix.

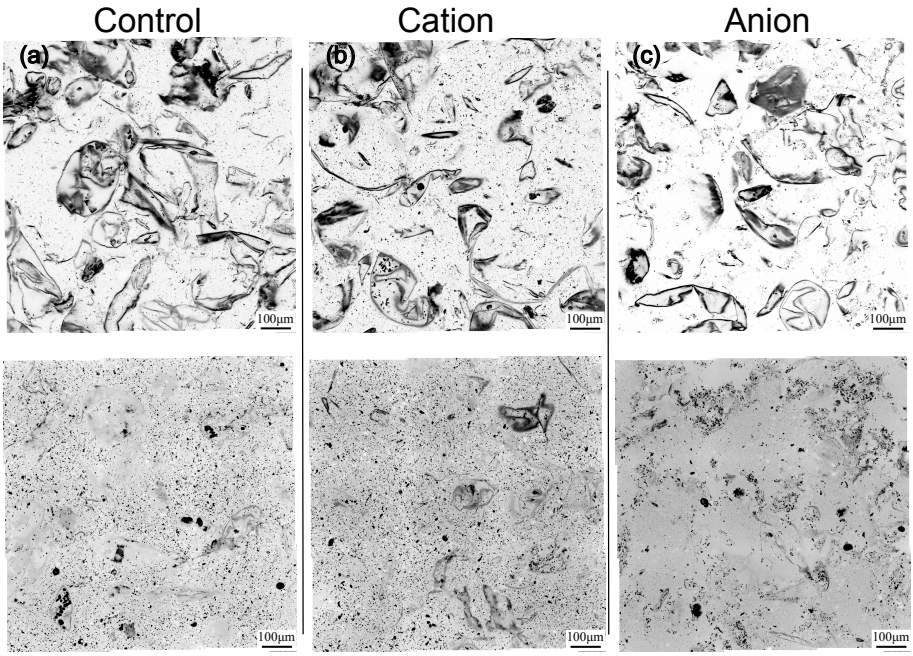

Figure 3.3.3: Confocal laser scanning microscopy images of resin treated and untreated tomato samples. Top series of images highlight cellulosic materials tagged with Congo red and the bottom series of images highlight proteins and smaller compounds tagged with Rhodamine. (a) Control sample (G': 287Pa), (b) Cation treated sample at pH of 5.3 (G': 275Pa) and (c) Anion treated sample at a pH of 5.3 (G': 550Pa).

3.3.5 Qualitative enzyme tests

As a qualitative step to verify this hypothesis, the tomato suspensions were incubated with enzymes, either before or after treatment with the anion resin. All samples were adjusted to a pH of 4.5 prior to enzyme treatment. The order of treatments and their modulus measurements are shown in table 3.3.2. A tomato cell suspension that was treated with protease followed by the anion resin did not result in a higher storage modulus. This is probably because the protease breaks down the proteins before processing it with the anion resin, resulting

in either a lower tendency for interaction with the pectins, hence lowering the storage modulus. On the contrary, when the protease was added after the anion resin treatment the storage modulus was similar to the anion resin treatment alone. This shows that the protease has no effect on the electrostatic interactions that were formed after processing with the anion resin. Most likely the steric hindrance caused by the new structure as a result of the anion resin treatment resulted in a lower availability of the protein for action of the protease, hence not lowering the rheological properties. This unique behavior of the protease provides further evidence to suggest that the anion resin treatment could alter the natural conformation of the proteins. In the case of pure pectinase, the storage modulus decreased when the enzyme was incubated both before and after the anion resin treatment. This indicates how important pectins are in contributing to the structure of these cell suspensions.

Table 3.3.2: Impact on the storage modulus of the order of enzymatic treatment, in anion resin treated tomato samples at a pH of 4.5.

Order of treatment	Storage modulus (Pa)
Control	260 ± 11
Anion resin	483 ± 20
Anion resin -> protease	520 ± 39
Protease -> Anion resin	279 ± 16
Anion resin -> Pectinase	220 ± 20
Pectinase -> Anion resin	203 ± 8

3.3.6 Molecular weight changes

To quantify the extent of enzyme hydrolysis, the molecular weight (Mw) of the serum phase of the suspension was analyzed by SEC MALLS. Figure 3.3.4 shows the RI signal strength (refractive index) vs the elution time for the samples, while the weight average molecular weight (Mw) of the biopolymers in the serum phase

is presented in the attached table. It is clear that the anion treatments increased the Mw of the biopolymers while decreasing the total amount of filterable mass most likely by inducing the formation of large unfilterable aggregates. This could be partially accounted by the demethoxylation of pectin at the high pH that when combined with the presence of ions, can induce gelation. By observing the absorbance at 280 nm (not shown) we could not detect significant concentrations of proteins in the elution region related to large biopolymers (up to elution time of 60 min), while large protein peaks were observed at elution times starting from 61-62 min. Such high elution times suggest that either the Mw of the proteins present is low (mono galacturonic acid elutes at 63 min) or that the proteins present are very compact in structure. While a clear trend in the Mw cannot be observed most likely due to the complexity of the system it is clear that enzymatic treatment prior to the anion treatment results in a smaller observed Mw than in the systems where the order of events is the opposite. When visually observing the RI elution profile we can notice that pectinase treated samples have very similar elution patterns suggesting similar obtained biopolymers, insensitive to the order of treatments. On the other hand, the protease treated samples both by observing the RI elution profile and the weight average Mw show a dependency to the order of treatment (figure 3.3.5). When anion resin treatment was followed by protease treatment the obtained particles were the largest while when the order was reversed the size of the polymers was quite close to the control. This result indicates the sensitivity in the order of treatments for the proteins present in the suspensions. The results from the chromatograms further strengthens our hypothesis that resin treatment alters the nature of proteins and their interaction with pectins. Although the extent of pectin hydrolysis is yet unknown, the enzyme treatment is merely a qualitative step to help in formulating the hypothesis. Structural changes are further analyzed by spectroscopic techniques in the following paragraphs.

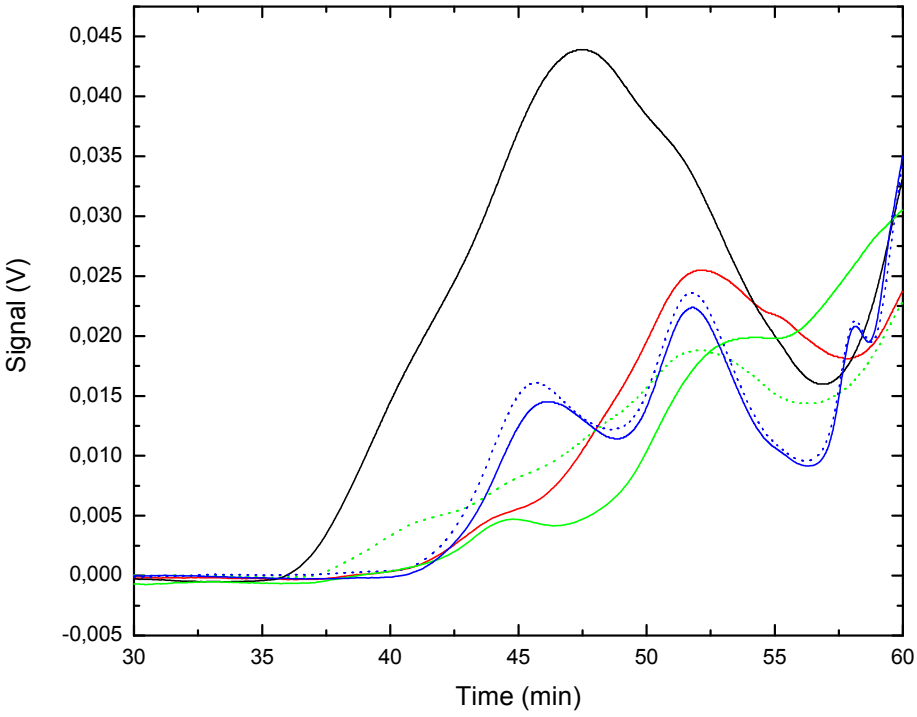

Legend	Mw (Da)	Std dev (Da)
Anion Resin	1,22E+06	1,34E+05
Control	3,69E+05	2,97E+04
Anion resin ➔ Protease	2,09E+06	1,20E+05
Protease ➔ Anion resin	7,70E+05	1,42E+05
Anion resin ➔ Pectinase	1,13E+06	5,66E+04
Pectinase ➔ Anion resin	5,29E+05	5,66E+04

Figure 3.3.4: Refractive index elution profile of enzymatically and anion treated tomato slurries. The table shows the weight average molecular weight.

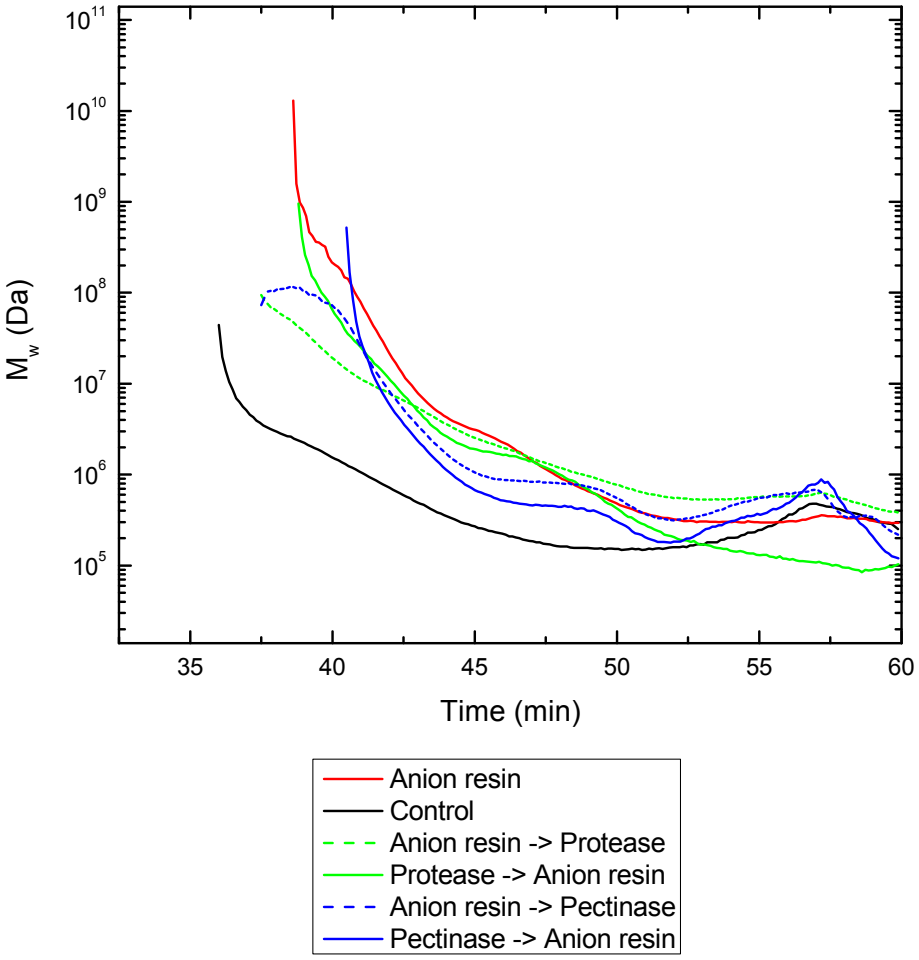

Figure 3.3.5: Mw profile of enzymatically and anion treated tomato slurries.

3.3.7 Infra-red spectroscopy

To further investigate protein-pectin interactions, the anion resin treated tomato suspension and an untreated tomato suspension both at pH 9.9 were lyophilized and analyzed in an infrared spectrometer. The pH of 9.9 was chosen as it was the pH after treatment with 15% w/v concentration of anion resin. The

region of interest in the absorbance spectra is in the region of 1500-1700 cm^{-1}, which is known to absorb amide stretching of the proteins [124] and carboxylic groups of pectins [87]. The region below 1500 cm^{-1} is known as the "finger-print zone" where severe peak overlap and overtones occur due to the heterogeneous nature of the samples [77]. The absorbance spectra of the tomato suspension in 1500^{-1} to 1700 cm^{-1} show a significant difference between the untreated (just pH corrected) and the anion treated tomato suspension without applying band narrowing methods as seen in figure 3.3.6. The strong signal in the amide-II band region, due to the COO^- stretches is close to the 1600 cm^{-1} peak from the pectins as previously observed by McCann et al. [77]. This band seems to shift due to the processing with the resins, being at 1578 cm^{-1} for the untreated while it appears at 1592 cm^{-1} after the anion treatment. In the amide-I region there is a subtle shoulder between 1625 $cm^{-1}$and 1675 cm^{-1} that is higher for the anion treated suspensions. A series of smaller peaks also appear within this shoulder at 1653 $cm^{-1}$and 1646 cm^{-1}, which are probably due to the amide stretches from the proteins. In both cases, there is a severe overlaying of the peaks due to inherent heterogeneity present (protein and pectin) and possibly more than one protein structure overlies on each other. These differences suggest that the anion resin causes an additional structural effect to the protein over the expected effect of pectin demethoxylation of pectins due to the pH increase. From observing the spectral data practically a full demethoxylation can be suggested as no peak is visible around 1740-1750 cm^{-1}[116].

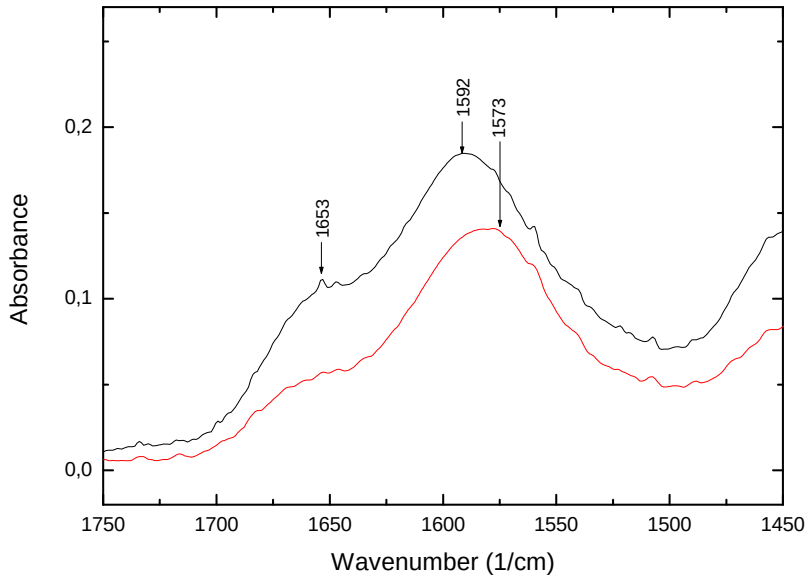

Figure 3.3.6: Infra red spectrum of an anion treated tomato suspension (black line, on the top) and non-resin treated tomato suspension (red line, on the bottom) at a pH of 9.9.

To obtain more quantitative information, the individual areas of the peaks in the amide-I and II regions were obtained from curve fitting. The result of the curve fitting is shown in figure 3.3.7. There are large differences between the samples in both the amide-I and amide-II regions. In the amide-II region, there are small shifts in the peaks that are observed and their corresponding areas show significant changes due to the treatment. This change in peaks is not a conclusive indicator of the change in the protein conformation. The amide-I region seems to provide more clear data regarding conformational changes, as the peaks in this region show significant shifts as a result of treatment. Additionally the large peak of the pectin (1588-1590 cm^{-1}) which is associated with the carboxylate

group is not located in this region. The fitted band profile is different in the absorbance wavelength and peak intensity. Band assignments and area under the curves in the amide-I region are analyzed in a similar manner to Byler and Susi [22], who verified the band assignments for 21 different proteins in FTIR with other established techniques. The pH corrected treated tomato suspensions were suggested to have about 75% random structures indicated by the peak at 1645 cm^{-1}, and about 16% extended chains indicated by the peak at 1670 cm^{-1}. After the treatment with the anion resin, this distribution changes drastically, as there is about 55% beta-sheet structures indicated by the peak at 1664 cm^{-1} and 40% of extended chains indicated by the peak at 1640 cm^{-1}. This result from the deconvoluted curve fitting further provides evidence to support the hypothesis that the anion resin alters the pectin-protein interactions present in the tomato suspensions. It is plausible that the resin treatment removes certain components which increase possible binding sites of the protein with pectin.

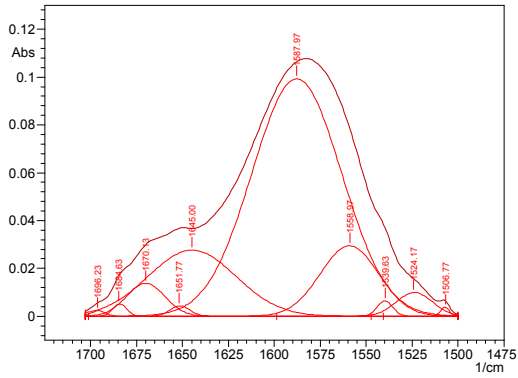

	Wavenumber (1/cm)	Peak Area (%)	Band Assignments
Amide-II	1507	0,29	
	1524	3,21	
	1540	0,89	
	1559	15,49	
	1588	80,12	
Amide-I	1645	77,09	Unordered
	1652	2,75	α-helix
	1670	16,88	Extended chains
	1685	2,25	Turns and bends
	1696	1,03	Turns and bends

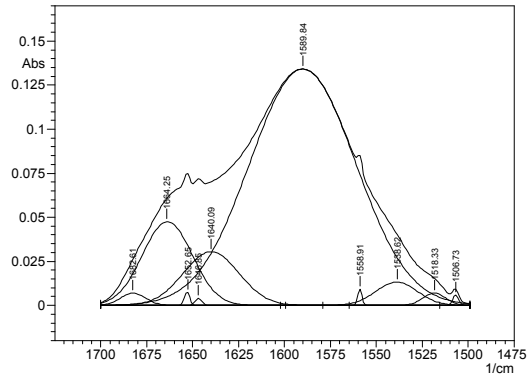

	Wavenumber (1/cm)	Peak Area (%)	Band Assignments
Amide-II	1507	0,22	
	1518	1,05	
	1539	3,66	
	1559	0,25	
	1590	94,81	
Amide-I	1640	39,38	Extended chains
	1647	0,61	Unordered
	1653	0,89	α-helix
	1664	55,09	β-sheets
	1683	4,02	Turns and bends

Figure 3.3.7: Deconvoluted curve fit spectra of figure 3.3.6. The table shows the respective peak locations with their area percentages within the Amide-I region. The top graph is for the untreated tomato suspension treated sample (red line) and the bottom graph shows the band assignments for the anion resin (black line).

Processing of tomato suspensions with resin exchangers appears to have significant impact on the physical properties of tomato suspensions. Although not all questions are answered in this work, it directs towards a potential of a novel processing method with the use of resin exchangers. Future work should aim at understanding the type of compounds removed, and at a further understanding of the mechanism of interactions. It is believed that this method can be further applied to other systems and only further research will allow to fully exploit this processing method.

3.4 Conclusions

Treatment of tomato suspensions with ion exchange resins was investigated. The anion resin treatment resulted in a higher storage modulus compared to treatment with the cation resin and the untreated tomato sample. The resins did not alter the physical cellulose micro-structure of the cell walls and only altered the particle-serum interactions. The anion exchange resin caused a structure formation which was sensitive to pH. Processing tomato suspensions with a cation resin resulted in a system with lower rheology than the untreated material and did not alter electrostatic interactions significantly. There is a strong indication that changes in pectin-protein interactions are the dominant cause of rheological changes in anion resin treated tomato suspensions. It is most probable, as shown using infra red spectroscopy that the anion resin alters the conformation of proteins present in the tomato suspensions, triggering their interaction with pectins. Possibly the anion resin removes certain compounds which trigger changes in protein conformation, allowing an enhanced binding with pectins (that also undergo pH induced changes). The study reported here is a first step in better understanding these interactions, but more research with model systems will be needed to study the nature of such interactions.

Chapter 4

Effect of enzymes on serum and particle properties of carrot cell suspensions[1]

4.1 Introduction

Suspensions of plant material, that are rich in polysaccharides, are widely used in products such as paper, biofuels, foods and bioplastic. Engineering these materials requires an in-depth understanding of how the polysaccharides affect bulk properties. These suspensions are chemically heterogeneous with a variety of particle shapes and sizes. This makes a complete understanding of the structure-property relationship of these systems very challenging. It is

[1] A.K. Sankaran, J. Nijsse, R. Cardinaels, L. Bialek, A. Shpigelman, M.E. Hendrickx, P. Moldenaers and A.M. Van Loey, Effect of enzymes on serum and particle properties of carrot cell suspensions, Food Biophysics (Accepted)

known that in these suspensions, there are cellulosic particles suspended in a serum phase of solubilized pectin, proteins and other solutes [149]. There is also sufficient evidence to show that there are complex interactions between either the serum-particle or particle-particle phases of the suspensions . The nature of these interactions could be electrostatic, frictional or elastic, depending on the particular system [64]. Electrostatic interactions in the serum phase are common to occur either between protein-pectin [111, 126] or pectin-pectin compounds [82]. It is not yet completely clear what is the relative effect of the particle and serum phases to the rheological properties of the whole suspension [84]. As these particles are also deformable, it has been suggested that the elasticity of plant particles can be important to fully understand the rheological properties of plant based suspensions. On shearing, the particles behave like folded elastic sheets that contribute to the storage modulus [64]. It is clear that there are two possible mechanisms of interaction between plant particles, depending on their concentration in the suspensions. They can interact either by an excluded volume effect from electrostatic interactions or by particle elasticity from particle-particle contact. Both types of interactions strongly affect the physical properties such as storage modulus and yield stress. However, a definite link between the polysaccharides and mechanical properties is not clear. Even a qualitative understanding of these relationships would pave way for further quantitative research in the field.

From the world of botany, there has been extensive research on the elasticity and plasticity of cell walls [29, 32]. Viscoelasticity of the cell wall plays an important role during the growth phase of the plant, as it is related to cell wall elongation. This elongation mechanism is driven by polymer rearrangements within the cell wall over long periods of time which affect the “cell wall viscoelasticity” [141]. It has been suggested that the cellulose fibrils are bound by various polysaccharides present within the cell wall [100]. There are various factors

suggested to affect the mechanical properties of the cell wall, including: cross linking of matrix polysaccharides, friction between the polysaccharides and/or non-covalent interaction of polysaccharides. The elasticity of the cell wall can be tuned by either breaking such bonds/interactions or by depolymerizing the backbone of major polysaccharides [29].

In this study, a multidisciplinary approach was used to understand the relative importance of particle hardness and electrostatic interactions on the rheology of carrot cell suspensions. It was also aimed to qualitatively connect the function of pectins and proteins to these properties. Enzymes were used to selectively hydrolyze the polysaccharides. These chemical changes were reflected on the measured physical properties. The enzyme treated samples were investigated using rheology, microscopy and multiple angle laser light scattering measurements. Compression experiments were developed to compare the particle hardness between enzyme treated and untreated carrot cell suspensions. This enabled to decouple the effects of particle hardness from electrostatic effects on the rheology of semi-dilute carrot cell suspensions. Carrots were chosen in this study as the cell walls were hard enough to be measured in the rheometer. The results from the cell wall hardness can be applied to other systems as most cell walls are made up of similar architecture. However, the results from the particle-particle interactions is specific for the case of carrots.

4.2 Materials and methods

The following experiments were performed on different fractions obtained from carrot cell suspensions, as shown in figure 4.2.1.

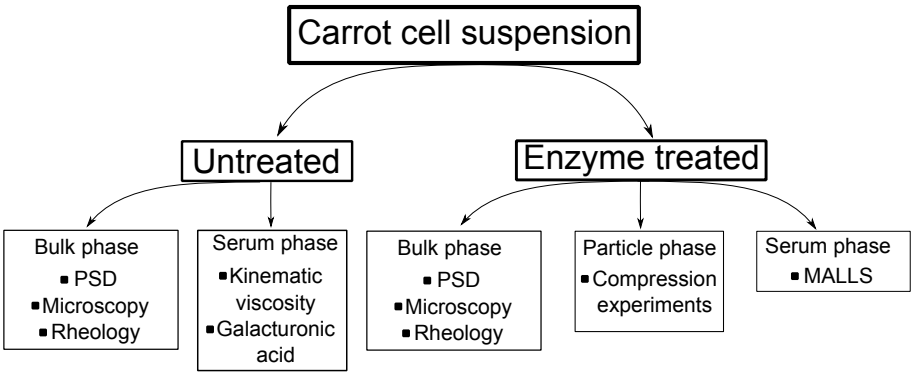

Figure 4.2.1: Schematic of experiments performed for different carrot cell fractions.

4.2.1 Sample preparation

Semi-dilute concentrations of suspensions were prepared as they are relevant to industrial products. Frozen carrots were procured from Ploegmakers Food Ingredients BV (Breda, Netherlands). Carrot cubes of size 1 cm were blanched at 80 °C for 2 minutes by the supplier to inactivate endogenous enzyme activity. The cubes were stored and transported at -20 °C. Before experiments, the cubes were thawed overnight at room temperature. Thawed carrot cubes were cooked at 90 °C for 45 minutes. Cooked carrots were cooled to room temperature in an ice bath. Evaporated water determined by weight loss was replenished with deionized water. The mixture was then blended using an industrial Waring Variable Speed Lab Blender LB20EG 0.40 HP (Waring commercial, Stamford USA) at maximum speed for 5 minutes to obtain a puree of carrot cells. This

reference sample was centrifuged at 12000 g and the supernatant was decanted from the pulp. To further remove colloidal particles the supernatant was passed through a 0.45 μm filter. This obtained filtrate (serum phase) was characterized separately.

4.2.2 Enzyme treatment

Two types of enzymes were used to treat the carrot suspensions, namely a protease (Promod 144GL, Biocatalysts Ltd UK) and a pectinase. The pectinase was a mixture of pure endo-polygalacturonase (EC 3.2.1.15, Megazyme International Ireland) and pectin methylesterase (EC 3.1.1.11, Novozyme International Denmark). The mix was made up of ten parts endo-polygalacturonase to one part of pectin methylesterase by volume. The enzyme activity for pure endo-polygalacturonase was 1800 U/ml and pectin methylesterase was 10 U/ml as reported by the suppliers. Both types of enzymes were used at a concentration of 0.1% w/w in carrot suspensions. All enzymatic treatments were performed at pH 4.5 and a temperature of 45 °C for a period of three hours. After enzyme treatment the samples were heated to 90 °C for 5 minutes to inactivate the enzymes .

The enzymatically treated samples were centrifuged at 12000 g and the supernatant was decanted from the pulp. To further remove colloidal particles the supernatant was passed through a 0.45 μm filter. The obtained filtrate (serum phase) was characterized separately using MALLS.

4.2.3 Determination of Galacturonic acid content

Galacturonic acid content was determined in the serum phase of the carrot suspensions. First the pectin polymers in the serum were hydrolyzed by the

addition of concentrated sulphuric acid. To 2 ml of serum solution 8 ml of concentrated H_2SO_4 was added dropwise while stirring in an ice bath for 5 minutes. 2 ml of deionized water was added to this solution which was then stirred for a period of 60 minutes for hydrolysis by the method of Ahmed and Labavitch [2]. This solution was then filled up to 50 ml in a volumetric flask. The method for quantitative determination of the uronide fraction was adapted from Blumenkrantz and Asboe-Hansen [18]. 0.6 ml of the above mentioned solution was mixed with 3.6 ml chilled sodium tetraborate solution and transferred to a test tube. This test tube was vortex mixed and immersed in an oil bath of 100 °C for 5 minutes. After placing the test tubes in an ice bath, 60 µl of methahydroxydiphenyl reagent was added. A blank sample with only 60 µl of methahydroxydiphenyl was used as reference. The emission at a wavelength of 520 nm was measured using a spectrophotometer. Acid hydrolysis was performed in duplicate and determination of the uronide component was performed in triplicate. For absolute determination of the galacturonic acid content, a standard curve was prepared using monogalacturonic acid.

4.2.4 Kinematic viscosity of the serum

A fully automated Ubbelohde viscometer (iVisc Capillary viscometer, Lauda-Brinkman, New Jersey USA) was used to accurately determine the intrinsic viscosity of the serum phase. The capillary ID was 0a with an internal diameter of 0.53 mm, capillary constant of 0.005 mm^2/s^2 and the calculated Hagenbach correction was approximately 1.57 seconds. The capillary was rinsed with deionized water and subsequently cleaned with ethanol/acetone and dried with air before use. The clean capillary with the sample was immersed into a water bath at 25 °C. The sample was allowed to equilibrate for 10 minutes. First the fluid was drawn up the glass to wet the glass surface. Subsequently, kinematic

viscosity of the sample was evaluated by measuring the time taken for the fluid to drain between the two marked lines on the capillary. Three measurements were performed and the average viscosity was reported.

4.2.5 Small angle oscillatory shear (SAOS)

A stress controlled rheometer (TA Instruments AR-2000ex, USA) with a parallel plate geometry of 40 mm diameter was used for all measurements. Wall slip commonly occurs in two-phase systems due to steric, hydrodynamic, viscoelastic and chemical constraints acting near the boundaries [6]. This wall slip was apparent for the concentrated carrot suspensions using a smooth geometry. To avoid this, the plates were covered with a 800 grit sand paper (3M, USA). In such setup the effects of slip were found to be negligible. For all SAOS measurements the gap between the plates was 2500 μm, being an order of magnitude larger than the mean particle size but small enough to avoid flow effects arising from large gaps. The sample was subjected to a pre-shearing step at a shear rate of 5 1/s for 30 seconds followed by 7 minutes of rest prior to measuring. The storage modulus within the linear viscoelastic region was measured by performing strain sweeps from 0.01-100% strain at a frequency of 10 rad/sec. Each point in the strain sweep was averaged over 6 cycles of oscillations to ensure good quality data. All measurements were repeated at least three times within each experimental batch and averaged over 2 batches.

4.2.6 Compression experiments

Compression experiments were performed on the suspensions to qualitatively understand the effect of enzyme treatment on carrot particles. A smooth plate-plate geometry of 40 mm diameter with an initial gap of 1 mm was used for

the compression experiments. Due to the slip occurring in such a geometry, the flow is dominated by axial compression whereas shear effects were largely eliminated [68].

After loading the sample into the rheometer, it was pre-conditioned as mentioned in section 4.2.5. Subsequently, the top plate was lowered to a gap of 10 µm at a speed of 10 µm/sec, thus compressing the particles. The gap was held constant at 10 µm while measuring the normal force. All measurements were repeated at least three times within each experimental batch and averaged over two batches.

4.2.7 Data analysis

All experiments were repeated at least three times within each experimental batch and averaged over 2 batches. To determine significant differences in the means between samples, a pairwise Tukey test followed by a Bonferroni correction was used, with a p value of 95 %.

4.3 Results and discussion

4.3.1 Linear viscoelastic properties of carrot suspension

Figure 4.3.1 presents the particle morphology of the untreated samples which present mostly single cells due to the hot break treatment [64]. The mean particle size for the reference sample was found to be 83 µm. Mean particle size (figure 4.3.2), particle morphology (figure 4.3.1) and total solid content did not change significantly after the enzymatic treatments. Hence, the volume fraction is comparable between the enzyme treated and reference samples with the same solid content. The storage modulus of the various samples was measured as a

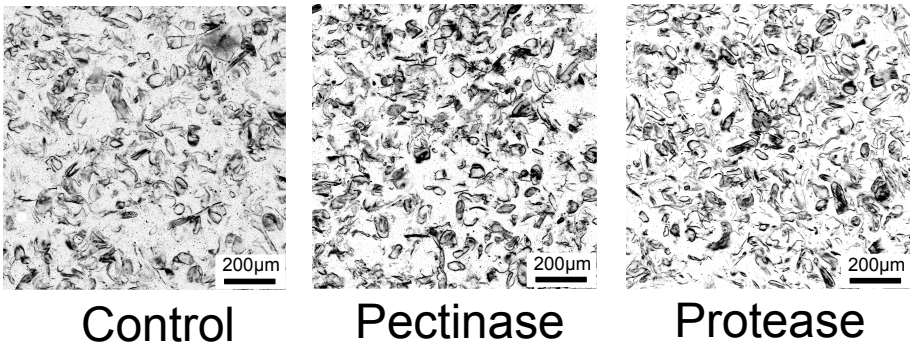

Figure 4.3.1: Confocal microscopy images of the untreated and enzyme treated carrot suspensions.

function of the total solid content, shown in figure 4.3.3. The storage modulus is known to have a power law dependence on the total solid content (equation 4.3.1) within the semi-dilute region [34, 64, 84]. After fitting the curves with a power law model the coefficients obtained for the respective samples are shown in figure 4.3.3. The results were statisticaly significant after being tested with the Tukey test. For similar systems, the values of "b" reported earlier are 2.99 [64] and 4 [84]. The reason for the differences in "b" is possibly due to the nature of the starting material.

$$log(G') = log(a) + b \cdot log(w) \tag{4.3.1}$$

where, G' is the storage modulus [Pa], a is the prefactor, b is the power law exponent and w is the total solid content.

The storage modulus of the carrot puree after pectinase treatment is lower throughout the concentration range investigated. This results in the prefactor "a" being lower. However, the coefficient "b" is higher compared to the untreated sample. The changes are significantly different from each other. The storage modulus of the carrot puree after protease treatment appeared

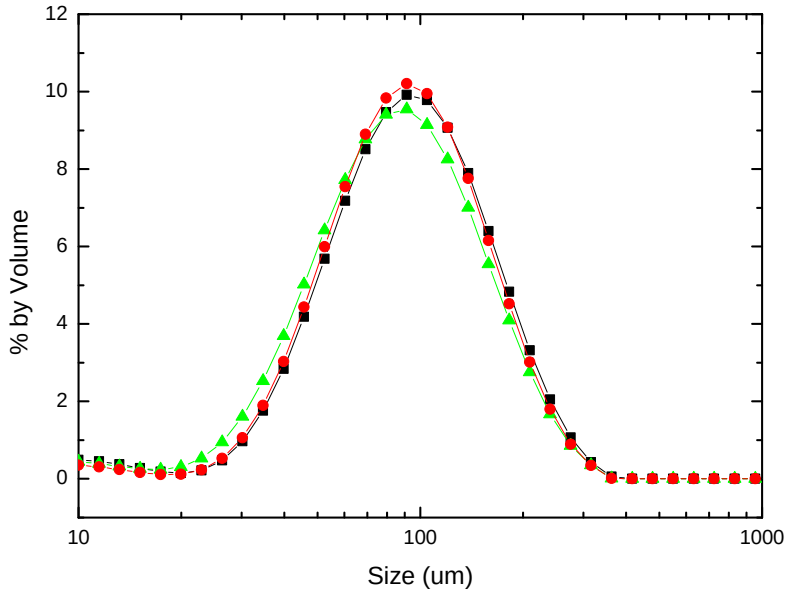

Figure 4.3.2: Particle size distribution of the carrot suspensions before and after enzyme incubation. Black squares indicate the untreated sample, green triangles the protease treated sample and red circles indicate the pectinase treated sample.

similar to the control sample at higher concentrations but is lower at more dilute concentrations. Upon comparing the power law coefficients, it is evident that there are differences between the suspensions. The prefactor “a” for the protease treated sample is lower compared to the untreated sample but higher than the pectinase treated sample, whereas, the coefficient “b” for the protease treated sample is similar to the pectinase treated sample. The lower value of “a” for enzyme treated systems is due to the lower storage modulus. Both pectinase or protease enzyme treatments of the carrot puree resulted in a higher “b” value compared to the untreated sample, indicating that the enzyme treatment

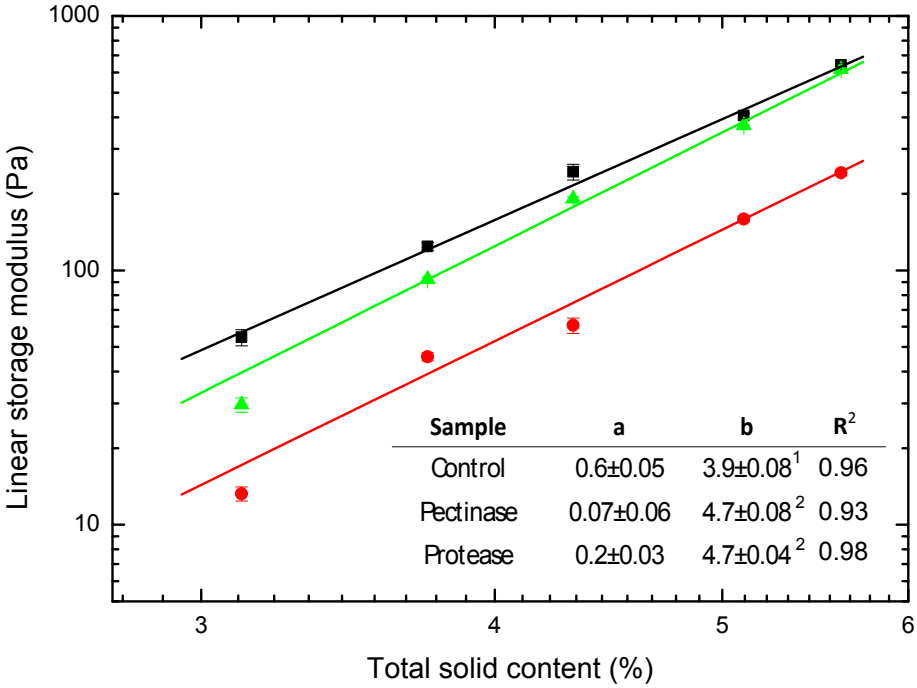

Figure 4.3.3: Linear storage modulus as a function of concentration. Black squares indicate the control sample, green triangles the protease treated sample and red circles indicate the pectinase treated sample. a, b are the prefactor and powerlaw exponent in eq 4.3.1. Error bars are smaller than the symbols.

induces a more "open" network structure [10, 84]. This could be the result of the enzymes altering the pectin and protein structures present within the serum or particle phase of the suspensions [84, 111]. As a result of enzymatic action, the inter particle interactions are altered either by pectin hydrolysis and demethoxylation (pectinase) or by changing the nature of protein-polysaccharide interactions (protease).

To investigate the nature of interactions between the particles, NaCl was added to two different packing fraction of particles. Varying the particle concentration enabled to qualitatively control the inter-particle distance. A

higher concentration of particles results in more crowding (higher packing fraction) and vice-versa. Logically, the particle properties are more important at higher particle concentrations and the properties of the serum phase are probably more important at lower particle concentrations. The concentration of NaCl was quantified relative to the total solid content. This gives a better indication of how much salt is needed to screen charges on the particles as compared to an absolute measure such as molarity. Figure 4.3.4 shows the variation of storage modulus with NaCl addition at two different particle concentrations. In both concentrations of the particles, the storage modulus of the particles after pectinase treatment is not very sensitive to salt addition. At a higher concentration, the particles are tightly packed bringing the particles closer to each other. This increases the potential for particle-particle interactions and the effect of particle properties becomes predominant on the rheology. The untreated sample is very sensitive to the addition of salt at a higher concentration of particles. This contrasting behavior of the pectinase treated and untreated samples with addition of salt suggests that the pectins present on the particles could contribute to electrostatic interactions. The combination of PG and PME would cause a reduction in Mw and increase the charge on the pectic backbone. The salt insensitivity of the pectinase treated sample suggests that the smaller but more charged pectins have little contribution to particle-particle and particle-serum electrostatic interaction. After protease treatment on the other hand, at the higher particle concentration a similar salt dependent trend to the control sample is observed, while at a lower concentration of particles the storage modulus is insensitive to the salt addition. From these observations, it is suggested that particle-particle interactions in the untreated systems are mainly electrostatic in nature through pectins. The effect of proteins on the rheology is not conclusive from these experiments. From the results it is suggested that the proteins present in these suspensions affect the rheology in more dilute

systems. The protease treatment probably alters the protein-polysaccharide interactions which can significantly change the dynamics of such systems. Due to the partially charged pectin backbone and possibly an oppositely charged

protein, they are most likely to interact [111, 126].

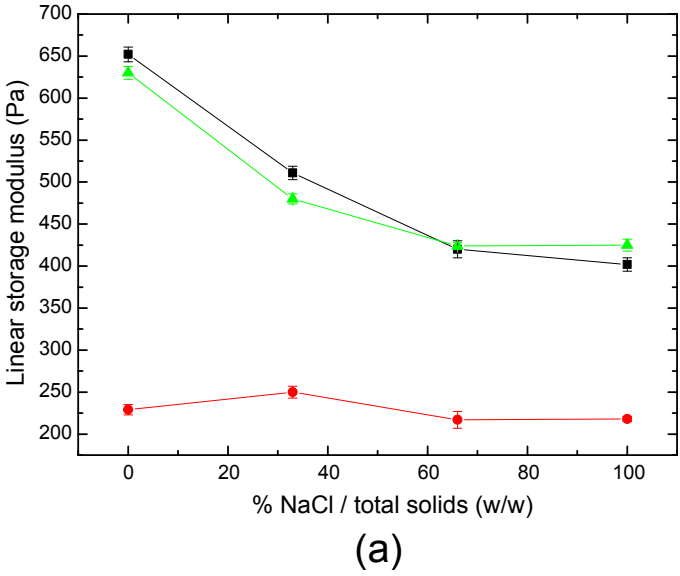

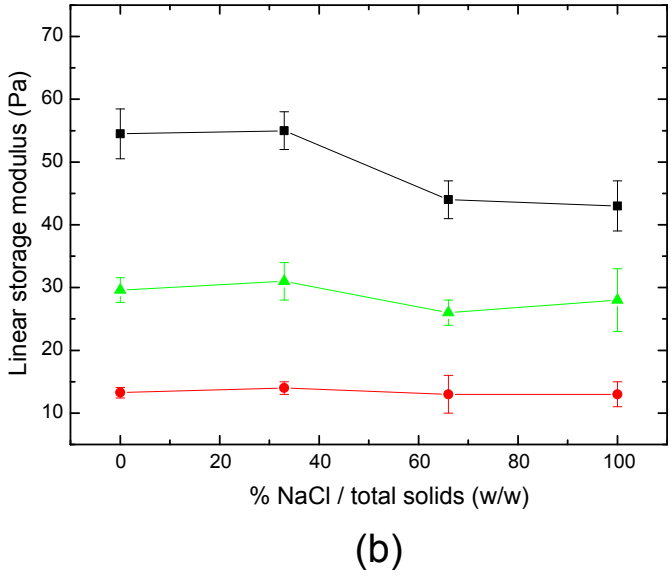

Figure 4.3.4: Effect of NaCl on the storage modulus of the samples at a total solid content of (a) 5.6% (high) and (b) 3.1% (low). Black squares indicate the untreated sample, green triangles the protease treated sample and red circles indicate the pectinase treated sample.

4.3.2 Serum phase

The serum phase of the suspensions was characterized by measuring the relative viscosity in absence and presence of salt. This allowed investigating the effect of the serum phase on particle-particle interactions by determining the intrinsic viscosity. Relative viscosity of the serum phase decreased in 2M NaCl (figure 4.3.5). Intrinsic viscosity was determined from fitting a line to the relative viscosity vs galacturonic acid content as shown in equation 4.3.2. The line was fit to the limit of zero concentration (0,1) and the intrinsic viscosity was measured from the slope. The measured intrinsic viscosity of the serum decreases from 0.68 to 0.44 in the presence of 2M NaCl. Hence, the apparent molecular weight of the solubilized polymers in the serum phase also has decreased as given by the Mark–Houwink rule (equation 4.3.3). The serum phase properties play an important role at a lower packing fraction. However, the decrease in the storage modulus with the addition of salt is not drastic at a lower fraction of particle compared to the higher packing fraction (figure 4.3.4b). Furthermore, the serum phase polymers result in a lower apparent Mw with the addition of NaCl. Hence, it is unlikely that the serum phase polymers affect particle-particle interactions. This result further strengthens the notion that pectins on the particle surface are responsible for the electrostatic interactions.

$$\frac{\eta}{\eta_o} = 1 + [\eta] \cdot \phi \tag{4.3.2}$$

$$[\eta] \propto M_w^a \tag{4.3.3}$$

where, η is viscosity [Pa.s], η_o is solvent viscosity [Pa.s], ϕ is the volume fractions, a is the constant and M_w is the molecular weight.

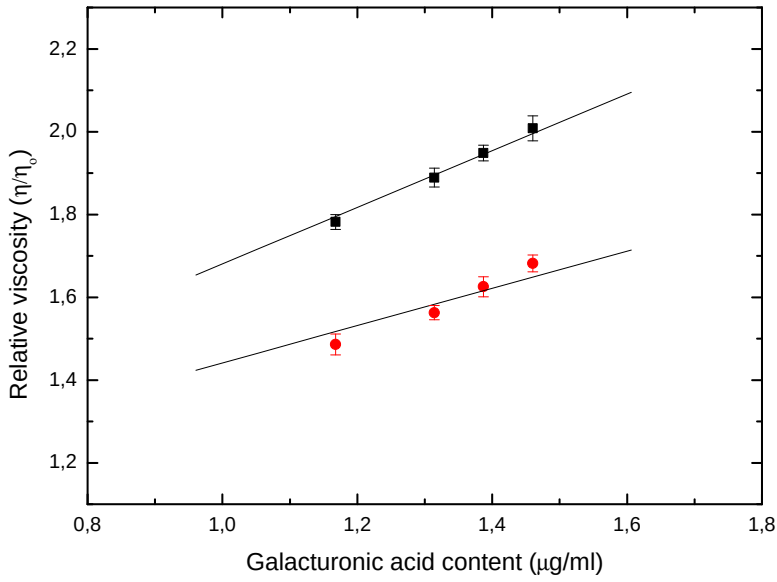

Figure 4.3.5: Intrinsic viscosity of the serum phase of the untreated carrot puree. No salt (black squares) and with 2M NaCl (red circles). The fit linear line is made to pass through (0,1).

The molecular weight distribution of the serum phase was measured to understand the effect of enzymes on the biopolymers in the serum phase. The results of the RI detector are presented in figure 4.3.6 a. The elution profile of the polymeric compounds shows a clear shift to the left after the treatment with pectinase as expected due to the hydrolysis of the pectic backbone (with minimal changes to the RI profile of the protease treated samples). On the other hand, when observing the UV (at 280 nm, figure 4.3.6b) profile a relatively large increase of the peak around 40 minutes is visible after the protease treatment, most likely suggestive that due to the enzymatic treatment some large Mw UV

absorbing material from the particle phase or unfilterable from the serum phase (at 0.45 μm) before the treatment dispersed into serum phase and/or became filterable. As a result the weight average molecular weight (assuming that the dn/dc of the polymers did not change very significantly due to the increased but still small fraction of proteins in the elution profile) of the pectinase treated sample insignificantly decreased from $2.3x10^6$ to $1.8x10^6$ gr/mol while due to the treatment with protease a significant increase to $4.9x10^6$ gr/mol was observed (figure 4.3.7). Changes in the concentration and size of the polymers in the serum phase are likely to affect the rheological properties of the whole system especially in samples where the rheology of the whole system is dominated by the serum phase (as was suggested for the protease treated samples). A suggested hypothesis is that the protease treatment changes the nature in which pectin binds proteins in the serum phase. However, the precise mechanism is difficult to elucidate within this study due to the limitation of the filter and removal of fully hydrolyzed polymers that result in a superposition of effects in the filterable serum phase. At least, this MALLS study shows that the protease treatment enriches the serum phase with large polymers coming from the particle phase.

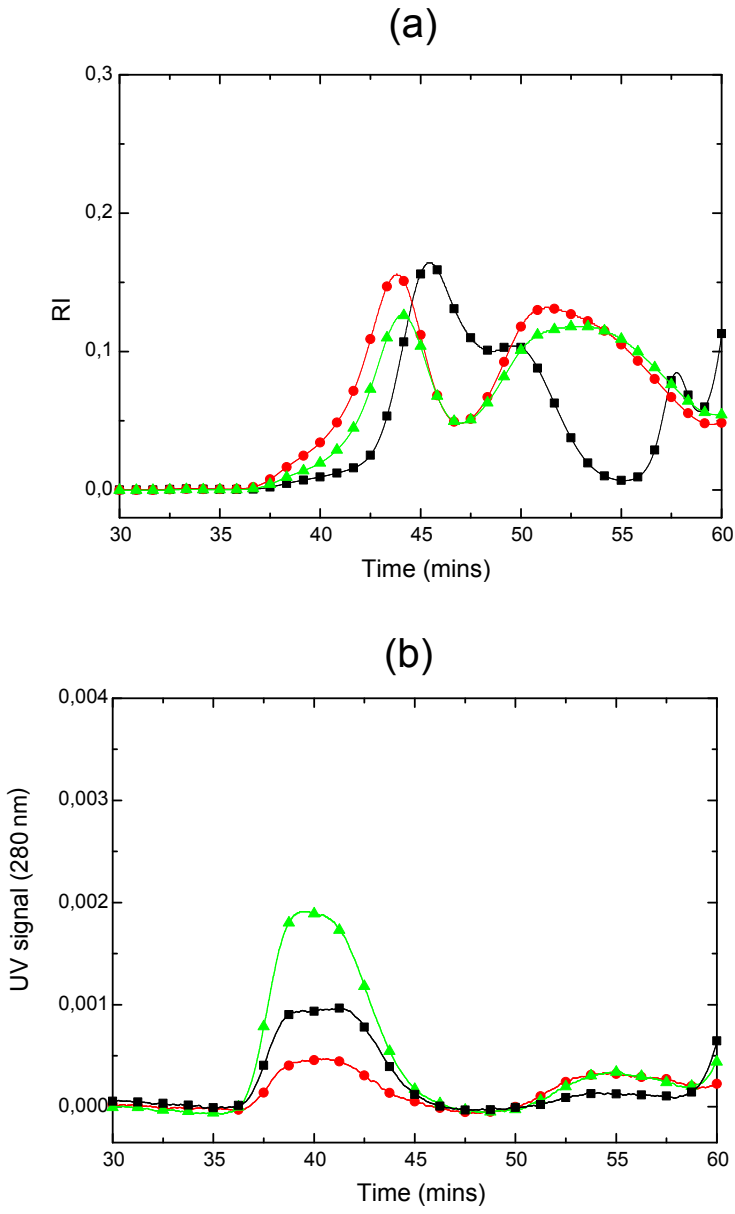

Figure 4.3.6: Size exclusion elution profile of the serum phase of the enzymatically treated and untreated samples. (a) Refractive index profile, (b) UV signal profile at 280nm. Black squares indicate untreated serum, green triangles indicate protease treated serum and red circles indicate pectinase treated serum phase.

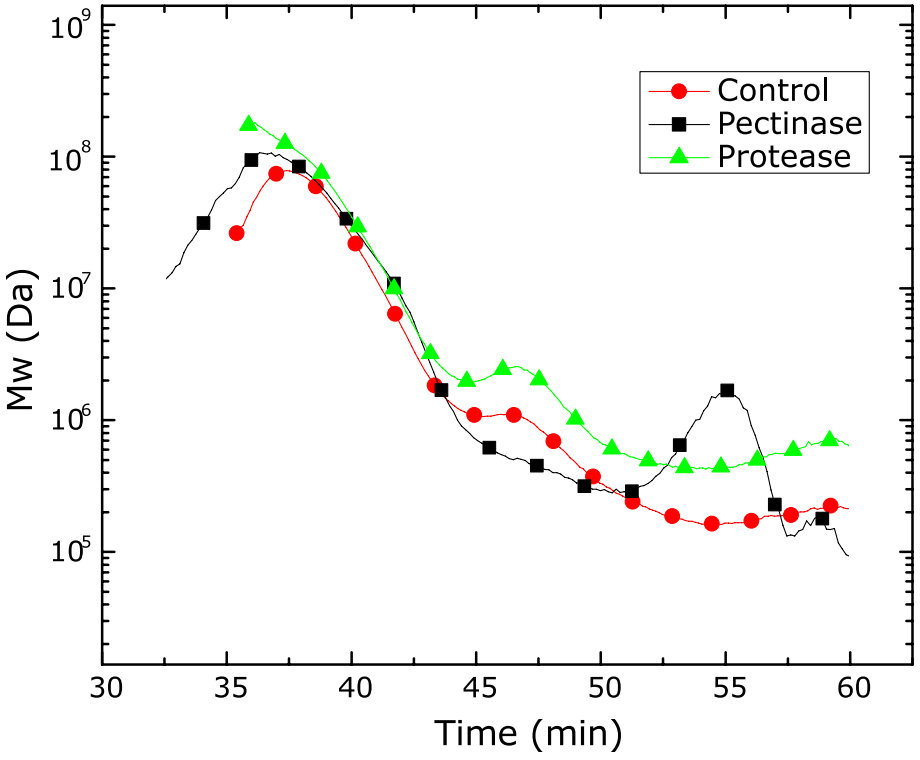

Figure 4.3.7: M_w elution profile vs time for the different samples.

4.3.3 Particle phase

The enzymes affect the cell wall microfibrillar architecture as visualized from cryo-SEM images shown in figure 4.3.8. Pectins on the cell wall were possibly hydrolyzed by the pectinase enzyme treatment which resulted in significant loosening of the cell wall. Even the protease enzyme treatment resulted in some cell wall loosening. Pectins and proteins are known to crosslink with cellulose fibrils. Upon enzymatic hydrolysis the crosslinks are reduced facilitating the loosening of the cellulose architecture [29].

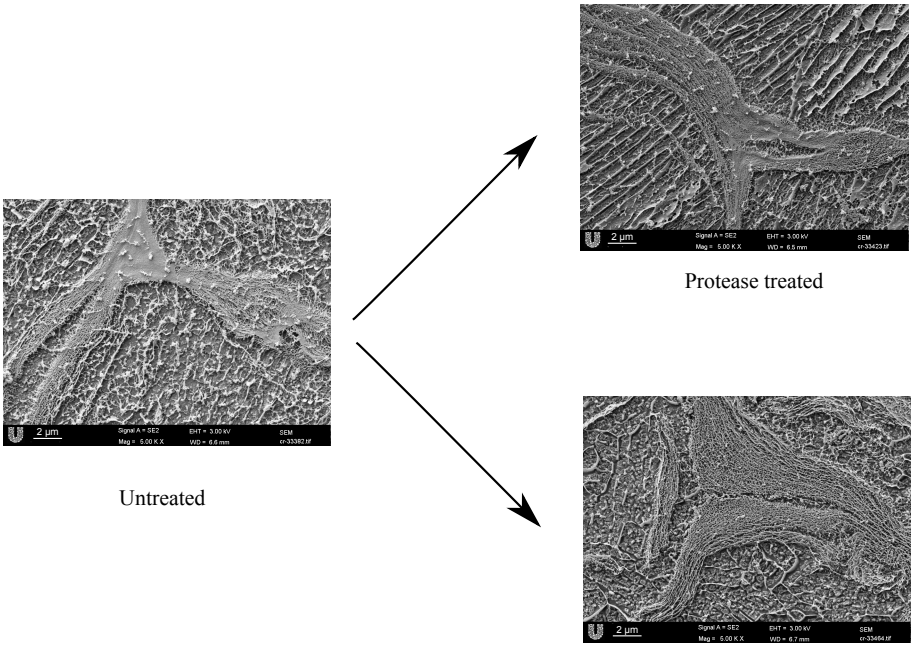

Figure 4.3.8: cryo-SEM images of cell wall architecture for untreated, pectinase treated and protease treated carrot systems.

Due to visible changes in the cell wall architecture after enzyme treatment (figure 4.3.8), the question arises whether the enzymes affect the rheology by changing the physical properties of particles? To answer this, squeeze experiments were performed using a rheometer. The top plate of the rheometer was lowered at a constant rate. This caused the serum phase of the suspensions to percolate through, leaving the particles constrained by the narrow gap. As the gap width tended towards the mean particle size, a direct strain was applied on the particles. The resulting stress response of the particles was measured by the normal force transducer on the bottom plate of the rheometer. Translating the force response to obtain precise rheological material functions is not trivial as the materials are very heterogeneous. Conventional models are applicable only for small deformation typically less than 10% [17]. Furthermore for anisotropic materials like cell walls, the particle properties depend on the direction of the strain applied [81, 125]. Direct visualization of the particle deformation was not possible with the current setup. It is suggested that compressive strain on the originally ellipsoidal particles would cause the cell wall to bend (figure 4.3.9). The advantage of this method is its robustness and special instrumentation is unnecessary. The downsides are the inability to determine particle properties, the measurement of the average response over many particles and the fact that deformation applied is possibly non-linear. Hence, this method can only be used to qualitatively compare related systems.

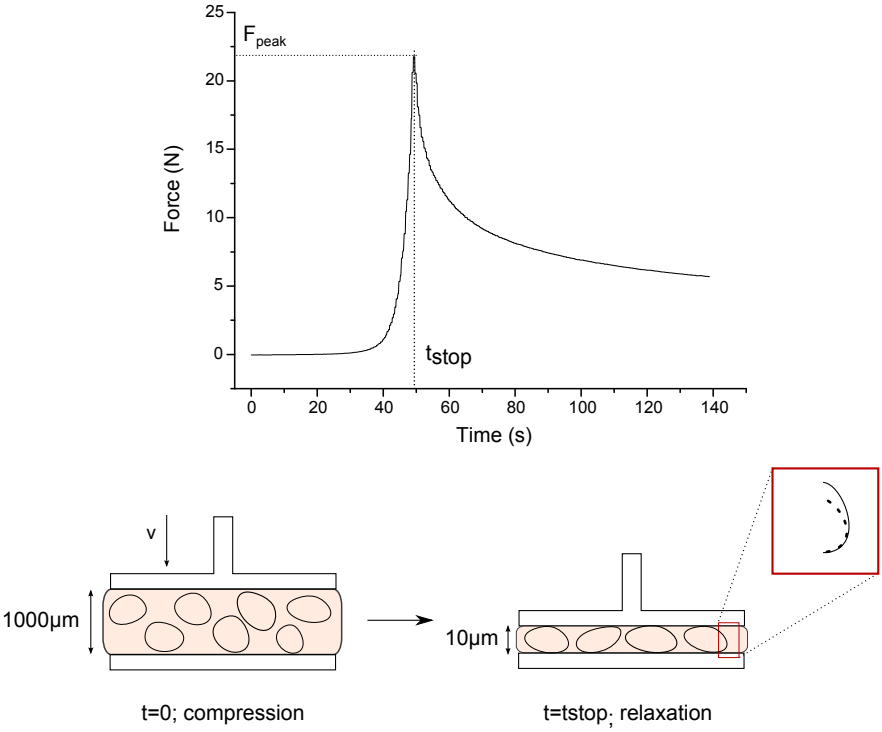

Figure 4.3.9: Schematic of compression experiment. Inset highlights the possible deformation experienced by the cell wall, dotted lines indicate the compressed cell wall and solid lines indicate the quiescent state of the cell wall.

The protocol described here is optimized for the specific rheometer and system. Faster compression rates or higher strains resulted in a normal force larger than specifications of the rheometer. A slower compression rate or lower strain, resulted in poor force resolution. Peak normal force was measured when the plate was stopped and the subsequent normal stress relaxation was fit with a 1-D Maxwell model, shown in equation 4.3.4.

$$\sigma(t) = c + \sigma_0 \cdot exp(-t/\lambda) \tag{4.3.4}$$

where, σ is stress (Pa); λ is relaxation time scale (s); σ_0 is peak stress (Pa); t is time (min) and c is residual stress (Pa).

Previous research to evaluate cell hardness has been performed with the use of a micro-manipulator [143] or atomic force microscope [47]. Under a compressive strain the force response has been suggested to be a superposition of two phenomena, the stress response due to particle deformation and water transport through the cell wall [67]. It is difficult to decouple these effects in heterogeneous suspensions. Based on the experiments performed using a micro-manipulator, it is suggested that the peak force is indicative of cell wall elasticity [17], while the time scale of relaxation is indicative of the water transport that would occur as a result of the applied strain [17].

The peak force from the compression test was investigated for a range of concentrations as shown in figure 4.3.10. It can be observed directly that the control sample shows a lower peak force compared to the enzyme treated samples throughout the concentration range investigated. Statistical analysis shows that the difference observed between the enzyme treated and untreated sample was found to be significantly different at the 95% level. There was no significant difference found between the peak force values of the pectinase and protease treated samples. From previous studies, enzyme treatment was reported to “soften” the cell wall in the surface plane to facilitate extension [29, 109, 125]. However, it is to be highlighted that this cell wall elasticity is not being measured in the current experimental protocol. The force measured here is the response from a complex cell wall deformation and from pressurized water inside the cells. The deformation of the cell wall results in a combination of bending stress and elastic force measured in the normal direction to the cell

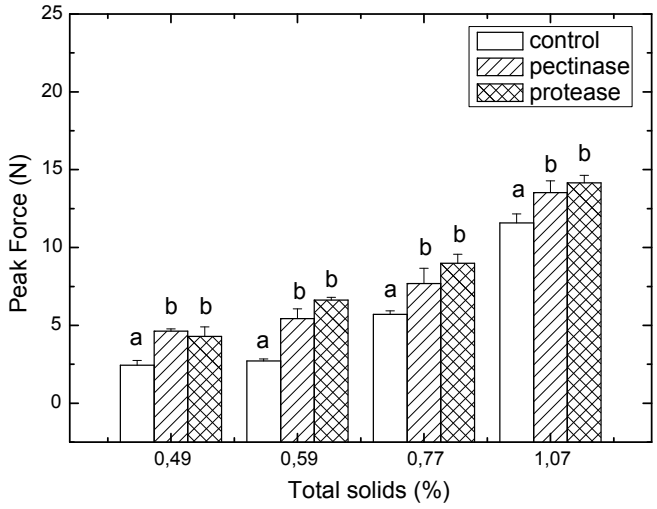

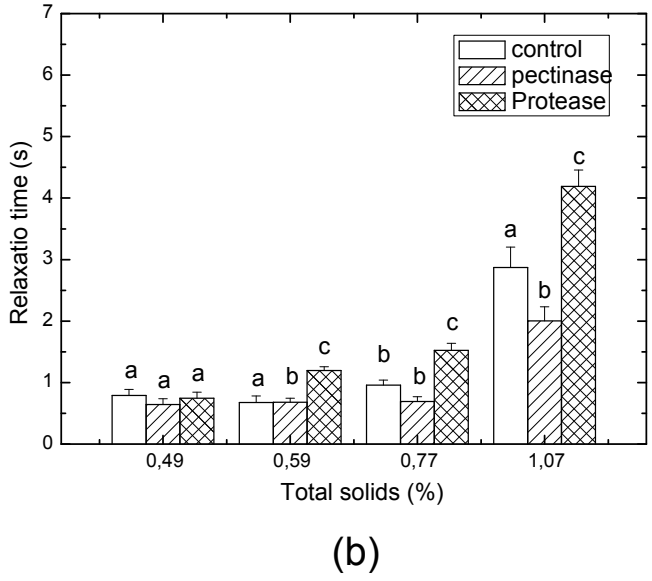

Figure 4.3.10: Graphs showing (a) peak force (b) relaxation time scales from compression experiments for the untreated, pectinase and protease treated carrot cell suspensions.

wall. A loosened cell wall architecture results in a thicker cell wall. This could cause both the pectinase and protease treated samples to have a significantly higher normal force when compressed. Previous experiments have shown that there is a direct correlation with pectin demethyloxylation and an increased rigidity of the cell wall in growing cells [94, 96]. Hence, the result that the enzyme treated samples shows a higher force is not entirely surprising The PME induces demothoxlyation of the pectic chains which could potentially make the particles stiffer.

The pectinase treated system had a lower storage modulus (figure 4.3.10) and a higher peak force (figure 4.3.10) compared to the untreated system in all the concentrations. Furthermore, the pectinase treated samples were insensitive to the addition of salt (figure 4.3.4). From these observations, it is suggested that the particle hardness did not affect the bulk rheological properties as significantly as the electrostatic interactions. This is probably due to the low occurrence of elastic particle-particle interactions in concentrations below the packing limit. Contrastingly, the storage modulus of the protease treated sample was lower than the untreated sample only at a lower particle concentration (figure 4.3.3), whereas, the peak force of the protease treated sample was consistently higher than the untreated system in all the concentrations investigated (figure 4.3.10). It could be hypothesized that pectin-protein interactions present in the serum phase affected the rheological properties after protease treatment.

From previous investigations using a micro manipulator, it has been suggested that the force relaxation is a result of water drainage [17]. The relaxation time scale from the Maxwell model is shown in figure 4.3.10b. At higher concentrations, the protease treated sample had the highest relaxation time, followed by the control and pectinase samples. As the concentration decreased the difference between the treatments became insignificant. These results do not indicate a consistent trend. Relaxation time scale for a cell with only turgor

pressure was measured to be 10-20 seconds which is longer than what is observed here for cooked systems without turgor pressure [143]. Here the relaxation time scales also vary with the particle concentration. It is possible that in concentrated systems particle-particle interactions affect the stress relaxation. When the concentration of the particles is reduced, the effect of elastic particle-particle interactions also decreases. In that case, the relaxation time scale at the lowest concentration would be the best indicator for each system. However, at the lowest concentration of the particles there is no significant difference in the relaxation time between the different treatments. This suggests that the porosity and tortuosity of the different samples are similar under compression [67].

4.4 Conclusions

The effect of protease and pectinase enzymatic treatments on the serum and particle phase properties of carrot cell wall suspensions was investigated. It was shown that both pectinases and proteases altered the network structure present in the serum phase. This was done by both pectin hydrolysis and demethoxylation (pectinase) or changing the protein-polysaccharide interactions by de-polymerization of proteins (protease). The pectinase treated material was insensitive to the addition of NaCl at both higher and lower concentrations, suggesting that pectins present on the surface of the particles were responsible for the electrostatic particle–particle interactions. This was further verified by measuring the relative and intrinsic viscosity of the untreated serum phase with the addition of NaCl. To investigate the effect of particle properties a series of compression experiments was performed. It was seen that the pectinase and protease treated samples had a higher peak force response compared to the control. However, the time scale for stress relaxation was similar between all the

samples investigated. This suggested that particle stiffness had increased due to cell wall loosening caused by the pectinase or protease enzyme treatment. Even though the pectinase treated sample had 'harder' particles the storage modulus was lower compared to the untreated system. This leads to the conclusion that rheological properties of carrot suspensions in the semi-dilute regime were affected by electrostatic interactions rather than by particle hardness effects.

Chapter 5

Conclusions and future outlook

The aim of this study was to investigate structure-function relationships of biopolymers in cell suspensions. Knowledge of these relationships will allow engineering of the physical properties of cell suspensions and develop new food products. It is known that the rheology of these suspensions depend on both the serum and particle phases. The effects of particle size, particle-particle interactions, particle-serum interactions and particle hardness on the bulk properties are discussed over three chapters. Throughout the thesis, a reverse engineering approach was used to understand the function of polysaccharides and their interactions with proteins by using enzymes. Cell suspensions were incubated with enzymes which hydrolyzed a specific polysaccharide or proteins. The physical properties were affected by these bio-chemical changes, and thus a hypothesis for the structure-function relationship of these polymers could be formulated.

In the second chapter, the effect of enzymes (pure and mixed) on particle size, particle morphology and rheological properties was investigated. Carrots were cooked, blended and homogenized (reference sample). This material was incubated with pure cellulase, hemicellulase or pectinase, which resulted in different microstructures and physical properties. Linear storage modulus was measured over an 8 hour period of enzyme incubation. There was a decrease in the storage modulus for all enzymes investigated. Among the pure enzymes, pectinase had the largest drop in storage modulus in the first two hours followed by hemicellulase and cellulase. Enzyme cocktails had a more severe impact on the storage modulus compared to the pure enzymes. They resulted in a lower storage modulus than the pure enzymes, showing a synergistic effect in hydrolyzing the bio-polymers. Enzymes hydrolyzed the polysaccharides that were present both within the cell wall and serum phase. This resulted in a decrease in the particle size and reduced particle-serum interactions, which caused the lower storage modulus for the enzyme treated systems. From microscopic images, it was observed that the enzymes also affected the morphology of the particles. As enzymes hydrolyzed the polysaccharides cross linking with the cell wall biopolymers, there was loosening of the cellulose fibrils in the absence of these crosslinks. An additional homogenization step performed on the enzyme treated systems was able to mechanically disintegrate the cellulosic fibers from the cell wall. The cellulose fibers fracture along the weak points created by the enzyme hydrolysis. This resulted in new microstructures of the particles and physical properties. Storage modulus of the enzyme-homogenized samples was higher compared to only enzyme treated throughout the time period investigated. This increase was attributed to the increase in the particle size as a result of the ruptured cellulose fibers. The enzyme-homogenization step changed the microstructure and resulted in fiber bundles for the pure enzymes and microfibrilated networks for the enzyme cocktails. Only the

heterogenous enzyme cocktail 'Cellulase' from *Aspergillus niger* showed complete microfibrilated cellulose upon homogenizing, which seems to be the first report of microfibrilated cellulose from carrot cell walls.

In the next chapter, the effect of particle-serum interactions on rheological properties of tomato suspensions was investigated by ion exchange resins. The serum phase of tomato suspensions was treated with either an anion or cation exchanger resin. Resin treated serum was reconstituted into the tomato pulp and re-suspended. Each resin was capable of replacing ionic compounds of molecular weight less than 1000 Daltons with a hydroxide or hydrogen ion respectively. The treatment did not alter the physical micro-structure of the cell walls as only the serum phase of the suspensions underwent resin treatment. The anion resin treated tomato slurry resulted in a higher storage modulus compared to the cation treated and untreated tomato slurries. Interestingly, the storage modulus of the anion resin treated system was more sensitive to pH changes compared to the reference sample. This indicated the existence of long range electrostatic interactions. To establish the nature of these interactions, enzymes (pectinase and protease) were used to treat the samples before and after anion resin treatment. Incubation with the pectinase enzyme caused a drop in the storage modulus when performed before and after anion resin treatment. Whereas, the protease enzyme caused a drop in the modulus only when it was incubated before the anion resin treatment. This suggested that the anion resin treatment changed pectin-protein interactions which affected the rheological properties. Possibly the anion resin removed certain compounds which triggered changes in the protein conformation, allowing an enhanced binding with pectins (that also undergo pH induced changes). To further prove this, the untreated and anion resin treated samples at the same pH were analyzed using Fourier transform infrared spectroscopy. After performing Fourier deconvolution within the Aminde-I region, protein conformations were identified. It was observed

that the anion resin treated sample had predominantly beta-sheet like structures compared to random coil structures in the untreated suspension. This change in protein conformation has apparently altered the protein-pectin interactions which resulted in the increased storage modulus of tomato suspensions.

In the final chapter, the effect of enzyme (pectinase and protease) treatment on the serum and particle properties of carrot cell suspensions was discussed. Storage modulus of the enzyme treated and untreated samples were measured as a function of total solid content. Pectinase treated samples had a lower storage modulus compared to the untreated system over the entire concentration range. The protease enzyme treatment, on the other hand, affected the rheological properties only at a lower concentration of carrot cells. The storage modulus had a power law dependence with the total solid content of the sample. Enzyme treatment resulted in a higher power law index and a lower pre-factor. A higher power law index indicated a change in the network structure after enzyme treatment. This was correlated to the changes within the system due to either pectin hydrolysis (pectinase) or pectin-polysaccharide interactions (protease). To investigate particle-particle interactions, NaCl was added at a high and low packing fraction of particles. The untreated and protease treated samples showed a decrease in the storage modulus in both cases. Pectinase treated systems on the other hand, did not show a decrease in the storage modulus upon NaCl addition for both high and low concentrations. From these observations, it was suggested that the electrostatic interactions between the particles was due to the pectins present on the surface of the particles. Further investigation showed that the relative and intrinsic viscosity of the untreated system's serum phase reduced with addition of salt. This indicates that the polymeric chains in the serum phase contract due to electrostatic screening, further supporting the hypothesis. After pectinase treatment the molecular weight of the polysaccharides in the serum phase was lower than the

untreated system. This was due to the pectinase hydrolyzing the galacturonic acid backbone into smaller polymeric chains. Surprisingly the molecular weight increased after protease treatment, probably the protease enzyme released higher molecular weight polysaccharides into the serum phase from the particles. The enzymes changed the microfibrillar architecture within the cell wall as observed in chapter II. A new method was developed to compare the particle properties using a conventional rheometer. A direct compressive strain was applied on the particles while measuring the normal force response. The untreated and protease treated sample showed similar peak force at different concentrations. Pectinase treated sample, on the other hand, showed a higher peak force than the other two. Even though the pectinase enzyme treatment results in a higher peak force it has a lower storage modulus compared to the untreated sample. This result suggests that in semi-dilute carrot cell suspensions the effects of electrostatic interactions are more predominant on the rheology than particle elasticity. The relaxation of the force was also measured and fit with a 1D Maxwell model. Characteristic relaxation time did not yield a consistent trend with enzyme treatment at a higher concentration of the particles. This was suggested to be caused by the superposition of two forces, the water transport through the cell wall and cell wall relaxation. In concentrated systems, these two phenomena occur simultaneously and it is difficult to decouple them.

Three possible ways of engineering the physical properties of cell suspensions were investigated, namely, particle volume fraction, particle-serum, particle-particle interaction and particle hardness. It was further shown that pectins played an unequivocal role in each mechanism. The learnings can be used to process food systems to tailor the physical propertie. In Chapter II the effect of enzymes showed a reduction in the storage modulus of carrot cell suspensions. This method can be used for products that require high pulp content with a reduced viscosity. By changing enzyme composition and incubation time the

physical properties of the final product can be controlled with high precision. Processing tomato suspensions with anion resins resulted in an increased storage modulus (Chapter III). Maybe using ion exchange resins directly may not find suitable applications in food. However, pectin-protein interactions can be used to formulate products such as ketchups or dressing. This enables to engineer the rheology of these products without the addition of artificial thickeners and additives. Only by using different processing methods, this work describes how to engineer the flow properties of food products at constant solid content. Future work should concentrate both on application of the ideas discussed in this work into products and further the understanding of these systems. One of the major drawbacks in the current work is the lack of bio-chemical charaterization. Thus, future studies should focus on linking the chemical structure to the physical properties of cell suspensions. In terms of applications, future studies should investiate the effects studied here in current food formulations. This will directly aid in product development using learnings from the latest science

Dissemination

Publications

(1) A.K. Sankaran, J. Nijsse, L. Bialek, M.E. Hendrickx, and A.M. Van Loey, Effect of Enzyme Homogenization on the Physical Properties of Carrot Cell Wall Suspensions, Food and bioprocess technology 8, 1377 (2015)

(2) A.K. Sankaran, J. Nijsse, L. Bialek, A. Shpigelman, M.E. Hendrickx, and A.M. Van Loey, Enhanced electrostatic interactions in tomato suspensions, Food Hydrocolloids 43, 442 (2015).

(3) A.K. Sankaran, J. Nijsse, R. Cardinaels, L. Bialek, A. Shpigelman, M.E. Hendrickx, P. Moldenaers and A.M. Van Loey, Effect of enzymes on serum and particle properties of carrot cell suspensions, Food Biophysics (Accepted, 2015)

Conferences

(1) A.K. Sankaran, J. Nijsse, L. Bialek, S. van Buggenhout and A.M. Van Loey, Structure property relationships in enzyme treated carrot cell suspensions at EPNOE, Nice (2013).

(2) A.K. Sankaran, J. Nijsse, L. Bialek, A. Shpigelman, and A.M. Van Loey, Structure property relationships in enzyme treated carrot cell suspensions at International food hydrocolloids conference, Taiwan (2014).

(3) A.K. Sankaran, J. Nijsse, R. Cardinaels, L. Bialek, A. Shpigelman, M.E. Hendrickx, and A.M. Van Loey, Structure property relationships in enzyme treated carrot cell suspensions at EFFoST, Sweeden (2014).

Bibliography

[1] J. M. Aguilera. Why food microstructure? *Journal of Food Engineering*, 67(1-2):3–11, 2005.

[2] A. E. R. Ahmed and J. M. Labavitch. A simplified method for accurate determination of cell wall uronide content. *Journal of Food Biochemistry*, 1(4):361–365, 1978.

[3] M. Anastasakis, J. Lindamood, G. Chism, and P. Hansen. Enzymatic hydrolysis of carrot for extraction of a cloud-stable juice. *Food Hydrocolloids*, 1(3):247–261, 1987.

[4] P. E. D. Augusto, A. Ibarz, and M. Cristianini. Effect of high pressure homogenization (HPH) on the rheological properties of a fruit juice serum model. *Journal of Food Engineering*, 111(2):474–477, 2012.

[5] C. Barbana and A. El-Omri. Viscometric behavior of reconstituted tomato concentrate. *Food and Bioprocess Technology*, 5(1):209–215, 2012.

[6] H. A. Barnes. A review of the slip (wall depletion) of polymer solutions, emulsions and particle suspensions in viscometers: its cause, character, and cure. *Journal of Non-Newtonian Fluid Mechanics*, 56(3):221–251, 1995.

[7] D. M. Barrett, E. Garcia, and J. E. Wayne. Textural modification of processing tomatoes. *Critical Reviews in Food Science and Nutrition*, 38 (3):173–258, 1998.

[8] G. K. Batchelor. The effect of brownian motion on the bulk stress in a suspension of spherical particles. *Journal of Fluid Mechanics*, 83(1): 97–117, 1977.

[9] G. K. Batchelor and J. T. Green. The hydrodynamic interaction of two small freely-moving spheres in a linear flow field. *Journal of Fluid Mechanics*, 56(2):375–400, 1972.

[10] E. Bayod, P. Mansson, F. Innings, B. Bergenstahl, and E. Tornberg. Low shear rheology of concentrated tomato products. effect of particle size and time. *Food Biophysics*, 2(4):146–157, 2007.

[11] L. Becu, S. Manneville, and A. Colin. Yielding and flow in adhesive and nonadhesive concentrated emulsions. *Physical Review Letters*, 96(13): 138302, 2006.

[12] N. Beresovsky, I. Kopelman, and S. Mizrahi. The role of pulp interparticle interaction in determining tomato juice viscosity. *Journal of Food Processing and Preservation*, 19(2):133–146, 1995.

[13] V. M. Bernal, C. H. Smajda, J. l. Smith, and D. W. Stanley. Interactions in Protein/Polysaccharide/Calcium gels. *Journal of Food Science*, 52(5): 1121–1125, 1987.

[14] L. Berthier, L. F. Cugliandolo, and J. L. Iguain. Glassy systems under time-dependent driving forces: Application to slow granular rheology. *Physical Review E*, 63(5):051302, 2001.

[15] S. Bhamidipati and R. K. Singh. Flow behavior of tomato sauce with or without particulates in tube flow. *Journal of Food Process Engineering*, 12(4):275–293, 1990.

[16] M. Bhat. Cellulases and related enzymes in biotechnology. *Biotechnology Advances*, 18(5):355–383, 2000.

[17] J. Blewett, K. Burrows, and C. Thomas. A micromanipulation method to measure the mechanical properties of single tomato suspension cells. *Biotechnology Letters*, 22(23):1877–1883, 2000.

[18] N. Blumenkrantz and G. Asboe-Hansen. New method for quantitative determination of uronic acids. *Analytical Biochemistry*, 54(2):484–489, 1973.

[19] P. Bottiglieri, F. Sio, G. Fasanaro, G. Mojoli, M. Impembo, and D. Castaldo. Rheological characterization of ketchup. *Journal of Food Quality*, 14(6):497–512, 1991.

[20] I. Braccini, R. P. Grasso, and S. Perez. Conformational and configurational features of acidic polysaccharides and their interactions with calcium ions: a molecular modeling investigation. *Carbohydrate Research*, 317(1-4): 119–130, 1999.

[21] H. C. Brinkman. The viscosity of concentrated suspensions and solutions. *The Journal of Chemical Physics*, 20(4):571, 1952.

[22] D. M. Byler and H. Susi. Examination of the secondary structure of proteins by deconvolved FTIR spectra. *Biopolymers*, 25(3):469–487, 1986.

[23] N. C. Carpita and D. M. Gibeaut. Structural models of primary cell walls in flowering plants: consistency of molecular structure with the physical properties of the walls during growth. *The Plant Journal*, 3(1):1–30, 1993.

[24] Z. Cheng, J. Zhu, P. M. Chaikin, S. E. Phan, and W. B. Russel. Nature of the divergence in low shear viscosity of colloidal hard-sphere dispersions. *Physical Review E*, 65(4):041405, 2002.

[25] M. J. Chrispeels. Biosynthesis, intracellular transport, and secretion of extracellular macromolecules. *Annual Review of Plant Physiology*, 27(1): 19–38, 1976.

[26] C. Christopoulou, G. Petekidis, B. Erwin, M. Cloitre, and D. Vlassopoulos. Ageing and yield behaviour in model soft colloidal glasses. *Philosophical Transactions of the Royal Society A: Mathematical, Physical and Engineering Sciences*, 367(1909):5051–5071, 2009.

[27] M. Cloitre, R. Borrega, F. Monti, and L. Leibler. Glassy dynamics and flow properties of soft colloidal pastes. *Physical Review Letters*, 90(6): 068303, 2003.

[28] E. G. D. Cohen and I. M. Schepper. Note on transport processes in dense colloidal suspensions. *Journal of Statistical Physics*, 63(1-2):241–248, 1991.

[29] D. J. Cosgrove. Enzymes and other agents that enhance cell wall extensibility. *Annual Review of Plant Physiology and Plant Molecular Biology*, 50(1):391–417, 1999.

[30] D. J. Cosgrove. Expansive growth of plant cell walls. *Plant Physiology and Biochemistry*, 38(1-2):109–124, 2000.

[31] D. J. Cosgrove. Growth of the plant cell wall. *Nature Reviews Molecular Cell Biology*, 6(11):850–861, 2005.

[32] D. J. Cosgrove and D. M. Durachko. Autolysis and extension of isolated walls from growing cucumber hypocotyls. (45):1711–1719, 1994.

[33] L. Day, M. Xu, S. K. Oiseth, Y. Hemar, and L. Lundin. Control of morphological and rheological properties of carrot cell wall particle dispersions through processing. *Food and Bioprocess Technology*, 3(6): 928–934, 2010.

[34] L. Day, M. Xu, S. K. Oiseth, L. Lundin, and Y. Hemar. Dynamic rheological properties of plant cell-wall particle dispersions. *Colloids and Surfaces B: Biointerfaces*, 81(2):461–467, 2010.

[35] C. de Kruif and R. Tuinier. Polysaccharide protein interactions. *Food Hydrocolloids*, 15(4-6):555–563, 2001.

[36] D. P. Delmer. Cellulose Biosynthesis: Exciting times for a difficult field of study. *Annual Review of Plant Physiology and Plant Molecular Biology*, 50(1):245–276, 1999.

[37] F. Den Ouden and T. Van Vliet. Particle size distribution in tomato concentrate and effects on rheological properties. *Journal of Food Science*, 62(3):565–567, 1997.

[38] J. V. Diaz, G. E. Anthon, and D. M. Barrett. Conformational changes in serum pectins during industrial tomato paste production. *Journal of Agricultural and Food Chemistry*, 57(18):8453–8458, 2009.

[39] J. L. Doublier, C. Garnier, D. Renard, and C. Sanchez. Protein-polysaccharide interactions. *Current Opinion in Colloid & Interface Science*, 5(3-4):202–214, 2000.

[40] A. Einstein. Eine neue bestimmung der molekuldimensionen [AdP 19, 289 (1906)]. *Annalen der Physik*, 14(S1):229–247, 2005.

[41] Z. El Rassi, D. Tedford, J. H. An, and A. Mort. High-performance reversed-phase chromatographic mapping of 2-pyridylamino derivatives of xyloglucan oligosaccharides. *Carbohydrate Research*, 215(1):25–38, 1991.

[42] L. T. Fan, Y. H. Lee, and D. H. Beardmore. Mechanism of the enzymatic hydrolysis of cellulose: Effects of major structural features of cellulose on enzymatic hydrolysis. *Biotechnology and Bioengineering*, 22(1):177–199, 1980.

[43] L. Fisher. Physics takes the biscuit. *Nature*, 397(6719):469–469, 1999.

[44] M. L. Fishman, H. K. Chau, F. Kolpak, and J. Brady. Solvent effects on the molecular properties of pectins. *Journal of Agricultural and Food Chemistry*, 49(9):4494–4501, 2001.

[45] I. Fraeye, T. Duvetter, E. Doungla, A. Van Loey, and M. Hendrickx. Fine-tuning the properties of pectin-calcium gels by control of pectin fine structure, gel composition and environmental conditions. *Trends in Food Science & Technology*, 21(5):219–228, 2010.

[46] U. Freudenberg, R. Zimmermann, K. Schmidt, S. H. Behrens, and C. Werner. Charging and swelling of cellulose films. *Journal of Colloid and Interface Science*, 309(2):360–365, 2007.

[47] M. Gad, A. Itoh, and A. Ikai. Mapping cell wall polysaccharides of living microbial cells using atomic force microscopy. *Cell Biology International*, 21(11):697–706, 1997.

[48] M. Girard, S. L. Turgeon, and S. F. Gauthier. Interbiopolymer complexing between beta-lactoglobulin and low- and high-methylated pectin measured by potentiometric titration and ultrafiltration. *Food Hydrocolloids*, 16(6): 585–591, 2002.

[49] G. T. Grant, E. R. Morris, D. A. Rees, P. J. Smith, and D. Thom. Biological interactions between polysaccharides and divalent cations: The egg-box model. *FEBS Letters*, 32(1):195–198, 1973.

[50] A. Gundurao, H. S. Ramaswamy, and J. Ahmed. Effect of soluble solids concentration and temperature on thermo-physical and rheological properties of mango puree. *International Journal of Food Properties*, 14 (5):1018–1036, 2011.

[51] D. Guzey and D. J. McClements. Influence of environmental stresses on O/W emulsions stabilized by beta-lactoglobulin-pectin and beta-lactoglobulin-pectin-chitosan membranes produced by the electrostatic layer-by-layer deposition technique. *Food Biophysics*, 1(1):30–40, 2006.

[52] P. Hebraud and F. Lequeux. Mode-coupling theory for the pasty rheology of soft glassy materials. *Physical Review Letters*, 81(14):2934–2937, 1998.

[53] R. Hohler and S. Cohen-Addad. Rheology of liquid foam. *Journal of Physics: Condensed Matter*, 17(41):R1041, 2005.

[54] F. M. Horn, W. Richtering, J. Bergenholtz, N. Willenbacher, and N. J. Wagner. Hydrodynamic and colloidal interactions in concentrated charge-stabilized polymer dispersions. *Journal of Colloid and Interface Science*, 225(1):166–178, 2000.

[55] K. M. Hua, M. Kay, and H. E. Indyk. Nutritional element analysis in infant formulas by direct dispersion and inductively coupled plasma-optical emission spectrometry. *Food Chemistry*, 68(4):463–470, 2000.

[56] G. B. Jeffery. The motion of ellipsoidal particles immersed in a viscous fluid. *Proceedings of the Royal Society of London. Series A*, 102(715): 161–179, 1922.

[57] D. A. R. Jones, B. Leary, and D. V. Boger. The rheology of a concentrated colloidal suspension of hard spheres. *Journal of Colloid and Interface Science*, 147(2):479–495, 1991.

[58] A. Kotcharian, H. Kunzek, and G. Dongowski. The influence of variety on the enzymatic degradation of carrots and on functional and physiological properties of the cell wall materials. *Food Chemistry*, 87(2):231–245, 2004.

[59] I. M. Krieger and T. J. Dougherty. A mechanism for non-Newtonian flow in suspensions of rigid spheres. *Transactions of the Society of Rheology*, 3 (1):137–152, 1959.

[60] D. T. A. Lamport. The protein component of primary cell walls. In *Advances in Botanical Research*, volume Volume 2, pages 151–218. Academic Press, 1966.

[61] D. T. A. Lamport, M. J. Kieliszewski, Y. Chen, and M. C. Cannon. Role of the extensin superfamily in primary cell wall architecture. *Plant Physiology*, 156(1):11–19, 2011.

[62] H. N. W. Lekkerkerker, W. C. K. Poon, P. N. Pusey, A. Stroobants, and P. B. Warren. Phase behaviour of colloid + polymer mixtures. *EPL (Europhysics Letters)*, 20(6):559, 1992.

[63] R. A. Lionberger and W. B. Russel. Microscopic theories of the rheology of stable colloidal dispersions. In *Advances in Chemical Physics*, pages 399–474. John Wiley & Sons, Inc., 2007.

[64] P. Lopez-Sanchez and R. Farr. Power laws in the elasticity and yielding of plant particle suspensions. *Food Biophysics*, 7(1):15–27, 2011.

[65] P. Lopez-Sanchez, J. Nijsse, H. C. G. Blonk, L. Bialek, S. Schumm, and M. Langton. Effect of mechanical and thermal treatments on the microstructure and rheological properties of carrot, broccoli and tomato dispersions. *Journal of the Science of Food and Agriculture*, 91(2):207–217, 2011.

[66] P. Lopez-Sanchez, C. Svelander, L. Bialek, S. Schumm, and M. Langton. Rheology and microstructure of carrot and tomato emulsions as a result of high-pressure homogenization conditions. *Journal of Food Science*, 76 (1):E130–E140, 2011.

[67] P. Lopez-Sanchez, M. Rincon, D. Wang, S. Brulhart, J. R. Stokes, and M. J. Gidley. Micromechanics and poroelasticity of hydrated cellulose networks. *Biomacromolecules*, 15(6):2274–2284, 2014.

[68] C. W. Macosko. *Rheology: Principles, Measurements, and Applications*. Wiley, 1994.

[69] R. S. J. Manley and S. G. Mason. Particle motions in sheared suspensions III.: Further observations on collisions of spheres. *Canadian Journal of Chemistry*, 33(5):763–773, 1955.

[70] G. I. Mantanis, R. A. Young, and R. M. Rowell. Swelling of compressed cellulose fiber webs in organic liquids. *Cellulose*, 2(1):1–22, 1995.

[71] A. Maroziene and C. G. de Kruif. Interaction of pectin and casein micelles. *Food Hydrocolloids*, 14(4):391–394, 2000.

[72] T. Mason, J. Bibette, and D. Weitz. Yielding and flow of monodisperse emulsions. *Journal of Colloid and Interface Science*, 179(2):439–448, 1996.

[73] P. Massiot, X. Rouau, and J.-F. Thibault. Characterisation of the extractable pectins and hemicelluloses of the cell wall of carrot. *Carbohydrate Research*, 172(2):229–242, 1988.

[74] P. Massiot, X. Rouau, and J.-F. Thibault. Isolation and characterisation of the cell-wall fibres of carrot. *Carbohydrate Research*, 172(2):217–227, 1988.

[75] P. Massiot, J.-F. Thibault, and X. Rouau. Degradation of carrot (daucus carota) fibres with cell-wall polysaccharide-degrading enzymes. *Journal of the Science of Food and Agriculture*, 49(1):45–58, 1989.

[76] M. C. McCann and K. Roberts. Architecture of the primary cell wall. In *The Cytoskeletal Basis of Plant Growth and Form*, pages 109–129. London: Academic Press, 1991.

[77] M. C. McCann, L. Chen, K. Roberts, E. K. Kemsley, C. Sene, N. C. Carpita, N. J. Stacey, and R. H. Wilson. Infrared microspectroscopy: Sampling heterogeneity in plant cell wall composition and architecture. *Physiologia Plantarum*, 100(3):729–738, 1997.

[78] J. Messiaen, P. Cambier, and P. V. Cutsem. Polyamines and pectins (i. ion exchange and selectivity). *Plant Physiology*, 113(2):387–395, 1997.

[79] J. Mewis and N. J. Wagner. *Colloidal suspension rheology*. Cambridge University Press, 2013.

[80] R. Mezzenga, P. Schurtenberger, A. Burbidge, and M. Michel. Understanding foods as soft materials. *Nature Materials*, 4(10):729–740, 2005.

[81] P. Milani, M. Gholamirad, J. Traas, A. Arneodo, A. Boudaoud, F. Argoul, and O. Hamant. In-vivo analysis of local wall stiffness at the shoot apical meristem in arabidopsis using atomic force microscopy. *The Plant Journal*, 67(6):1116–1123, 2011.

[82] K. R. Moelants, R. Cardinaels, K. De Greef, E. Daels, S. Van Buggenhout, A. M. Van Loey, P. Moldenaers, and M. E. Hendrickx. Effect of calcium ions and pH on the structure and rheology of carrot-derived suspensions. *Food Hydrocolloids*, 36:382–391, 2014.

[83] K. R. Moelants, R. Cardinaels, S. Van Buggenhout, A. M. Van Loey, P. Moldenaers, and M. E. Hendrickx. A review on the relationships between processing, food structure, and rheological properties of plant-tissue-based food suspensions: Plant-tissue-based food suspensions. *Comprehensive Reviews in Food Science and Food Safety*, 13(3):241–260, 2014.

[84] K. R. N. Moelants, R. Cardinaels, R. P. Jolie, T. A. J. Verrijssen, S. Buggenhout, L. M. Zumalacarregui, A. M. Loey, P. Moldenaers, and M. E. Hendrickx. Relation between particle properties and rheological characteristics of carrot-derived suspensions. *Food and Bioprocess Technology*, 6(5):1127–1143, 2013.

[85] D. Mohnen. Pectin structure and biosynthesis. *Current Opinion in Plant Biology*, 11(3):266–277, 2008.

[86] C. H. Montana, L. C. Greve, and J. M. Labavitch. Changes in cell wall pectins accompanying tomato (lycopersicon esculentum mill.) paste manufacture. *Journal of Agricultural and Food Chemistry*, 50(2):273–278, 2002.

[87] H. Morikawa, R. Hayashi, and M. Senda. Infrared analysis of pea stem cell walls and oriented structure of matrix polysaccharides in them. *Plant and Cell Physiology*, 19(7):1151–1159, 1978.

[88] S. Mueller, E. W. Llewellin, and H. M. Mader. The rheology of suspensions of solid particles. *Proceedings of the Royal Society A: Mathematical, Physical and Engineering Science*, 466(2116):1201–1228, 2010.

[89] K. Muhlethaler. Ultrastructure and formation of plant cell walls. *Annual Review of Plant Physiology*, 18(1):1–24, 1967.

[90] M. O'Neill, P. Albersheim, and A. Darvill. 12 - the pectic polysaccharides of primary cell walls. In P.M. DEY, editor, *Methods in Plant Biochemistry*, volume 2 of *Carbohydrates*, pages 415–441. Academic Press, 1990.

[91] M. A. O'Neill, D. Warrenfeltz, K. Kates, P. Pellerin, T. Doco, A. G. Darvill, and P. Albersheim. Rhamnogalacturonan-II, a pectic polysaccharide in the walls of growing plant cell, forms a dimer that is covalently cross-linked by a borate ester in vitro conditions for the formation and hydrolysis of the dimer. *Journal of Biological Chemistry*, 271(37):22923–22930, 1996.

[92] A. P. Ormerod, J. D. Ralfs, R. Jackson, J. Milne, and M. J. Gidley. The influence of tissue porosity on the material properties of model plant tissues. *Journal of Materials Science*, 39(2):529–538, 2004.

[93] W. Pabst. Fundamental considerations on suspension rheology. *Ceramics*, 48(1):6–12, 2004.

[94] E. Parre and A. Geitmann. Pectin and the role of the physical properties of the cell wall in pollen tube growth of solanum chacoense. *Planta*, 220 (4):582–592, 2005.

[95] S. E. Paulin, B. J. Ackerson, and M. S. Wolfe. Microstructure-dependent viscosity in concentrated suspensions of soft spheres. *Physical Review E*, 55(5):5812–5819, 1997.

[96] A. Peaucelle, S. A. Braybrook, L. Le Guillou, E. Bron, C. Kuhlemeier, and H. Hofte. Pectin-induced changes in cell wall mechanics underlie organ initiation in arabidopsis. *Current Biology*, 21(20):1720–1726, 2011.

[97] C. Pickardt, G. Dongowski, and H. Kunzek. The influence of mechanical and enzymatic disintegration of carrots on the structure and properties of cell wall materials. *European Food Research and Technology*, 219(3), 2004.

[98] W. C. K. Poon. The physics of a model colloid-polymer mixture. *Journal of Physics: Condensed Matter*, 14(33):R859, 2002.

[99] V. Prasanna, T. N. Prabha, and R. N. Tharanathan. Fruit ripening phenomena: An overview. *Critical Reviews in Food Science and Nutrition*, 47(1):1–19, 2007.

[100] R. D. Preston. Polysaccharide conformation and cell wall function. *Annual Review of Plant Physiology*, 30(1):55–78, 1979.

[101] P. N. Pusey and W. van Megen. Phase behaviour of concentrated suspensions of nearly hard colloidal spheres. *Nature*, 320(6060):340–342, 1986.

[102] P. N. Pusey and W. van Megen. Observation of a glass transition in suspensions of spherical colloidal particles. *Physical Review Letters*, 59 (18):2083–2086, 1987.

[103] C. G. Qiu and M. Rao. Role of pulp content and particle size in yield stress of apple sauce. *Journal of Food Science*, 53(4):1165–1170, 1988.

[104] U. Rani and G. Bains. Flow behaviour of tomato ketchups. *Journal of Texture Studies*, 18(2):125–135, 1987.

[105] M. Rao and H. Cooley. Rheological behavior of tomato pastes in steady and dynamic shear. *Journal of Texture Studies*, 23(4):415–425, 1992.

[106] R. J. Redgwell, D. Curti, and C. Gehin-Delval. Physicochemical properties of cell wall materials from apple, kiwifruit and tomato. *European Food Research and Technology*, 227(2):607–618, 2008.

[107] P. Roger, B. Baud, and P. Colonna. Characterization of starch polysaccharides by flow field-flow fractionation-multi-angle laser light

scattering-differential refractometer index. *Journal of Chromatography A*, 917(1-2):179–185, 2001.

[108] R. Roscoe. The viscosity of suspensions of rigid spheres. *British Journal of Applied Physics*, 3(8):267, 1952.

[109] A. L. Routier-Kierzkowska, A. Weber, P. Kochova, D. Felekis, B. J. Nelson, C. Kuhlemeier, and R. S. Smith. Cellular force microscopy for in vivo measurements of plant tissue mechanics. *Plant Physiology*, 158(4): 1514–1522, 2012.

[110] M. C. Sanchez, C. Valencia, C. Gallegos, A. Ciruelos, and A. Latorre. Influence of processing on the rheological properties of tomato paste. *Journal of the Science of Food and Agriculture*, 82(9):990–997, 2002.

[111] A. K. Sankaran, J. Nijsse, L. Bialek, A. Shpigelman, M. E. Hendrickx, and A. M. Van Loey. Enhanced electrostatic interactions in tomato cell suspensions. *Food Hydrocolloids*, 43:442–450, 2015.

[112] H. V. Scheller and P. Ulvskov. Hemicelluloses. *Annual Review of Plant Biology*, 61(1):263–289, 2010.

[113] E. Schijvens, T. van Vliet, and C. van Dijk. Effect of processing conditions on the composition and rheological properties of applesauce. *Journal of Texture Studies*, 29(2):123–143, 1998.

[114] P. N. Segre, S. P. Meeker, P. N. Pusey, and W. C. K. Poon. Viscosity and structural relaxation in suspensions of hard-sphere colloids. *Physical Review Letters*, 75(5):958–961, 1995.

[115] D. J. Shaw. 8 - colloid stability. In D. J. Shaw, editor, *Introduction to Colloid and Surface Chemistry (Fourth Edition)*, pages 210–243. Butterworth-Heinemann, Oxford, 1992.

[116] A. Shpigelman, C. Kyomugasho, S. Christiaens, A. M. Van Loey, and M. E. Hendrickx. Thermal and high pressure high temperature processes result in distinctly different pectin non-enzymatic conversions. *Food Hydrocolloids*, 39:251–263, 2014.

[117] D. Sila, S. Van Buggenhout, T. Duvetter, I. Fraeye, A. De Roeck, A. Van Loey, and M. Hendrickx. Pectins in processed fruits and vegetables: Part II: Structure-function relationships. *Comprehensive Reviews in Food Science and Food Safety*, 8(2):86–104, 2009.

[118] P. Sollich, F. Lequeux, P. HÃ©braud, and M. E. Cates. Rheology of soft glassy materials. *Physical Review Letters*, 78(10):2020–2023, 1997.

[119] H. K. Sreenath, M. D. Frey, B. J. Radola, and H. Scherz. Degradation of a washed carrot preparation by cellulases and pectinases. *Biotechnology and Bioengineering*, 26(7):788–796, 1983.

[120] A. M. Stephen. *Food polysaccharides and their applications*. CRC Press, 1995.

[121] F. C. Steward and K. Muhlethaler. The structure and development of the cell-wall in the valoniaceae as revealed by the electron microscope. *Annals of Botany*, 17(2):295–316, 1953.

[122] T. Stoll, U. Schweiggert, A. Schieber, and R. Carle. Process for the recovery of a carotene-rich functional food ingredient from carrot pomace by enzymatic liquefaction. *Innovative Food Science & Emerging Technologies*, 4(4):415–423, 2003.

[123] A. Sturcova, I. His, D. C. Apperley, J. Sugiyama, and M. C. Jarvis. Structural details of crystalline cellulose from higher plants. *Biomacromolecules*, 5(4):1333–1339, 2004.

[124] G. B. B. M. Sutherland. Infrared analysis of the structure of amino acids, polypeptides and proteins. In K. B. M.L. Anson and J. T. Edsall, editors, *Advances in Protein Chemistry*, volume Volume 7, pages 291–318. Academic Press, 1952.

[125] L. Taiz. Plant cell expansion: Regulation of cell wall mechanical properties. *Annual Review of Plant Physiology*, 35(1):585–657, 1984.

[126] N. Takada and P. E. Nelson. Pectin-protein interaction in tomato products. *Journal of Food Science*, 48(5):1408–1411, 1983.

[127] T. Tanglertpaibul and M. A. Rao. Flow properties of tomato concentrates: Effect of serum viscosity and pulp content. *Journal of Food Science*, 52 (2):318–321, 1987.

[128] T. Tanglertpaibul and M. A. Rao. Rheological properties of tomato concentrates as affected by particle size and methods of concentration. *Journal of Food Science*, 52(1):141–145, 1987.

[129] R. Tanner and K. Walters. *Rheology: An Historical Perspective*. Elsevier, 1999.

[130] G. I. Taylor. The viscosity of a fluid containing small drops of another fluid. *Proceedings of the Royal Society of London. Series A*, 138(834): 41–48, 1932.

[131] B. R. Thakur, R. K. Singh, and A. K. Handa. Effect of added soy protein on the quality of tomato sauce. *Journal of Food Processing and Preservation*, 20(2):169–176, 1996.

[132] B. R. Thakur, R. K. Singh, A. K. Handa, and M. A. Rao. Chemistry and uses of pectin - a review. *Critical Reviews in Food Science and Nutrition*, 37(1):47–73, 1997.

[133] J. Thibault, C. M. G. C. Renard, M. A. V. Axelos, P. Roger, and M. J. Crépeau. Studies of the length of homogalacturonic regions in pectins by acid hydrolysis. *Carbohydrate Research*, 238:271–286, 1993.

[134] L. H. Thomas, V. T. Forsyth, A. Sturcova, C. J. Kennedy, R. P. May, C. M. Altaner, D. C. Apperley, T. J. Wess, and M. C. Jarvis. Structure of cellulose microfibrils in primary cell walls from collenchyma. *Plant Physiology*, 161(1):465–476, 2013.

[135] S. Tiziani and Y. Vodovotz. Rheological effects of soy protein addition to tomato juice. *Food Hydrocolloids*, 19(1):45–52, 2005.

[136] S. M. Underwood, J. R. Taylor, and W. van Megen. Sterically stabilized colloidal particles as model hard spheres. *Langmuir*, 10(10):3550–3554, 1994.

[137] W. van Megen and S. M. Underwood. Glass transition in colloidal hard spheres: Measurement and mode-coupling-theory analysis of the coherent intermediate scattering function. *Physical Review E*, 49(5):4206–4220, 1994.

[138] V. Vand. Viscosity of solutions and suspensions. i. theory. *The Journal of Physical and Colloid Chemistry*, 52(2):277–299, 1948.

[139] V.B.Tolstoguzov. Functional properties of food proteins and role of protein-polysaccharide interaction. *Food Hydrocolloids*, 4(6):429–468, 1991.

[140] A. Vercet, C. Sánchez, J. Burgos, L. Montañés, and P. Lopez Buesa. The effects of manothermosonication on tomato pectic enzymes and tomato paste rheological properties. *Journal of Food Engineering*, 53(3):273–278, 2002.

[141] B. A. Veytsman and D. J. Cosgrove. A model of cell wall expansion based on thermodynamics of polymer networks. *Biophysical Journal*, 75(5): 2240–2250, 1998.

[142] L. Walker, D. Wilson, and D. Irwin. Measuring fragmentation of cellulose by thermomonospora fusca cellulase. *Enzyme and Microbial Technology*, 12(5):378–386, 1990.

[143] L. Wang, D. Hukin, J. Pritchard, and C. Thomas. Comparison of plant cell turgor pressure measurement by pressure probe and micromanipulation. *Biotechnology Letters*, 28(15):1147–1150, 2006.

[144] S. E. C. Whitney, M. G. E. Gothard, J. T. Mitchell, and M. J. Gidley. Roles of cellulose and xyloglucan in determining the mechanical properties of primary plant cell walls. *Plant Physiology*, 121(2):657–664, 1999.

[145] R. Whittenberger and G. Nutting. High viscosity of cell wall suspensions prepared from tomato juice. 8:420–424, 1958.

[146] K. Wickholm, P. T. Larsson, and T. Iversen. Assignment of non-crystalline forms in cellulose I by CP/MAS 13C NMR spectroscopy. *Carbohydrate Research*, 312(3):123–129, 1998.

[147] W. G. Willats, J. P. Knox, and J. D. Mikkelsen. Pectin: new insights into an old polymer are starting to gel. *Trends in Food Science & Technology*, 17(3):97–104, 2006.

[148] W. G. T. Willats, L. McCartney, W. Mackie, and J. P. Knox. Pectin: cell biology and prospects for functional analysis. *Plant Molecular Biology*, 47 (1-2):9–27, 2001.

[149] B. Yoo and M. Rao. Effect of unimodal particle size and pulp content on rheological properties of tomato puree. *Journal of Texture Studies*, 25(4): 421–436, 1994.

[150] A. Yoshimura and R. K. Prud'homme. Wall slip corrections for couette and parallel disk viscometers. *Journal of Rheology*, 32(1):53–67, 1988.

[151] E. B. Zhulina, O. V. Borisov, and V. A. Priamitsyn. Theory of steric stabilization of colloid dispersions by grafted polymers. *Journal of Colloid and Interface Science*, 137(2):495–511, 1990.

FACULTY OF BIOSCIENCE ENGINEERING

DEPARTMENT OF MICROBIAL AND MOLECULAR SYSTEMS

LABORATORY OF FOOD TECHNOLOGY

Kasteelpark Arenberg 22 box 2457

B-3001 Heverlee